DISSERTATION

submitted to the

Combined Faculties for the Natural Sciences
and for Mathematics
Ruperto-Carola University of Heidelberg, Germany

for the degree of
Doctor of Natural Sciences

presented by
Diplom-Ernährungswissenschaftler Daniel Habermehl

born in Lahn/Wetzlar

oral examination: April 24th, 2008

Analysis of glucocorticoid receptor function in murine lung development using cell type-specific gene ablation

Referees:

Prof. Dr. Günther Schütz
Prof. Dr. Felix Wieland

Table of Contents

1. Summary

A vast body of evidence from studies in humans as well as animals illustrates the pivotal role of glucocorticoid signalling during pre- and postnatal lung maturation. Consequently, corticosteroid treatment is the established standard regimen for pre-term infants and has served to reduce incidence and severity of the major complications, respiratory distress syndrome and bronchopulmonary dysplasia. Glucocorticoid effects are mediated by the glucocorticoid receptor (GR) which acts as a ligand-dependent transcription factor and controls target gene expression by DNA-binding-dependent as well as -independent mechanisms. In line with this, disruption of glucocorticoid signalling by germline inactivation of the GR gene in the mouse leads to respiratory failure and postnatal lethality. Intriguingly, mice carrying a point mutation which selectively impairs homodimeric binding of GR to its cognate response elements survive, indicating that the essential functions of GR during murine lung development are mediated via protein-protein interactions rather than DNA-binding.

To further elucidate the modes of GR action which mediate these critical effects, conditional gene inactivation was employed taking advantage of the Cre/loxP recombination system. A series of mutant mice was generated, lacking GR in the mesenchyme, endothelial cells or the lung epithelium, respectively, allowing the assessment of the relative contribution of these compartments to the phenotype of the germline mutation.

The beneficial effects of corticosteroids have commonly been attributed to their ability to induce the functional maturation of lung epithelial cells including the stimulation of surfactant synthesis as well as sodium and water transport across the epithelium. However, conditional inactivation of the GR gene in all epithelial cells of the developing lung did not impair survival. Although these mutant mice displayed a delayed progression through the late phases of lung maturation, this retardation did not affect respiratory function at birth and was compensated during the first days of life or an artificially prolonged pregnancy.

In contrast, mice lacking GR specifically in mesenchymal cells displayed a morphogenetic phenotype strongly reminiscent of GR knockout animals and succumbed to death immediately after birth. Comparable to the germline mutants, lungs of mutant embryos did not proceed through the canalicular and saccular phases of pulmonary development but remained in the pseudoglandular stage until birth. At E18.5, they were characterized by cuboidal epithelial cells and an expansion of the mesenchymal compartment resulting in an almost complete lack of presumptive alveolar airspace. Mutant lungs showed an increased proliferation rate and failed to induce general differentiation markers such as $p21^{cip1}$. Moreover, the mutation significantly altered the composition of the extracellular matrix which is known to be critical not only as a structural support but also for mesenchymal-epithelial interactions.

Finally, endothelium-specific inactivation of the GR gene neither affected postnatal survival nor morphogenetic development of the lung precluding an important function of GR in endothelial cells during the development of the pulmonary vasculature.

In summary, the present study demonstrates that GR in the developing murine lung epithelium is not essential for postnatal survival. Instead, critical glucocorticoid effects are mediated by GR action in the mesenchyme which is necessary to promote complete progression through the maturational phases of murine lung development. GR acts particularly in cells of the fibroblast lineage where it controls the composition of the extracellular matrix and is indispensible for the decrease in the general proliferation rate.

2. Zusammenfassung

Eine Vielzahl von Studien sowohl an Menschen als auch an Tieren hat gezeigt, dass Glucocorticoide eine zentrale Rolle in der prä- und postnatalen Lungenreifung ausüben. Daher gehört die Behandlung mit Corticoiden zur Standardtherapie frühgeborener Kinder und hat dazu beigetragen, Vorkommen und Ausmaß der wichtigsten Komplikationen zu verringern, der respiratorischen Insuffizienz sowie der bronchopulmonalen Dysplasie. Glucocorticoideffekte werden durch den Glucocorticoidrezeptor (GR) vermittelt, der als ligandengesteuerter Transkriptionsfaktor die Expression von Zielgenen über Mechanismen kontrolliert, die DNA-bindungsabhängig aber auch DNA-bindungsunabhängig sein können. In Übereinstimmung damit führt eine Blockade des Glucocorticoid-Signalwegs durch gezielte Inaktivierung des GRs in der Maus zu Atemversagen und postnataler Lethalität. Interessanterweise überleben Mäuse mit einer Punktmutation, die selektiv die Bindung von GR als Homodimer an seine entsprechenden responsiven DNA-Elemente verhindert, was darauf hindeutet, dass die wesentlichen Funktionen des GR in der Lungenentwicklung über Protein-Protein-Wechselwirkungen ausgeübt werden.
Um die Wirkungsweisen des GR, die diese essentiellen Effekte vermitteln, näher zu untersuchen, wurde das Cre/loxP Rekombinationssystem zur gewebs- und/oder zelltypspezifischen Geninaktivierung angewandt. Es wurde eine Reihe von Mausmutanten generiert, denen GR entweder im Mesenchym, endothelialen Zellen oder dem Lungenepithel fehlt. Dies ermöglicht eine Einschätzung, inwiefern diese Kompartimente für den Phänotyp der Keimbahnmutante verantwortlich sind.
Die positiven Effekte der Corticosteroide wurden gemeinhin ihrer Fähigkeit zugesprochen, Aspekte der funktionellen Reifung von Lungenepithelzellen zu induzieren wie die Synthese von Surfactant und den transepithelialen Transport von Natrium und Wasser. Eine konditionale Inaktivierung des GR-Gens in epithelialen Zellen der fötalen Lunge führte jedoch zu keiner Beeinträchtigung der Überlebensrate. Obwohl diese Mausmutanten eine Verzögerung der späten Phasen der Lungenreifung aufwiesen, hatte dies keinen Einfluss auf die Atemfunktion nach der Geburt und konnte in den ersten Lebenstagen oder durch eine künstlich verlängerte Schwangerschaft ausgeglichen werden.
Im Gegensatz dazu starben Mäuse mit einer mesenchymspezifischen Inaktivierung des GR-Gens sofort nach der Geburt und äußerten einen Phänotyp, der in weiten Teilen mit dem der GR Knockouttiere übereinstimmt. Die Lungen dieser Mutanten verblieben bis zur Geburt in der Pseudoglandulären Phase der Lungenentwicklung und durchliefen weder die Kanalikuläre noch die Sakkuläre Phase. Am Tag E18.5 waren sie durch kuboidale Epithelzellen sowie eine Zunahme des mesenchymalen Kompartiments charakterisiert, was ein praktisch vollständiges Fehlen von zukünftigem alveolärem Luftraum zur Folge hatte. Die Lungen der Mausmutanten wiesen eine erhöhte Proliferationsrate auf und die Induktion von allgemeinen Differenzierungsmarkern wie $p21^{cip1}$ blieb aus. Darüber hinaus bewirkte die Mutation eine signifikant veränderte Zusammensetzung der Extrazellulärmatrix, die zum einen als strukturelles Gerüst dient aber auch in der Lage ist, mesenchymal-epitheliale Interaktionen zu beeinflussen.
Schließlich beeinträchtigte eine endothelspezifische Inaktivierung des GR-Gens weder die postnatale Überlebensrate noch die morphogenetische Entwicklung der Lunge, was eine entscheidende Rolle des GR in Endothelzellen während der Entwicklung des pulmonalen Gefäßsystems ausschließt.
Zusammenfassend zeigt die vorliegende Arbeit, dass der GR im Epithel der Mauslunge für das Überleben nach der Geburt nicht essentiell ist. Im Gegensatz dazu vermittelt der mesenchymale GR Glucocorticoideffekte, die unabdingbar sind, um ein vollständiges Durchlaufen der Reifungsphase der Lungenentwicklung der Maus zu ermöglichen. GR wirkt spezifisch in Fibroblasten, wo er die Zusammensetzung der Extrazellulärmatrix kontrolliert und unabkömmlich ist, um die allgemeine Proliferationsrate zu reduzieren.

3. Introduction

Successful transition to air-breathing at birth strictly depends on the adequate functional maturation of the respiratory system *in utero*. Accordingly, fetal lung development is a complex and highly regulated process orchestrating branching morphogenesis, growth and differentiation to ultimately provide the extensive gas exchange area critical for postnatal survival. This requires an appropriate spatio-temporal activity of a large number of regulatory molecules and pathways, including glucocorticoids which act via the glucocorticoid receptor (GR) (Bourbon et al., 2005; Cardoso and Lu, 2006).

A vast body of evidence illustrates the fundamental role of glucocorticoid signalling during lung maturation in humans as well as rodents (Whitsett and Matsuzaki, 2006). While treatment with corticosteroids is accepted and widely employed as standard regimen for preterm infants, the precise mechanisms of glucocorticoid action remain elusive (Gilstrap et al., 1995).

3.1. Development and structure of the murine respiratory system

3.1.1. Lung morphogenesis

Murine lung development is initiated at embryonic day E9.5 and is commonly divided into four stages, the pseudoglandular, canalicular, saccular and alveolar phase (Bourbon et al., 2005; Warburton et al., 2005).

Formation of the respiratory tube starts with the evagination of endodermal cells from the anterior foregut into the surrounding mesenchyme (E9.5). The following pseudoglandular phase is characterized by growth and repeated dichotomous branching of this lung bud giving rise to bronchioles, respiratory bronchioles and alveolar ducts. As this respiratory tree evolves, one left and four right lung lobes are formed.

During the canalicular phase of lung development (E16.5 to E17.5), branching morphogenesis is completed, and the rapid growth rate diminishes to allow the transition to epithelial differentiation. This coincides with the maturation of the

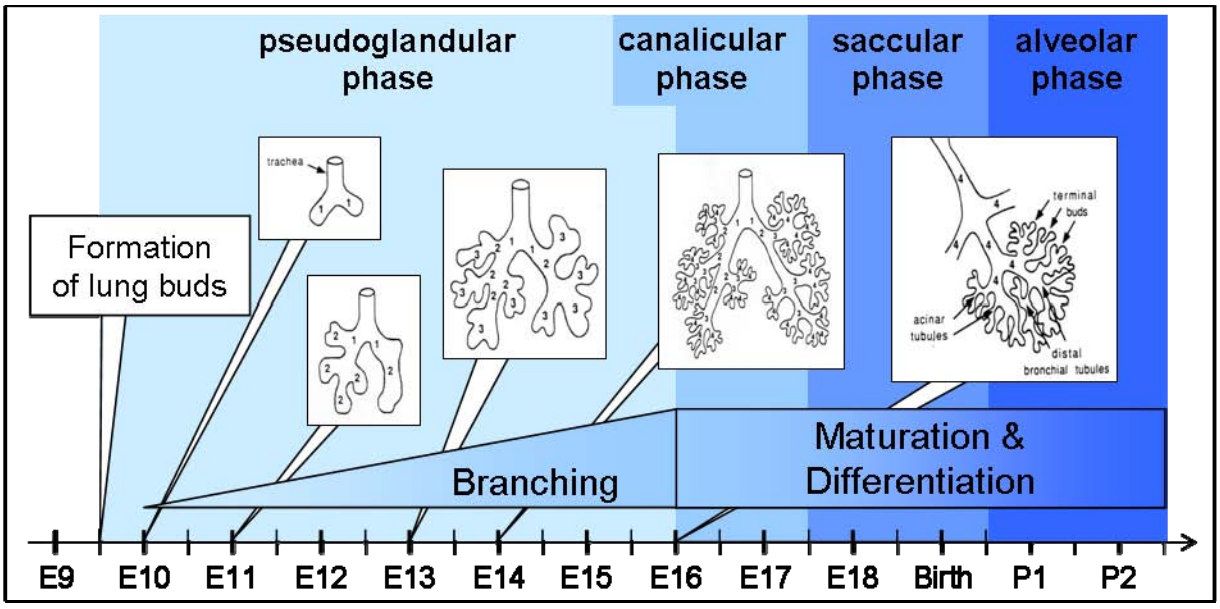

Figure 1: Phases of murine lung development

The pseudoglandular phase starts at E9.5 with the formation of the lung bud and is characterized by growth and dichotomous branching of the respiratory tube. With the onset of the canalicular phase at E16.5, branching morphogenesis seizes and alveolar dilation is initiated. During the saccular phase from E17.5 to birth, terminal differentiation occurs, the epithelium matures and forms close contact with the vascular system while the alveolar septae are attenuated. These processes continue until P5 in the alveolar phase when in addition secondary septae are formed.

primitive vascular and capillary network, which surrounds the respiratory tree and is formed in parallel with it.

From E17.5 to birth, terminal differentiation occurs in the saccular phase of murine lung development. The distal epithelium matures and becomes composed of alveolar type I and type II cells, it flattens and gets in close apposition with the underlying vascular system to form the alveolar gas exchange unit. In parallel, the presumptive alveoli expand while the mesenchymal stroma in the alveolar septae attenuates.

During the alveolar phase from birth to postnatal day 5, the interalveolar septae become progressively thinner and the initial double capillary layer fuses to the single layer of the adult lung. Moreover, secondary septae are formed as low ridges that protrude into the primitive airspace and increase the lung surface area.

3.1.2. Cell types of the developing and mature distal lung and their functions

The mature alveolar epithelium is mainly constituted of alveolar type I and type II cells (ATI and ATII). Even though both cell types are found with the same frequency, ATI cells cover about 95% of the alveolar epithelial surface. They are highly attenuated and form the interface between the luminal airspace and the endothelial cells of the pulmonary capillary system. While the basic function of ATI cells is to

allow and facilitate efficient gas exchange, ATII cells synthesize and secrete pulmonary surfactant, control the ion and fluid transport across the epithelium and are involved in the innate immune response. Moreover, they represent a pool of progenitor cells differentiating into ATI and other cell types when activated during repair and regeneration processes.

Pulmonary surfactant is a phospholipid-rich lipoprotein consisting primarily of phosphatidylcholine and dipalmitoylphosphatidylcholine on the one side as well as surfactant-associated proteins (SP)-A, SP-B, SP-C and SP-D on the other side (Mendelson, 2000). Produced by columnar ATII cells, surfactant is stored in vesicles termed lamellar bodies, and upon secretion into the alveolar lumen, it forms a monolayer surface film which serves to reduce surface tension, increase compliance, and prevent alveolar collapse (Lewis and Veldhuizen, 2003). In addition, surfactant-associated proteins have also been attributed with roles in the immune defence within the alveolus as well as during the initiation of birth (Condon et al., 2004; Wright, 2005).

In the developing lung, the epithelium of the respiratory tube is composed of precursor cells which resemble ATII cells due to their columnar appearance and the expression of proSP-C. The mesenchyme is derived from the splanchnic mesoderm and gives rise to a wide range of cell types including endothelial progenitors, lipofibroblasts, smooth muscle cells and alveolar myofibroblasts (McGowan and Torday, 1997).

3.1.3. Epithelial-mesenchymal interactions in the developing lung

Growth, morphogenic patterning and cellular differentiation in the developing lung depend on interactive signalling between the endodermal epithelium and mesenchyme derived from splanchnic mesoderm (Shannon and Hyatt, 2004). The best characterized model of epithelial-mesenchymal interactions in the developing lung is the integrative regulation of branching morphogenesis involving a number of signalling molecules: Fibroblast growth factor 10 (FGF10) is expressed in the distal mesenchyme and promotes directed growth of the primitive lung bud through induction of proliferation and chemotaxis towards the subpleural source (Bellusci et al., 1997b; Ramasamy et al., 2007). This stimulatory effect is enhanced by FGF10-induced expression of bone morphogenic protein 4 (BMP4) in the epithelium and the sub-epithelial mesenchyme (Bellusci et al., 1996; Weaver et al., 1999). During

elongation of the respiratory tube, epithelial expression of the factors sprouty-2 (SPRY2) and sonic hedgehog (SHH) block ectopic bud formation through local inhibition of FGF signalling in the lateral epithelium and mesenchyme, respectively (Bellusci et al., 1997a; Ding et al., 2007).

Initiation of branching occurs when the proliferation at the tip seizes due to increased WNT (wingless related MMTV integration site) and SHH signalling which oppose the action of FGF10 (Li et al., 2005a). This coincides with the deposition of fibronectin and other components of the extracellular matrix (ECM) at the tip acting as a physical block as well as by reducing growth factor availability at the presumptive cleft (Sakai et al., 2003). As a consequence, new buds form laterally and proliferate again towards the FGF10 sources in the sub-pleural mesenchyme. Epithelial expression of the secreted WNT inhibitor dickkopf-1 (Dkk1) restricts fibronectin deposition to the cleft by counteracting WNT activity at the new growth tips (De Langhe et al., 2005).

3.1.4. Glucocorticoid action during lung development

Among the numerous regulatory signalling molecules known to be involved in lung development, glucocorticoids belong to the most prominent ones. Initial experiments were performed already in 1969 by Liggins demonstrating that corticosteroid treatment of fetal lambs accelerates lung maturation (Liggins, 1969). The clinical benefit of glucocorticoids for the treatment of preterm infants was then confirmed three years later and it has since then served as an important therapy for the reduction of morbidity and mortality in these children (Liggins and Howie, 1972). It has been shown that incidence and severity of the major complications, respiratory distress syndrome (RDS) and bronchopulmonary dysplasia (BPD), are reduced by prenatal exposure to pharmacological doses of glucocorticoids resulting in increased perinatal survival (Sinclair, 1995). As a consequence, the “US National Institute of Health Consensus Developmental Panel on the Effect of Corticosteroids for Fetal Maturation on Perinatal Outcomes” strongly recommends the application of prenatal glucocorticoids for the treatment of woman at risk for preterm delivery (Gilstrap et al., 1995). While this therapy is now accepted as standard of care, it is known to have also harmful side-effects on other organs like the brain and thus, further refinement of indications, timing, dose and duration of glucocorticoid treatment for the prevention or treatment of lung disease in the pre- and postnatal period is warranted (Halliday, 2004).

3.2. Glucocorticoids

3.2.1. Glucocorticoid synthesis and its regulation via the hypothalamic-pituitary-adrenal axis

Glucocorticoids belong to the family of steroid hormones and are synthesized in the zona fasciculata and the zona reticularis of the adrenal cortex. Chemically, they are derivatives of cholesterol and as such characterized by a sterane ring system. Because of their common origin in the adrenal cortex and similar modes of action, they are grouped together with the mineralocorticoids under the denotation corticosteroids. In rodents, corticosterone represents the major glucocorticoid while in humans it is cortisone. Due to their lipophilic character, corticosteroids are not stored but directly released to the circulation where they are preferentially bound to their main transport protein called corticosteroid binding globulin or transcortin (Klieber et al., 2007).

Synthesis and levels of circulating corticosterone are tightly controlled by the hypothalamic-pituitary-adrenal (HPA) axis (Herman et al., 2003). The paraventricular nucleus of the hypothalamus integrates signals from the hippocampus and the amygdala and releases corticotropin releasing hormone (CRH) as well as arginine vasopressin (AVP). Via the portal blood system, these polypeptides are transported to corticotroph cells in the anterior lobe of the pituitary where they induce the expression of proopiomelanocortin (POMC). Apart from POMC synthesis, CRH and AVP also stimulate the secretion of the adrenocorticotropic hormone (ACTH) which is one of the POMC cleavage products. Through binding to its cognate receptors in the adrenal cortex, ACTH finally induces synthesis and release of corticosterone.

Apart from its primary action on other target tissues, circulating corticosterone mediates a negative feedback loop on both levels, secretion of CRH as well as ACTH in the hypothalamus and the pituitary, respectively (Herbert et al., 2006). The limbic structures which control the basal activity of the HPA axis additionally also influence this feedback inhibition. Studies using lesioning and electrical stimulation suggest an overall inhibitory effect of the hippocampus (Jacobson and Sapolsky, 1991), while the amygdala appears to have an excitatory influence (Herman et al., 2003).

The tone of the HPA axis displays a circadian rhythm which reflects the physiologic cycle of activity throughout the day. In nocturnal rodents, high glucocorticoid levels

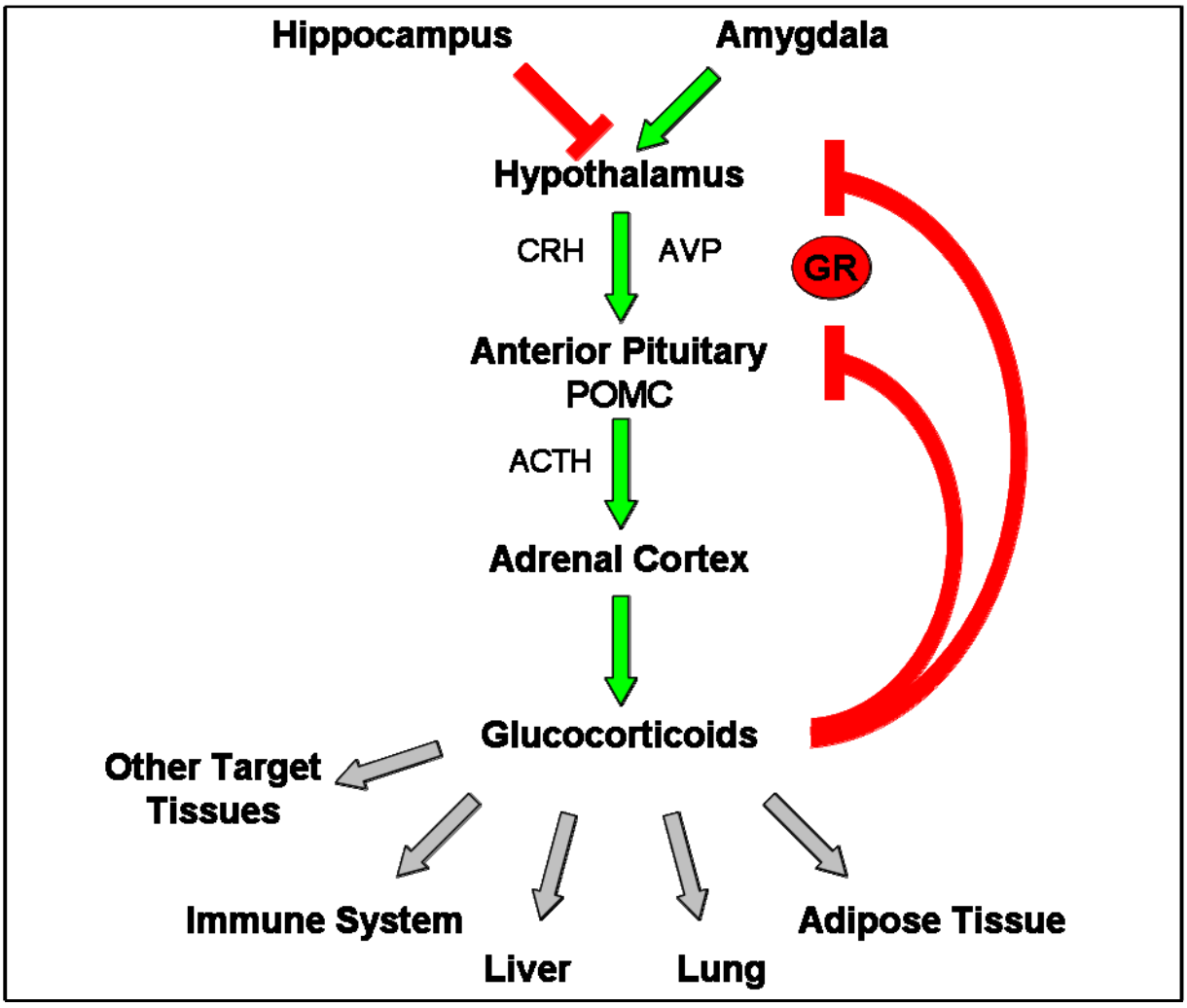

Figure 2: Schematic representation of the regulatory circuit of the hypothalamic-pituitary-adrenal (HPA) axis

Activation of the hypothalamic-pituitary-adrenal (HPA) axis is initiated with the release of the corticotropin-releasing hormone (CRH) from the hypothalamus, which activates the synthesis of proopiomelanocortin (POMC) in the adenohypophysis. POMC is processed into the adrenocorticotropic hormone (ACTH) which is released from the anterior lobe of the pituitary and activates synthesis and secretion of corticosterone in the adrenal cortex. Corticosterone-bound GR mediates the direct negative feedback at the level of the pituitary and hypothalamus, resulting in the return to homeostasis. Activated GR and MR in limbic structures like the hippocampus and amygdala control the tone of the HPA axis.

coincide with the beginning of the dark phase, whereas the HPA axis is most active at the beginning of the light phase in diurnal humans. Accordingly, the resting phase is paralleled by low levels of corticosteroids, respectively, and thus represents the circadian trough.

During murine embryonic development, glucocorticoid synthesis is initiated at E14.5 but the levels remain low until a tremendous surge is observed towards term. Starting at E16.5, the corticosterone levels strongly increase and reach their maximum between E18.5 and birth before they return to low levels during the first days after birth.

3.2.2. Glucocorticoid mediated effects

Apart from their role during embryonic lung development, glucocorticoids exert pleiotropic functions and play a pivotal role in the maintenance of homeostasis in mammalian organisms. As a consequence, dysregulation of the HPA axis and malfunction of glucocorticoid signalling are associated with certain pathophysiological circumstances. On the other hand and despite considerable side effects, corticosteroid therapy allows the treatment and/or alleviation of a wide variety of diseases.

Insufficient production of glucocorticoids by the adrenal cortex leads to Addison's disease, characterized by metabolic imbalances and disturbed fluid and salt homeostasis but also disorders of the central nervous system (Ten et al., 2001). In contrast, Cushing's disease describes the symptoms associated with increased glucocorticoid levels: for instance a catabolic shift with reduced glucose tolerance, osteoporosis, and muscular atrophy due to increased proteolysis, redistribution of adipose tissue with consequent central obesity, hypertension and atherosclerosis as well as repression of the immune system (Krieger, 1983).

In general, glucocorticoids are the principal mediators of stress responses to external stressors such as predators or infections, but also internal imbalances for instance in energy or fluid homeostasis. Hence, glucocorticoids are well known for their role in the metabolic regulation where they generally exert catabolic and anti-insulinergic effects with the exception of the liver (Vegiopoulos and Herzig, 2007). Glucocorticoids increase blood glucose levels by inhibiting cellular uptake and utilization of glucose in peripheral organs and stimulate in particular hepatic gluconeogenesis as well as glycogen synthesis (Pilkis and Granner, 1992). They also induce proteolysis in the musculature, lymphatic tissue, skin and bones providing free amino acids to sustain gluconeogenesis in the liver (Schacke et al., 2002). In adipocytes, glucocorticoids inhibit the uptake of glucose and stimulate lipolysis, thus increasing the availability of free fatty acids (Simmons et al., 1984). Many glucocorticoid effects are mediated via a direct transcriptional control of regulatory enzymes, for example in the case of the phosphoenolpyruvate-carboxykinase or the tyrosine aminotransferase (Hanson and Reshef, 1997; Jantzen et al., 1987; Schmid et al., 1985). However, it is noteworthy that some of those actions such as enhanced

lipolysis are only permissive, allowing and/or increasing the effects of other signalling molecules such as glucagon or catecholamines (Pilkis and Granner, 1992).

Other very crucial effects of glucocorticoids are the suppression of the immune system and the inhibition of inflammational reactions which are the basis for their widespread and valuable clinical application (Barnes and Adcock, 1993; Calandra et al., 1995). They repress the expression as well as secretion of a variety of cytokines and block histamine release, leading among others to the inhibition of T-cell proliferation (Vacca et al., 1992). Glucocorticoids were shown to act pro-apoptotic in T-lymphocytes (Khan et al., 1996; Thompson, 1994) and chronically elevated glucocorticoid levels result in a regression of thymus size in mice (Tronche et al., 1998).

Extensive progress has also been made in the understanding of glucocorticoid actions in the central nervous system. Among the various influenced processes are neuronal excitability and plasticity, neurogenesis and neuronal cell death as well as neuroendocrine control and behavioural responses like learning, memory and anxiety (De Kloet et al., 1998; Herbert et al., 2006). In addition, research both in humans and in animal models has implicated the forebrain GR in depression (Calfa et al., 2003; Gass et al., 2001). In animal models of depression it was shown that a depression-like phenotype is associated with decreased hippocampal GR expression (Boyle et al., 2005; Ridder et al., 2005).

3.3. The glucocorticoid receptor

3.3.1. Corticosteroid receptors

The effects of the two corticosteroid hormones corticosterone and aldosterone are mediated by two closely related steroid hormone receptors, the glucocorticoid receptor (GR) and the mineralocorticoid receptor (MR). GR and MR belong to the superfamily of ligand-activated transcription factors including other steroid receptors such as the estrogen or androgen receptor but also receptors for vitamin D3, retinoic acid and thyroids as well as orphan receptors (Beato and Klug, 2000; Mangelsdorf et al., 1995). Cloning and sequencing of the genes for GR (NR3C1) (Hollenberg et al., 1985; Miesfeld et al., 1986) and MR (NR3C2) (Arriza et al., 1987; Patel et al., 1989)

revealed a high degree of homology and allowed analysis of their binding activities and expression pattern.

While GR shows a very widespread expression and is found in almost every cell, prominent sites of glucocorticoid action are the liver, the lung, the brain and the immune system (Cole et al., 1993). In contrast, MR expression is much more restricted and predominantly found in the distal segments of the renal tubuli but also in the colon, the sweat and salivary glands and certain structures of the brain (Arriza et al., 1988; Zennaro et al., 1997).

Although both receptors are able to bind each of the two ligands, GR binds corticosterone (K_D ~ 5nM) with a tenfold higher affinity than aldosterone (K_D ~ 50nM) (Funder, 1992). Therefore, GR is expected to be occupied predominantly by glucocorticoids under physiological circumstances due to the considerably higher plasma concentration of corticosterone (0.5-50nM) compared to aldosterone (0.1-0.5nM).

In contrast, MR shows similar affinities for both corticosteroids (K_D ~0.5nM) and the affinity of MR for glucocorticoids is about one order of magnitude higher than that of GR to its preferred ligand corticosterone. Thus, MR does not exhibit intrinsic specificity for aldosterone but is protected by a pre-receptor mechanism from the higher plasma glucocorticoid levels. To allow exclusive mineralocorticoid activity, aldosterone target tissues such as the distal segments of the renal tubuli or the colon express the enzyme 11β-hydroxysteroid-dehydrogenase type 2 (11βHSD2) which converts corticosterone into the receptor-inactive 11-dehydrocorticosterone (Albiston et al., 1994; Funder et al., 1988).

3.3.2. Functional domains of the glucocorticoid receptor

Similar to other nuclear receptors, the GR as well as its close homologue MR are composed of several domains and subdomains, depicted in Figure 3. For the corticosteroid receptors, six different domains were described and denoted A to F from the aminoterminal to the carboxyterminal end. Three major functional units can be classified: the aminoterminal transactivation domain AF1 (TAD), the DNA-binding domain (DBD) and the carboxyterminal ligand-binding domain (LBD) (Beato et al., 1995; Beato and Klug, 2000).

The AF1 domain comprises the domains A and B and is a ligand-independent, constitutive activation domain. The transactivation domain performs specific

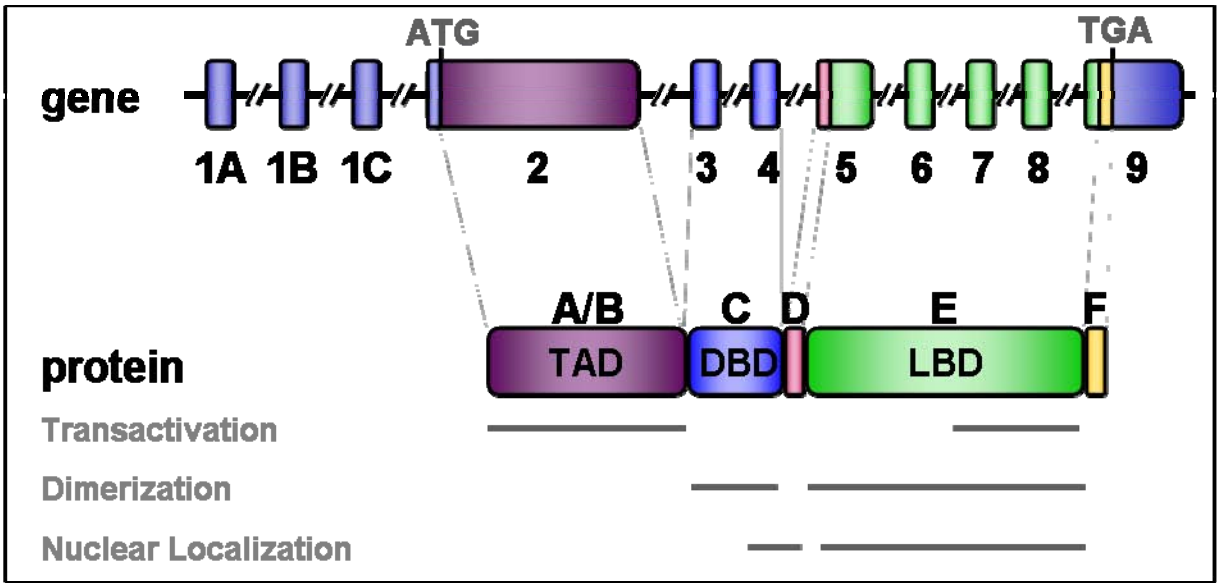

Figure 3: Functional domains of the glucocorticoid receptor

The GR gene comprises nine exons. Exon 2 contains the start codon (ATG) and encodes the domain A/B which forms the aminoterminal transactivation domain (TAD). Exons 3 and 4 encode the DNA binding domain (domain C, DBD) containing two zinc finger motifs and the dimerization domain. The hinge domain (D) connects the DBD with the ligand-binding domain (domain E, LBD) encoded by exons 5 to 9. Nuclear localization sequences are found in domain D and E and the LBD contains a second transactivation as well as a second dimerization domain.

interactions with other transcription factors and components of the basal transcription machinery allowing promotor and cell type-specific activation of receptor-mediated transcription.

The central DBD (domain C) consists of two zinc finger motifs characterized by a zinc ion which is complexed by four cystein residues (Luisi et al., 1991; Umesono and Evans, 1989). The DBD recognizes and binds to specific palindromic DNA sequence motifs, called glucocorticoid response element (GRE). The aminoterminal zinc finger has been shown to define the hormone response element recognized by the receptor since replacement by the zinc finger of another steroid hormone receptor changes the specificity of DNA binding (Green et al., 1988). The crystal structure of the GR DNA-binding domain bound to DNA revealed that three specific amino acids within one α-helix of the first zinc finger form the P-box which provides DNA sequence-specific binding to the GRE in the major groove of the DNA helix (Mader et al., 1989). The second zinc finger binds non-specifically to the minor groove of the DNA helix stabilizing the interaction of the DBD with the GRE. Moreover, it harbours the D-box comprised of five amino acids which are important for the formation of GR homodimers and thus cooperative high affinity binding of GR dimers at the GRE (Beato, 1989; Luisi et al., 1991). The hinge region (domain D) connects the DBD with

the LBD, contains a nuclear localization sequence and mediates conformational changes of the steroid hormone receptors upon ligand binding.

The carboxyterminal LBD (domain E) forms a pocket with the ligand binding site which provides the specificity and selectivity of steroid hormone binding. In addition, it contains a ligand-dependent transactivation domain and sequences important for dimerization and nuclear localization as well as interactions with either chaperones or other transcription factors (Beato and Klug, 2000). No specific function has been described for domain F so far.

3.3.3. Molecular action of the glucocorticoid receptor

Due to their lipophilic character, glucocorticoids diffuse freely through the cell membrane to the cytosol where they bind to GR. In the absence of the ligand, the receptor is part of a large heteromeric complex which prevents it from entering the nucleus but also supports an optimal conformation for high-affinity ligand binding (Morishima et al., 2003; Pratt and Toft, 2003). A number of chaperones and cofactors participate in the formation of this complex, for instance hsp90, hsp70, Imunophilins, FKBPs, CyP-40 and p23 (Gehring, 1993; Pratt and Toft, 1997). Binding of the hormone induces a conformational change of the receptor resulting in dissociation of the receptor from the protein complex and exposure of the nuclear localization sequences, the dimerization domains and the DNA binding domain. This activated state of the receptor allows importin α and β to mediate translocation into the nucleus where GR binds to GREs within the regulatory regions of target genes (Freedman and Yamamoto, 2004). The glucocorticoid, mineralocorticoid, progesterone and androgen receptors all recognize the identical DNA sequence, which does therefore not confer specificity of the hormone response. The consensus sequence for dimeric high-affinity binding of the receptors is a palindromic 15bp sequence (GGRACAnnnTGTYCT, where Y is a pyrimidine and R a purine base). Once bound to its response element, GR interacts with the basal transcription machinery and various cofactors to enhance the expression of the regulated gene.

Apart from this classical direct transactivation activity as a homodimer, GR can also participate in the regulation of target genes by multiple modes of interaction with other transcription factors. According to the molecular mechanisms involved the following types of interactions can be distinguished:

First, composite response elements bind both, GR and another transcription factor, leading to crosstalk which may be positive or negative. For example, GR and cAMP response element binding protein (CREB) co-operate on the promotor of the phosphoenolpyruvate-carboxykinase, mutually enhancing their binding and transactivation activity (Imai et al., 1993). Adding another level of complexity, the result of GR interaction with the dimeric transcription factor AP-1 in some cases depends on the particular subunit composition: While it enhances the transcriptional activation of c-Jun homodimers on the mouse proliferin gene, GR represses the induction of the same gene by c-Jun/c-Fos heterodimers (Diamond et al., 1990).

In the second case of overlapping response elements, transcription factor binding sites share common sequences and thus, binding of one factor precludes the interaction of the other with its cognate binding site. GR-mediated repression of the osteocalcin gene by blocking the interaction of TFIID of the general transcription machinery with the TATA box is one example for this mode of action (Stromstedt et al., 1991).

Third, according to the tethering mechanism, GR modulates gene expression independent from DNA-binding by interacting with another transcription factor which is bound to DNA or *vice versa*. In most cases, this crosstalk results in repression and has therefore been named trans-repression. For instance, GR blocks AP-1-dependent induction of the genes for collagenase 1 and 3 (Kassel et al., 2004; Rogatsky et al., 2001) while AP-1 has also been described to inhibit GR-mediated transactivation on promotors containing only GREs (Schule et al., 1990). Similar observations were made for a number of other transcription factors such as NF-κB, Smad3 and 4, IRF3, PU.1/Spi1 or COUP-TFII (De Martino et al., 2004; Gauthier et al., 1993; Luecke and Yamamoto, 2005; Reily et al., 2006; Song et al., 1999). Nevertheless, co-operation of GR and Stat5 exemplifies that tethering interactions can result in positive synergistic action as well. Recently, the *in vivo* relevance of this mechanism has been demonstrated in mice lacking GR and/or Stat5 specifically in the liver. A subset of hepatic Stat5 target genes strictly depends on GR-Stat5 interaction and this positive crosstalk was shown to be indispensible for normal postnatal growth (Engblom et al., 2007).

Finally, interaction of GR with other transcription factors can also be independent from DNA binding and lead to sequestration of both factors away from their

respective binding sites or even to the proteasome as in the case of GR and p53 (Sengupta et al., 2000; Sengupta and Wasylyk, 2001).

Although GR and MR both bind glucocorticoids under physiological conditions and recognize the same HREs, they are able to elicit receptor-specific responses by differential interaction with additional transcription factors (Arriza et al., 1988; Rupprecht et al., 1993). Thus, the specificity of GR transactivation activity depends on the individual combination of transcription factor binding sites in the promotor/enhancer elements of target genes as well as the differential and cell type-specific expression of the interacting transcription factors (Pearce and Yamamoto, 1993).

3.4. Analysis of GR function *in vivo*

3.4.1. GR mutant mice

Many initial studies of GR function relied either on pharmacologic interference with the receptor or adrenalectomy with subsequent hormone replacement. However, antagonists often provide only incomplete blockade and the implication of unspecific effects is difficult to exclude. Adrenalectomy, on the other side, removes in addition to glucocorticoids also mineralocorticoids and catecholamines, thus impairing direct association of the observed effects with GR function only. To circumvent these caveats, mouse models were implemented which took advantage of genetic inactivation of the GR gene.

Two distinct mutations leading to germ-line inactivation of the GR gene have been reported. The first approach targeting exon 2 was later shown to allow the expression of a truncated protein due to alternative splicing and this allele was therefore termed hypomorphic (Cole et al., 1995; Mittelstadt and Ashwell, 2003). The null allele, in contrast, was generated by deletion of exon 3 and results in complete ablation of GR protein expression overcoming the incomplete penetrance observed in the hypomorphic allele (Tronche et al., 1998).

Mutant mice homozygous for the hypomorphic or the null allele (GR^{null}) die shortly after birth due to respiratory failure. They manifest a strong dysregulation of the HPA axis leading to elevated plasma levels for corticosterone as well as ACTH and consequently hyperplasia and hypertrophy of the adrenal cortex. Moreover, the hepatic induction of gluconeogenic enzymes was shown to be impaired and GR deficient thymocytes were resistant to glucocorticoid-induced apoptosis (Cole et al.,

1995). In the following, a number of conditional mutants has been generated using the Cre/loxP recombination system to analyze specific GR function in adult animals (see chapter 3.4.2.).

Moreover, a function-selective mutation has been established by introducing a point mutation into the dimerization domain of GR (GR^{dim} mice). This alteration selectively perturbs homodimeric binding of GR to its cognate response elements while the modulation of gene expression via protein-protein interaction is preserved (Heck et al., 1994). Surprisingly, this mutation did not impair survival highlighting the importance of DNA-binding independent GR functions (Reichardt et al., 1998). Whereas established GRE-dependent target genes such as tyrosine aminotransferase were non-responsive to glucocorticoid stimulation, important anti-inflammatory activities mediated by protein-protein interaction were maintained.

3.4.2. Conditional gene inactivation using the Cre/loxP recombination system

Early lethality of knockout mice and pleiotropic functions in different organs have complicated the analysis of gene function in the adult organism in the case of the GR but also a number of other genes. The two components of the Cre/loxP recombination system allow inactivation of a gene of interest in a cell type- or tissue-specific manner (Figure 4A). First described in P1 bacteriophages, it employs the Cre recombinase which recognizes and mediates recombination of DNA molecules containing specific palindromic motifs called loxP sites (Gu et al., 1994). The flanking of an essential part of the gene of interest with these loxP sites in the same direction allows Cre-mediated recombination and hence gene inactivation. Cell type-specific ablation of a desired gene is achieved by the expression of the Cre recombinase under control of specific regulatory elements (Nagy, 2000).

More recently, this system has been further advanced by the development of a fusion protein of the Cre recombinase with a mutated ligand binding domain of the estradiol receptor ($CreER^{T2}$; Figure 4B). The latter retains the fusion protein in the cytoplasm, and only upon binding of the synthetic ligand tamoxifen it translocates into the nucleus, where it mediates the excision of the loxP-flanked DNA sequence (Feil et al., 1997; Kellendonk et al., 1999; Kellendonk et al., 1996; Weber et al., 2001). Appropriate application of tamoxifen in combination with specific regulatory elements to control Cre expression allows not only cell type-specific but also inducible inactivation of the gene of interest.

In the case of the conditional GR allele (GR^{flox}), exon 3 encoding the first zinc finger of the DNA binding domain has been flanked by loxP sites. Importantly, GR expression remains unaffected in the absence of the recombinase whereas Cre-mediated excision results, if splicing occurs from exon 2 to exon 4, in a frame shift of the coding sequence which results in ablation of GR protein expresion (Berger et al., 2006; Tronche et al., 1999).

Originally, short promotor/enhancer fragments of genes with desired expression pattern have been cloned in front of a Cre cassette to drive the expression of the Cre recombinase (Mantamadiotis et al., 2002; Tronche et al., 1999; Tsien et al., 1996). However, these plasmid-derived transgenes often show copy number-independent, mosaic or ectopic expression (Otto et al., 2001; Shimshek et al., 2005). Since the development of the recombineering technology, the use of BAC (bacterial artificial chromosome)- or YAC (yeast artificial chromosome)-derived transgenes has therefore become the method of choice (Copeland et al., 2001; Lee et al., 2001; Muyrers et al., 1999; Zhang et al., 1998). In contrast to plasmids, these vectors harbor large genomic regions containing almost all regulatory elements of the gene locus that was chosen to drive Cre expression. Accordingly, this results in faithful cell type-specific and copy number-dependent Cre expression (Muyrers et al., 1999; Schedl et al., 1993b).

Further illustrating the pleiotropic functions of this receptor, conditional GR mutants have been employed in a variety of studies. Mice with prenatal onset of GR deficiency in neurons and glial cells showed a strongly activated HPA axis which caused Cushing-like symptoms including altered fat distribution and reduced bone density. In addition, the mutant mice displayed reduced anxiety (Tronche et al., 1999). As mentioned before, mice lacking GR specifically in hepatocytes have been used to investigate GR functions in the control of metabolism and postnatal growth signalling (Engblom et al., 2007; Tronche et al., 2004). Finally, different cell types of the immune system have been targeted leading to advanced understanding of glucocorticoid action in inflammation and therapy (Kleiman and Tuckermann, 2007).

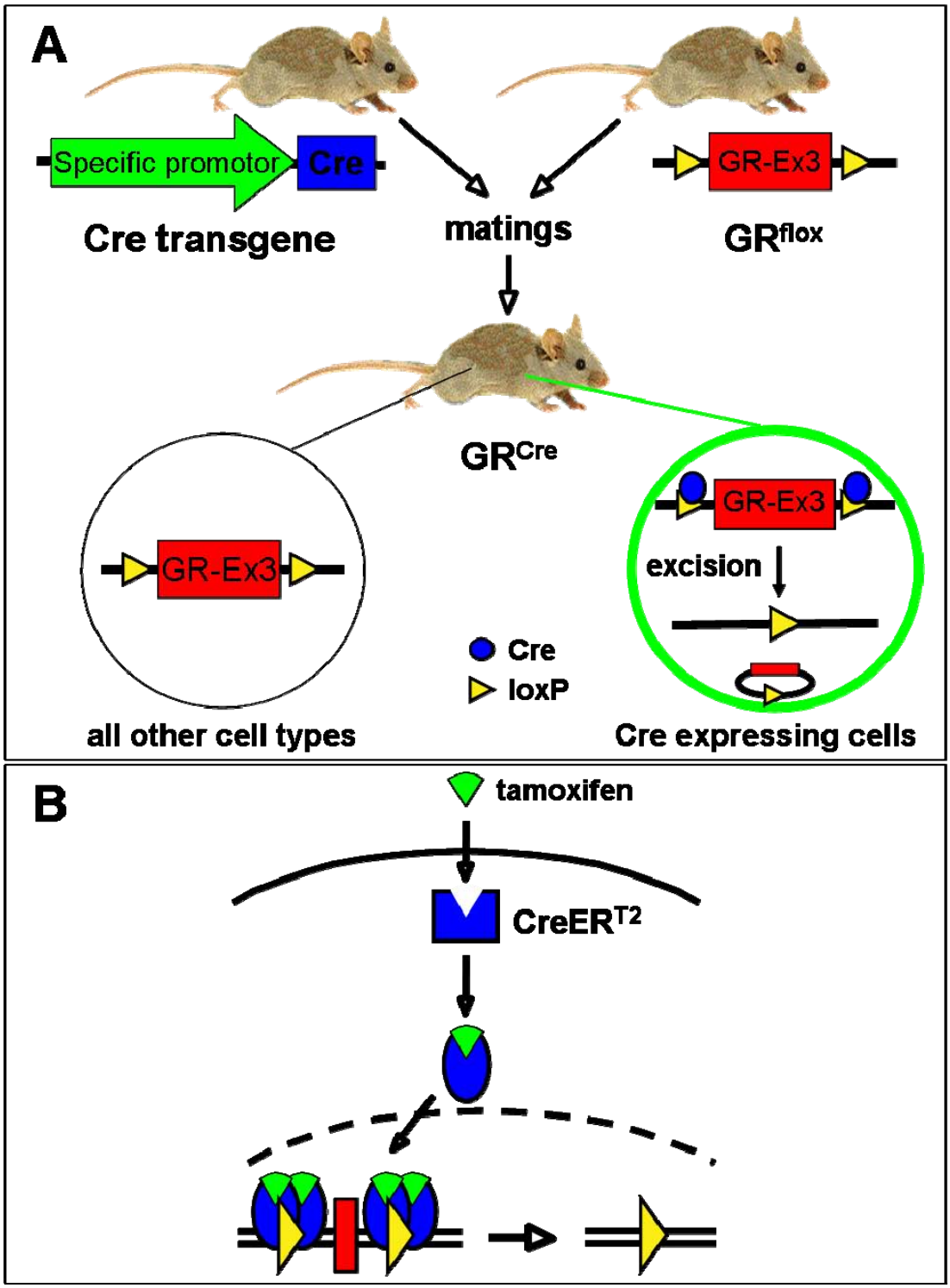

Figure 4: The Cre/loxP recombination system allows cell type-specific constitutive and inducible inactivation of a target gene

(A) To achieve cell type-specific gene inactivation with the Cre/loxP-recombination system, an essential part of a gene has to be flanked by loxP sequences without affecting the expression of the gene. The cell type/tissue-specific expression of the Cre recombinase under control of specific regulatory elements results in deletion of the loxP-flanked part and thereby in gene inactivation only in these Cre-expressing cells. (B) The Cre/loxP-recombination system has been advanced with the tamoxifen-inducible fusion protein consisting of the Cre recombinase and the mutated ligand binding domain of the human estrogen receptor ($CreER^{T2}$) to achieve ligand-dependent Cre activity. The unliganded form of the $CreER^{T2}$ fusion protein resides in the cytoplasm and upon tamoxifen binding it translocates into the nucleus and mediates site-specific recombination of the loxP-flanked DNA sequence.

3.5. Aim of the thesis

Clinical application and animal experiments provide ample evidence for an important role of the GR-mediated glucocorticoid signalling during murine lung development. In line with this, previous studies in our lab showed that mice with a germline inactivation of the GR gene die postnatally due to respiratory failure. In contrast, mice carrying a point mutation in the GR gene which prevents DNA binding of the receptor as a homodimer survive. These findings indicated that the essential functions of GR during murine lung development are mediated via protein-protein interactions.

The aim of the present study was to further elucidate these modes of action using the Cre/loxP recombination system for conditional inactivation of the GR gene. To identify the cell types mediating the critical glucocorticoid effects during murine lung development, a series of mutants was generated lacking GR specifically in the mesenchyme, endothelial cells or the lung epithelium, respectively.

Beneficial effects of corticosteroids for lung maturation have commonly been attributed to their ability to induce the functional maturation of lung epithelial cells including the synthesis of surfactant. Therefore, we took advantage of a mouse line expressing the Cre recombinase under control of a 3.7kb promotor of the human Sftpc gene (Spc-Cre) to generate mice lacking GR specifically in lung epithelial cells. In the course of these experiments, this mutation was shown not to impair survival of the mice, pointing towards an important role of GR in the mesenchyme. To verify this assumption, mice lacking GR specifically in mesenchymal cells were generated. This was achieved using a transgenic mouse line which expresses the Cre recombinase from a BAC containing the regulatory elements of the collagen type (I)-alpha 2 locus. To assess the participation of GR in the regulation of vascular development in the lung, a Tie2-Cre line was finally employed to inactivate GR specifically in endothelial cells.

The mutant animals were analyzed by a series of methods including histology, immunohistochemistry and gene expression profiling to investigate glucocorticoid effects in specific cell types. The resulting findings should further contribute to the understanding of the mechanisms behind the essential GR effects during lung development and may help to identify potential interaction partners.

4. Results

4.1. Generation of a lung epithelium-specific Cre line (mSftpc-Cre)

To allow conditional recombination specifically in lung epithelial cells of the mouse, a BAC-derived transgene was generated expressing the codon-improved Cre recombinase (Shimshek et al., 2002) under control of the regulatory elements of the mouse gene for the surfactant-associated protein C (mSftpc). The BAC RP24-252D18 was selected from the NCBI CloneFinder and contained a genomic insert including ~80kb upstream as well as ~80kb downstream of the mSftpc gene. Homologous recombination in bacteria was used to insert the sequence encoding the Cre recombinase at the ATG into the reading frame of the mSftpc locus (Figure 5A) (Lee et al., 2001).

In the applied targeting construct, two homology arms flanked the coding sequence of the Cre as well as a cassette containing an ampicillin resistance gene in between two FRT recognition sites for the Flp recombinase. At the 3'end of the 5'homology arm, the ATG of the mSftpc gene was cloned in frame with the sequence encoding the Cre recombinase while the 3'homology arm started at its 5'end with the first intron of the mSftpc gene.

The linearized targeting construct was electroporated into competent bacteria of the EL250 strain (Lee et al., 2001) containing the BAC, and clones showing ampicillin resistance were analyzed for correct recombination by analytical restriction digestion. The ampicillin resistance cassette was subsequently removed by induced expression of the Flp recombinase, before the integrity and correct modification of the genomic insert were confirmed by pulse-field gel electrophoresis as well as Southern Blot analysis (Figure 5B). The BAC backbone was removed by NotI digestion, and the modified genomic insert was isolated using a gel filtration column (Figure 5C). Finally, the construct was introduced into the mouse germline by pronuclear injection (Schedl et al., 1993a).

Analysis of the potentially transgenic progeny by Dot Blot and PCR identified three mice carrying the mSftpc-Cre transgene (Figure 5D). However, none of these was able to generate transgenic offspring, thus precluding further analysis as well as any application of the mouse line.

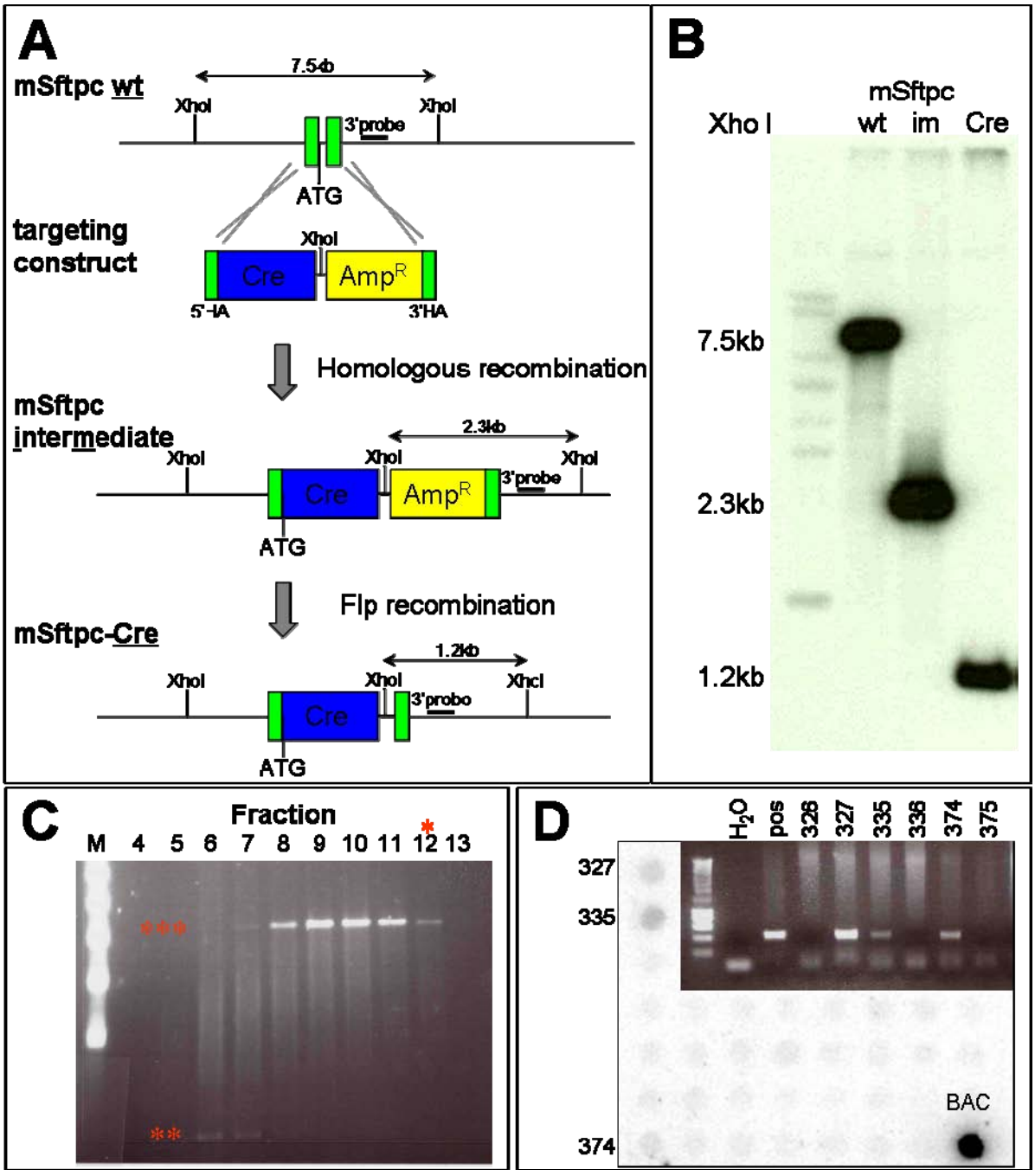

Figure 5: Generation of a transgenic mouse line expressing the Cre recombinase from a BAC containing the mSftpc locus

A) Using homologous recombination in bacteria, a cassette encoding the Cre recombinase was inserted in frame with the ATG of the mSftpc gene contained in the BAC RP24-252D18. After identification of homologous recombinant clones (mSftpc intermediate) the ampicillin resistance cassette was removed by Flp recombination. B) Southern blot was performed to confirm the correct modification of the BAC using a probe recognizing a sequence in the 3' homology arm as represented in A. Band sizes are indicated and reflect the XhoI fragments depicted in A. C) Subsequently, the genomic insert of the BAC was released by NotI digestion and purified on a gel filtration column. Samples of the fractions were analyzed by pulse field gel electrophoresis and fraction 12 (*) was used for pronuclear injection. ** and *** mark the sizes of the BAC backbone (~15kb) and the modified genomic insert (~160kb), respectively. D) Three animals carrying the mSftpc-Cre transgene were identified by DotBlot and PCR (insert).

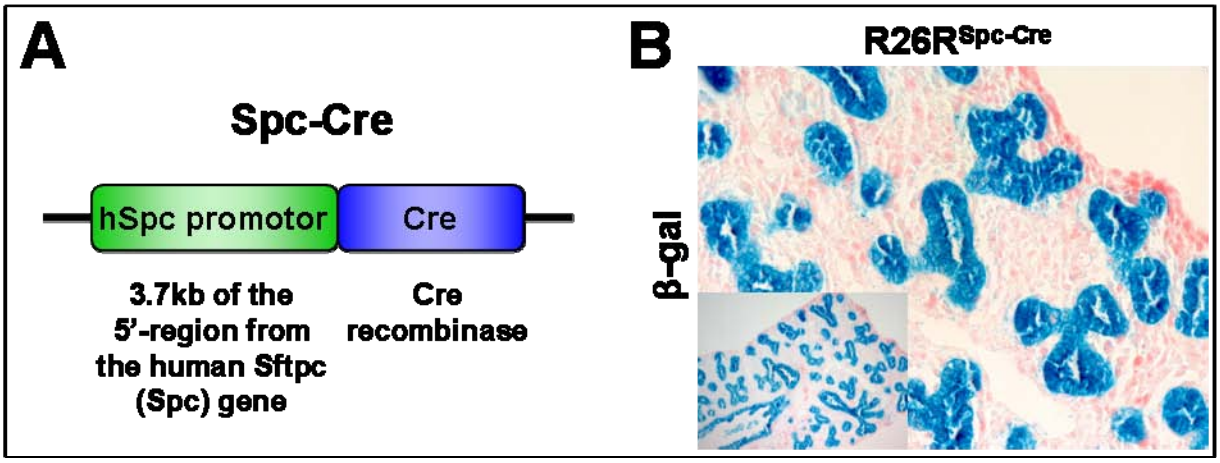

Figure 6: The plasmid-based Spc-Cre transgene mediates lung epithelium-specific recombination

A) 3.7kb of the 5'-flanking region of the human Sftpc gene are used to drive Cre expression. B) Faithful recombination in the lung epithelium by the Spc-Cre line was verified using whole mount β-galactosidase staining of E16.5 $R26R^{Spc\text{-}Cre}$ lungs. Paraffin sections were prepared of these specimens and lightly counterstained with eosin. Prominent blue staining is observed throughout all epithelial cells.

Yet, in the course of these experiments, another lung epithelium-specific Cre line was published and became available (Okubo and Hogan, 2004). This transgenic line exploits a well characterized 3.7kb promotor of the human Sftpc gene to drive Cre expression (Figure 6A) (Glasser et al., 1991; Wert et al., 1993). The Spc-Cre line was obtained by Brigid Hogan, and the specific recombination pattern was verified using a Rosa26 Cre reporter mouse (Soriano, 1999). This line carries a knock-in of the β-galactosidase preceded by a stop cassette in the Rosa26 locus. Since the stop cassette is flanked by two loxP sequences, Cre activity results in its excision and thereby allows expression of the β-galactosidase. As expected, animals positive for the Cre reporter as well as the Spc-Cre transgene showed strong β-galactosidase activity in the entire population of lung epithelial cells at all stages analyzed (from E16.5, depicted in Figure 6B, to E18.5, data not shown). Consequently, this line was employed for all further experiments to ablate GR in lung epithelial cells.

4.2. Lung epithelium-specific loss of GR does not impair survival

Mice lacking GR specifically in lung epithelial cells were generated using the Cre/loxP system. To this end, Spc-Cre mice expressing the Cre recombinase under control of the human Sftpc promotor were intercrossed with GR^{flox} animals. Genotyping of litters containing $GR^{flox/flox}$/Spc-Cre ($GR^{Spc\text{-}Cre}$) mice at weaning revealed the presence of all genotypes with the expected frequency (Figure 7A). This

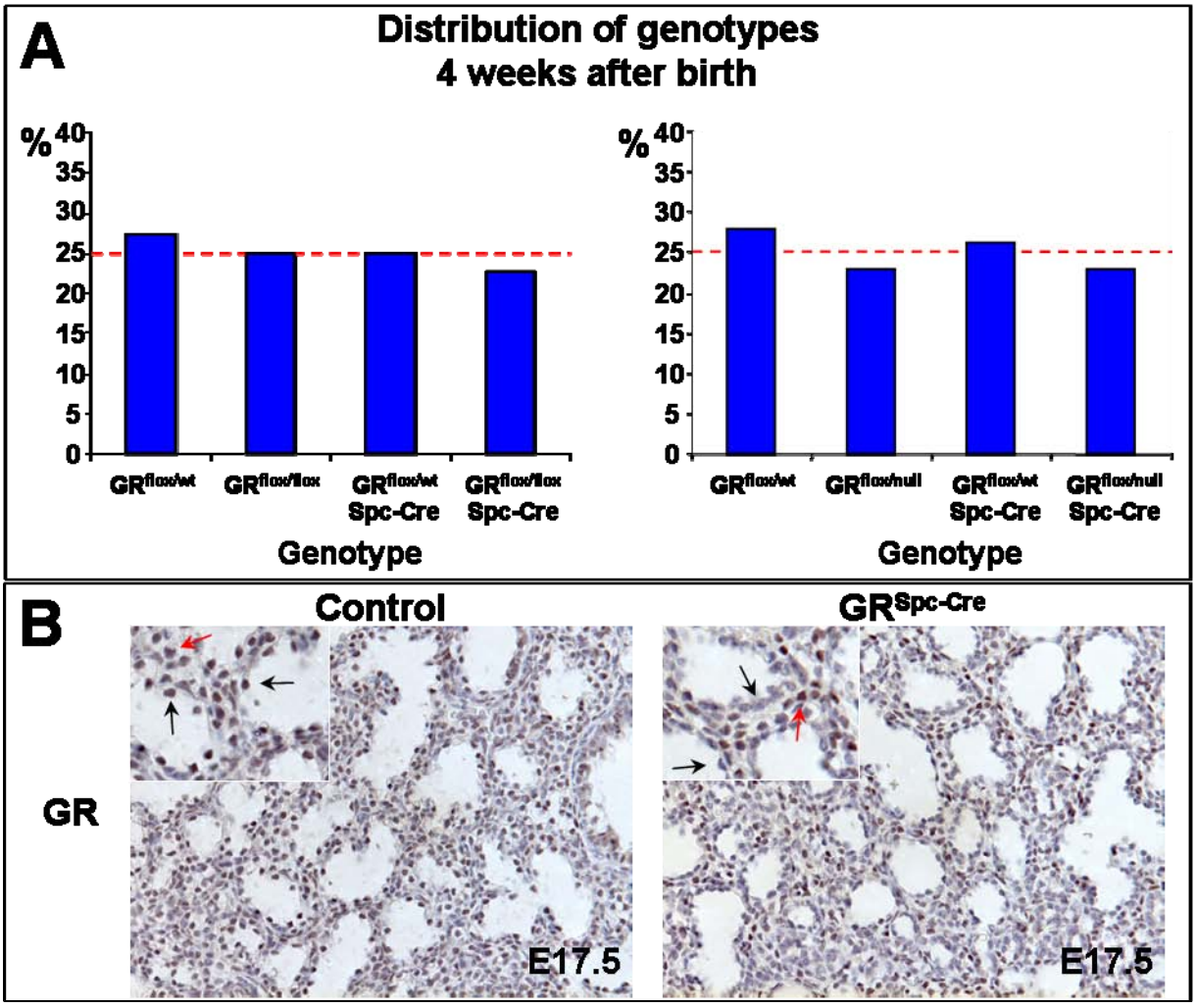

Figure 7: Lung epithelium-specific loss of GR does not impair survival

A) Genotypical analysis after weaning of offspring containing the genotypes $GR^{flox/flox}$/Spc-Cre (left hand side) or $GR^{flox/null}$/Spc-Cre (right hand side) - n~50, respectively. The litters contained all expected genotypes in mendelian frequencies. B) Immunohistochemistry for GR on 6µm paraffin sections demonstrated lung epithelium-specific protein loss in $GR^{Spc-Cre}$ animals. E17.5 lungs of control animals showed strong epithelial staining for GR protein (black arrows) compared to lower intensity in the mesenchyme (red arrow). In contrast, $GR^{Spc-Cre}$ lungs displayed immunoreactivity only in mesenchymal cells (red arrow) while no GR protein was detected in the epithelium (black arrows).

indicates that inactivation of the GR gene in lung epithelial cells did not impair survival.

To confirm the efficacy of the employed gene ablation system, GR immunohistochemistry was performed on paraffin sections from embryonic lungs at E17.5 when epithelial and mesenchymal cells are easy to distinguish (Figure 7B). As expected, control littermates showed strong GR expression in epithelial cells compared to lower immunoreactivity in the mesenchyme. In contrast, GR staining was absent in the epithelium of $GR^{Spc-Cre}$ mutant mice while expression was preserved in mesenchymal cells. Thus, efficient conditional gene inactivation was achieved in epithelial cells of $GR^{Spc-Cre}$ mice.

In an additional attempt to further reduce the GR dosage in the residual GR expressing cells of the mesenchyme, mice were generated carrying the Spc-Cre transgene in combination with one conditional GR^{flox} and one GR^{null} allele ($GR^{null/flox}$/Spc-Cre). $GR^{null/+}$/Spc-Cre mice were intercrossed with $GR^{flox/flox}$ animals and the resulting litters were genotyped at weaning. PCR analysis revealed that all expected genotypes were observed with mendelian frequency, including $GR^{null/flox}$/Spc-Cre mice (Figure 7A). This demonstrates that even a single intact GR allele in the mesenchyme suffices to complete lung development in the absence of epithelial GR.

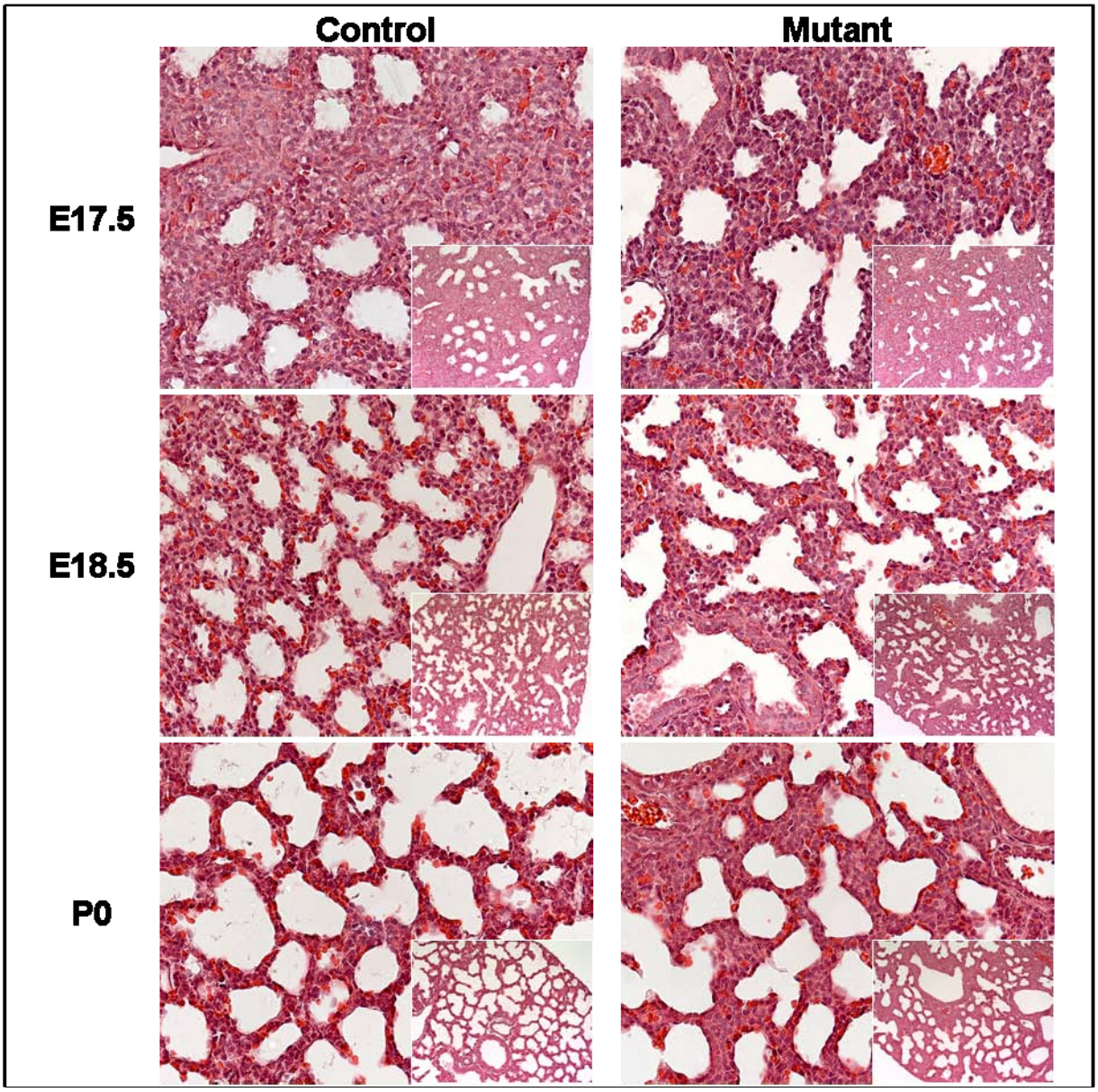

Figure 8: Lung morphogenesis in $GR^{Spc-Cre}$ embryos

HE staining of 4.5µm paraffin sections from $GR^{Spc-Cre}$ and control lungs collected at the indicated day. Mutant animals show a delay in the tubular dilation as well as the thinning of the alveolar septae and are characterized by mesenchymal accumulations at P0.

4.3. Lung epithelium-specific loss of GR transiently delays lung maturation

The effects of lung epithelium-specific inactivation of the GR gene on late lung development were further analyzed. Hematoxylin eosin (HE) staining of paraffin sections illustrates the morphogenetic progress of $GR^{Spc\text{-}Cre}$ lungs compared to those of littermate control mice (Figure 8). Mutant animals display less dilated alveolar saccules and correspondingly a higher frequency of unexpanded rosettes. At E18.5 and P0, their lungs are also characterized by a higher incidence of regions with mesenchymal accumulation compared to control animals.

Electron microscopy demonstrates that the thinning of the alveolar septae is incomplete in $GR^{Spc\text{-}Cre}$ animals at E18.5 resulting in an increased thickness of the

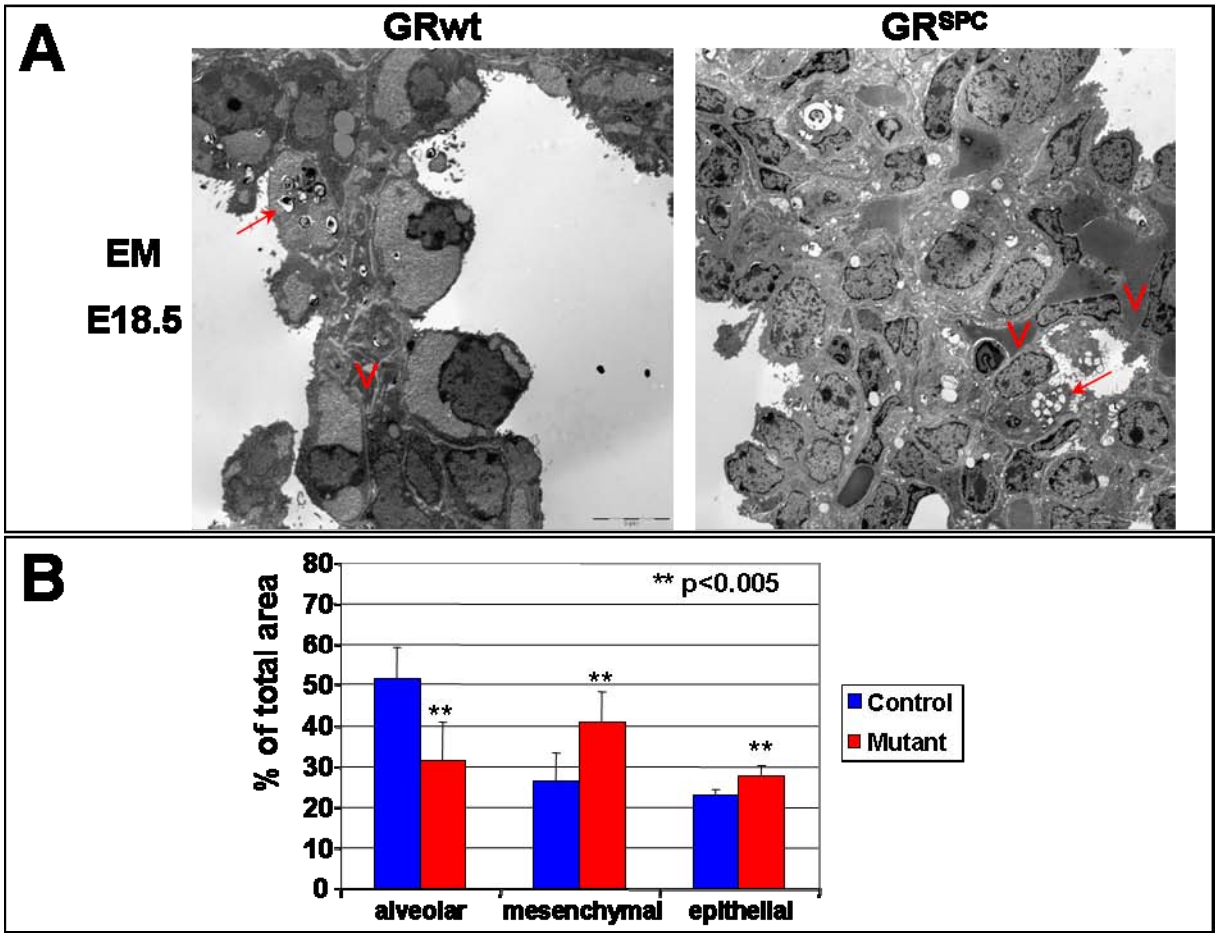

Figure 9: $GR^{Spc\text{-}Cre}$ lungs display increased thickness of the alveolar septae at the expense of alveolar airspace

A) Electon microscopy of mutant and control lungs shows an increased thickness of the alveolar septae in $GR^{Spc\text{-}Cre}$ mice. Nevertheless, the epithelium attenuates and comes in close apposition with the capillary system (V indicates vessels). Surfactant-containing lamellar bodies are also observed (arrows) indicating proper functional maturation of alveolar type II cells. B) Morphometric measurements were performed on semi-thin sections and the percentage of the total area was determined for the alveolar, mesenchymal and epithelial compartments. Compared to controls, the alveolar compartment is reduced in mutant lungs while the mesenchymal compartment is increased. The epithelial compartment also shows a small but significant increase.

alveolar walls (Figure 9A). Finally, morphometric measurements on semi-thin sections revealed a significant reduction of the alveolar area at the expense of the mesenchymal compartment (Figure 9B).

Nevertheless, these techniques also demonstrated that the functional maturation of the alveolar gas exchange unit is not critically impaired in $GR^{Spc\text{-}Cre}$ mice. During this process, the epithelium flattens and comes in close apposition with the endothelium of the underlying capillary system. These findings were additionally substantiated by histological examination of differentiation markers such as proSpc, T1α or glycogen revealing no significant difference in staining pattern in mutant compared to control animals (data not shown).

To investigate whether the observed retardation in lung development was of transient nature or persistent as incomplete maturation, pregnant mothers were injected with progesterone to prolong the pregnancy. Embryos were collected at E20.5 (~1.5 days beyond the expected delivery) and lung morphology was analyzed using HE staining (Figure 10). $GR^{Spc\text{-}Cre}$ lungs were virtually indistinguishable from controls and both genotypes demonstrated a progression to the alveolar stage of murine lung development. This phase of final alveogenesis is characterized by the formation of secondary septae, visible as numerous small protrusions into the alveolar lumen. The associated rough appearance is observed in both, mutant and control animals, demonstrating that $GR^{Spc\text{-}Cre}$ mice overcome their morphogenetic delay and recover to normal progression through the final alveolar phase of murine lung development.

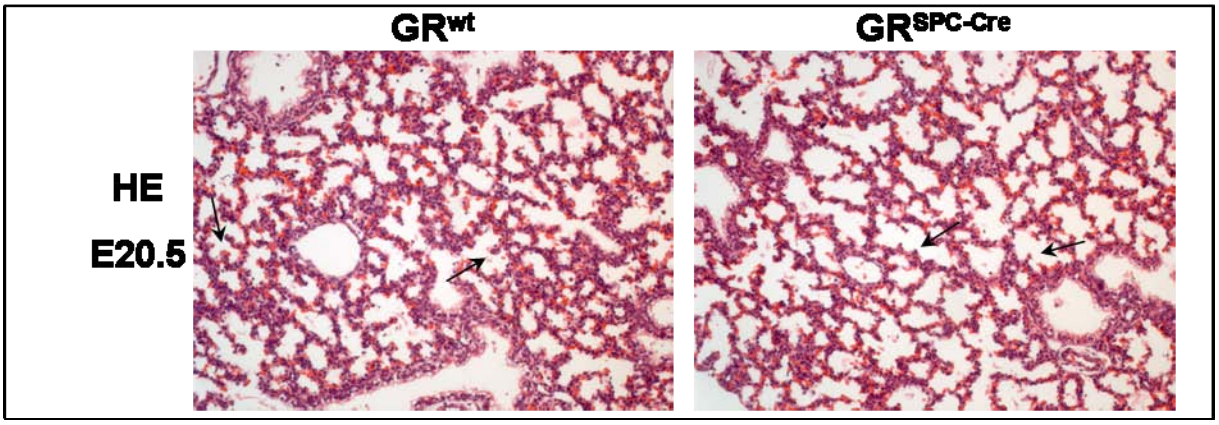

Figure 10: A prolonged pregnancy enables $GR^{Spc\text{-}Cre}$ embryos to compensate their developmental delay

Pregnancies were artificially prolonged by progesterone treatment. Mutant as well as control lungs progressed to the alveolar phase of murine lung development, indicated by formation of secondary septae which are visible as small protrusions into the lumen (arrows).

4.4. Inactivation of the GR gene in the mesenchyme leads to postnatal lethality

The results obtained by lung epithelium-specific inactivation of the GR gene in $GR^{Spc\text{-}Cre}$ mice indicated an important role of GR in the surrounding mesenchyme for fetal pulmonary maturation. In order to determine the contribution of mesenchymal GR to murine lung development, we employed a transgenic mouse line expressing the Cre recombinase from a BAC containing the locus of the collagen type (I)-alpha 2 gene (Col1-Cre) (Florin et al., 2004). The Cre transgene has been shown to mediate recombination in the mesenchyme and was crossed with GR^{flox} mice to obtain $GR^{flox/flox}$/Col1-Cre ($GR^{Col1\text{-}Cre}$) offspring. When the litters were genotyped after weaning, however, no mutant $GR^{Col1\text{-}Cre}$ animals were found pointing towards early lethality of these mice. Confirming this assumption, close inspection immediately after birth revealed that $GR^{Col1\text{-}Cre}$ neonates showed respiratory distress and cyanosis leading to death within the first hour of life.

Since the Col1-Cre transgenic mouse line has occasionally been reported to recombine unspecifically in the germline (P. Angel, personal communication) we sought to verify that GR was still expressed in non-targeted cells. Immunohistochemistry demonstrated persistent GR protein expression in the epithelium of P0 lungs from $GR^{Col1\text{-}Cre}$ animals which were compared to E17.5 control lungs due to their similarity in cellular morphology (Figure 11).

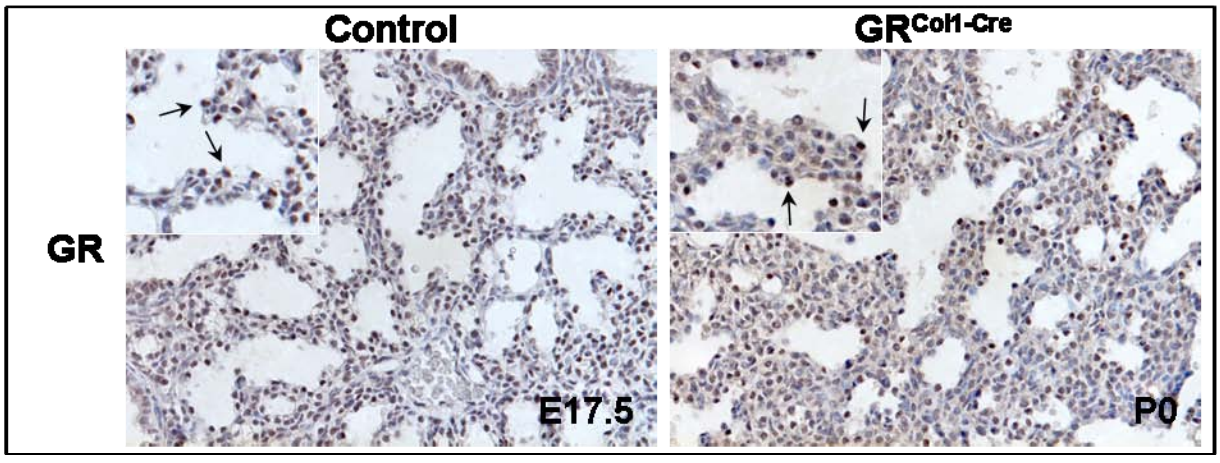

Figure 11: Persistent GR protein expression in epithelial cells of $GR^{Col1\text{-}Cre}$ embryos

6µm paraffin sections were stained with an antibody against GR and lightly counterstained with hematoxylin. Specimen from E17.5 control and P0 mutant embryos were compared due to their similarity in morphology. Persistent strong GR staining is observed in the epithelium of mutant lungs (arrows).

4.5. Loss of mesenchymal GR arrests lung development at the transition from the pseudoglandular to the canalicular phase and phenocopies the GR knockout mutation

Histological examination of embryonic lungs from $GR^{Col1\text{-}Cre}$ embryos and control littermates indicated that earlier lung development and branching morphogenesis were unaltered until E16.5 (data not shown). While control lungs subsequently further progressed through the canalicular and saccular phase, mutant lungs were still in the

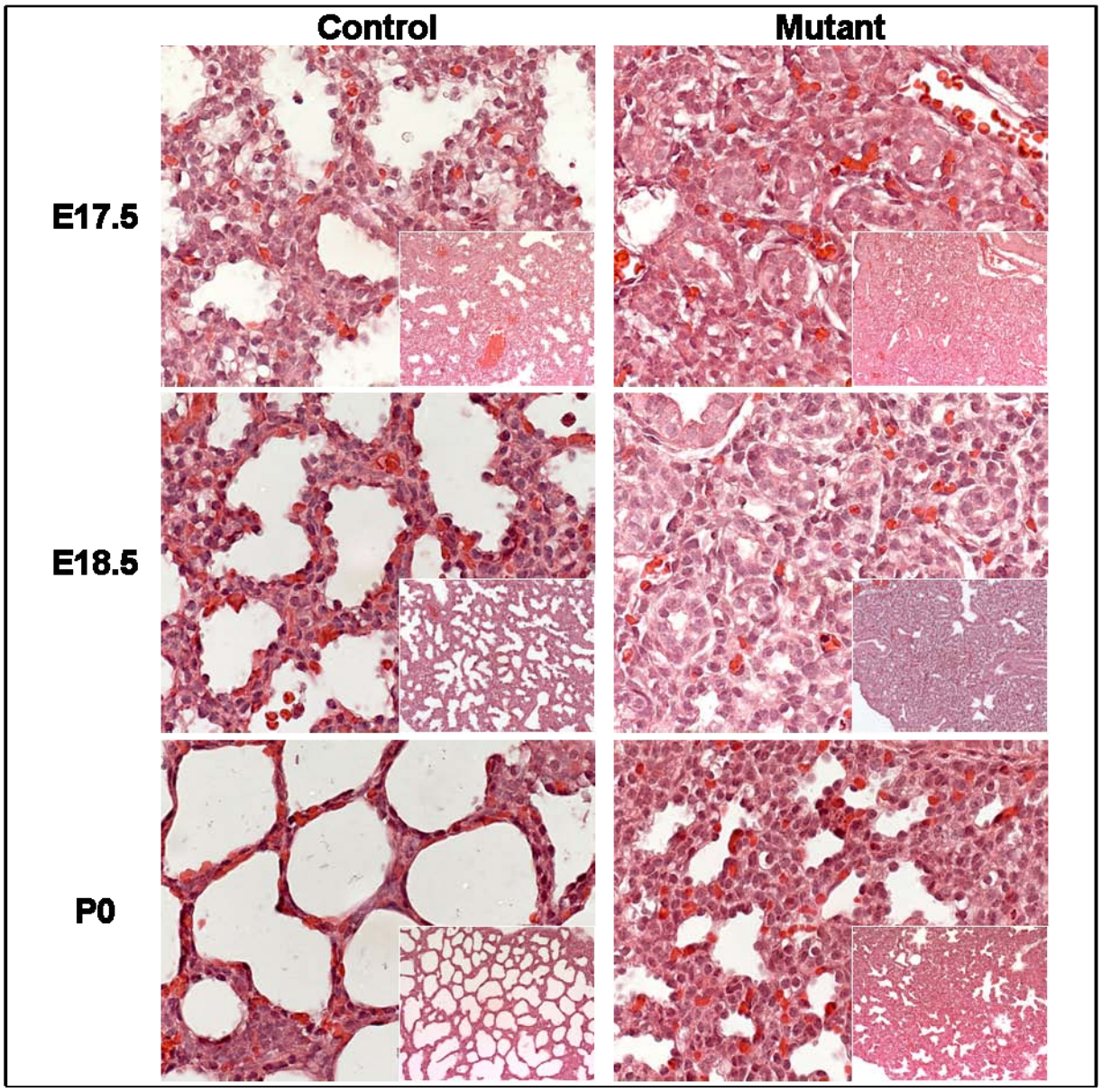

Figure 12: Lung morphogenesis in $GR^{Col1\text{-}Cre}$ embryos

HE stainings of 4.5µm paraffin sections from mutant and control lungs of the indicated age. Insets show a lower magnification overview. While control lungs display the normal morphogenetic development, mutant lungs remain in the pseudoglandular phase until E18.5. The respiratory tube does not dilate and is lined by immature cuboidal epithelial cells. At birth, $GR^{Col1\text{-}Cre}$ lungs show signs of the early canalicular phase visible as beginning dilation of the alveolar lumen in some areas but the alveolar septae remain thick and formation of the gas exchange unit is missing.

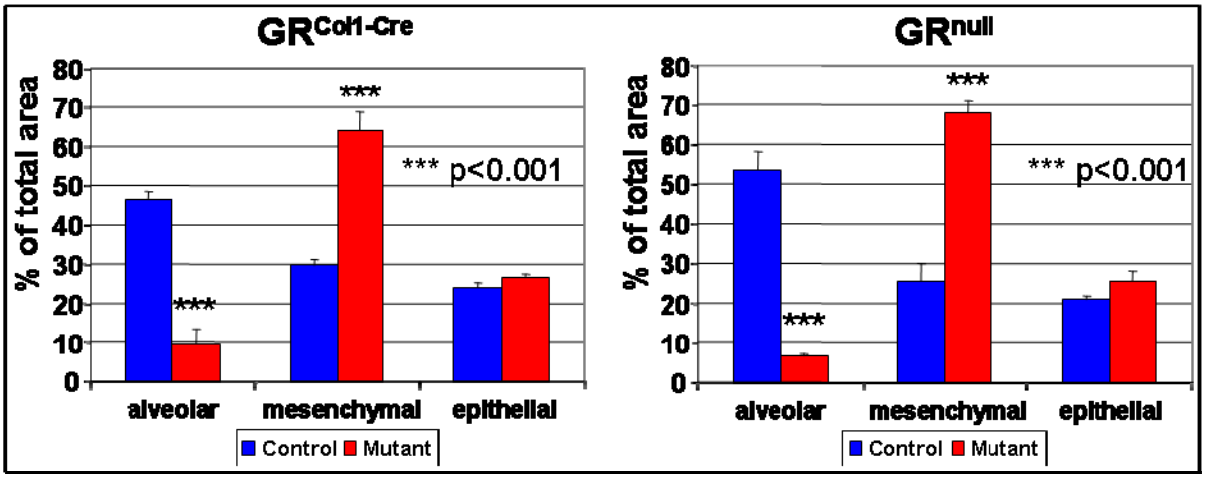

Figure 13: Morphogenetic phenotype of $GR^{Col1\text{-}Cre}$ animals

Morphometric measurements of E18.5 $GR^{Col1\text{-}Cre}$ and GR^{null} embryos as well as their respective littermate controls were performed on semi-thin sections. Both mutations lead to a similar strong and significant increase of the mesenchymal compartment at the expense of the alveolar compartment while the epithelium appears unaffected.

pseudoglandular stage at E18.5 (Figure 12). At this stage, alveolar space was virtually absent in $GR^{Col1\text{-}Cre}$ lungs and the mostly unexpanded rosettes were surrounded by thick mesenchyme. Figure 13 displays morphometric results of $GR^{Col1\text{-}Cre}$ and control lungs describing these findings in a quantitative manner. The alveolar compartment is strongly decreased to less than 10% of the total area whereas the mesenchyme expands to over 60%. In addition, these measurements were also performed on lungs from GR^{null} embryos and their littermates revealing the close quantitative similarity of the phenotypes observed in the conditional and the germ line mutation, respectively.

Periodic acid-Schiff (PAS) staining for the detection of glycogen as well as immunohistochemistry for T1α and proSPC demonstrated that the proximo-distal patterning of the respiratory tube was not affected in $GR^{Col1\text{-}Cre}$ animals (Figure 14). At E16.5, distal glycogen-rich epithelium could be clearly distinguished from proximal glycogen-free airways in mutant as well as control lungs. Moreover, both genotypes expressed the maturation-independent epithelial marker T1α at E18.5. However,

Figure 14 (next page): Proximo-distal patterning is unaffected in $GR^{Col1\text{-}Cre}$ animals

A) Violet periodic acid Schiff (PAS) staining visualizes the high glycogen content of the immature distal lung epithelium. At E16.5, both, controls and mutants show a clear separation of the distal glycogen-rich epithelium from the more proximal parts. Until birth, the staining becomes discontinuous in the alveolar sacs of controls while it appears in the larger airways. Although mutants preserve the glycogen pattern of the pseudoglandular phase until E17.5, they afterwards show a progressive loss of epithelial glycogen indicating an epithelial maturation which is advanced with respect to the morphological appearance. B) Immunohistochemistry for the epithelial differentiation marker T1α yields continuous staining of the epithelial cell layer in mutants as well as controls. C) Immunohistochemistry for the surfactant protein proSPC illustrates the retardation in epithelial differentiation. The transition from the continuous staining, which is still observed in the mutants at E17.5, to the punctual staining of the mature lung occurs with a delay of ~1-2 days.

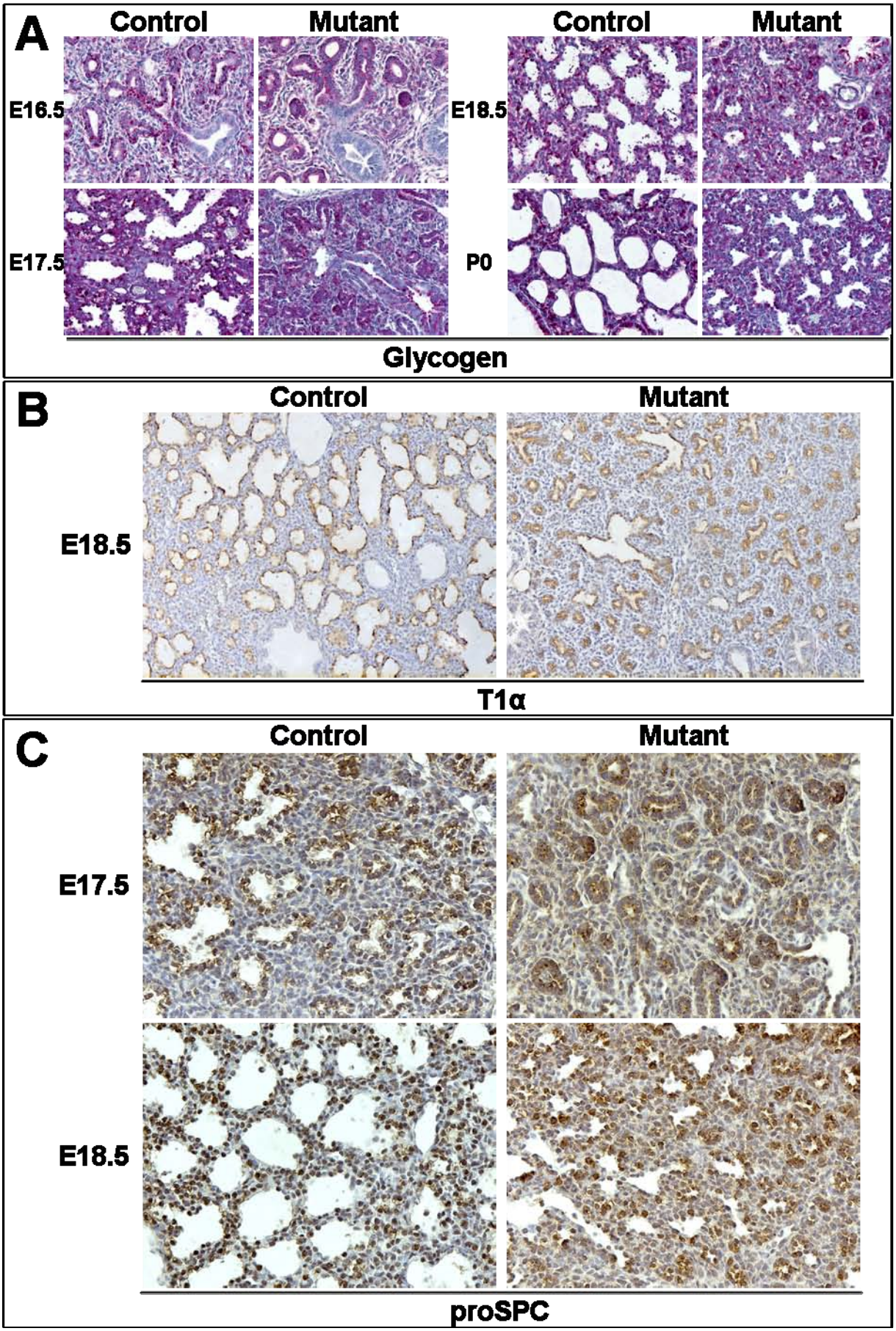
A
Control
Mutant
Control
Mutant
E16.5
E18.5
E17.5
P0
Glycogen
B
Control
Mutant
E18.5
T1α
C
Control
Mutant
E17.5
E18.5
proSPC

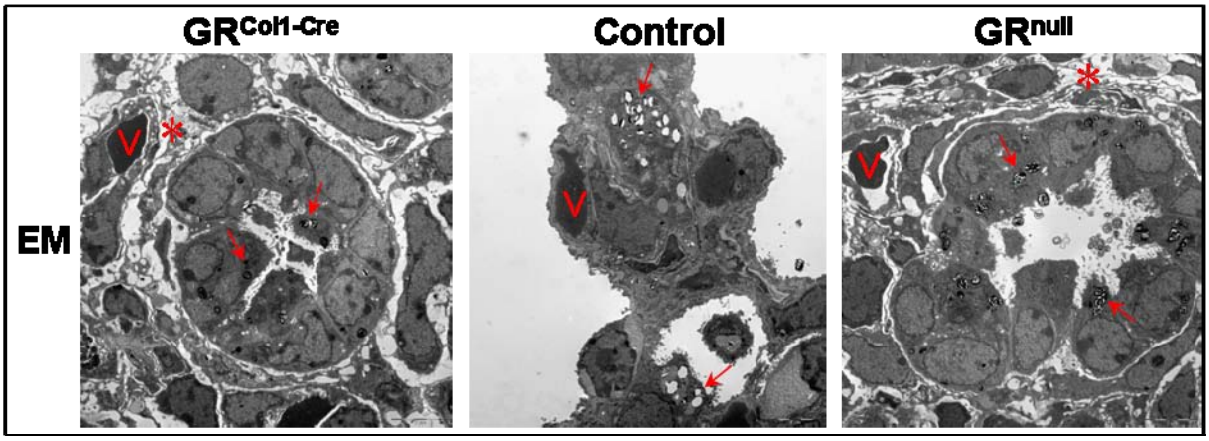

Figure 15: Ultrastructural phenotype of $GR^{Col1\text{-}Cre}$ and GR^{null} embryos

Electron microscopy shows that mutant epithelia are composed of immature, cuboidal type II cells which preserve the ability to synthesize and secrete pulmonary surfactant as indicated by the presence of multiple lamellar bodies within the cells as well as the alveolar lumen (arrows). Vessels (V) get close to the alveolar lumen in control but not in mutant lungs. * indicates exemplary areas with disorganized ECM and loose cell contacts which is in contrast to the fusion of the cell layers in control lungs.

distal epithelial differentiation was significantly delayed as indicated by the proSPC expression pattern and the preserved high glycogen content in epithelial cells until birth (Figure 14).

Electron microscopy was applied to monitor ultrastructural changes associated with the mesenchyme-specific inactivation of the GR gene. Type I cells are completely missing and type II cells display the typical cuboidal morphology of epithelial precursor cells. However, the ATII cells possess the ability to synthesize and secrete surfactant-containing vesicles. Between the unexpanded rosettes of the epithelium, the mesenchymal cells appear disorganized, form only loose contact and are surrounded by extensive deposition of extracellular matrix (ECM). Virtually indistinguishable observations were made in lungs of GR^{null} embryos showing that $GR^{Col1\text{-}Cre}$ animals recapitulate the lung phenotype observed in the germline mutation (Figure 15).

Furthermore, close ultrastructural inspection of $GR^{Col1\text{-}Cre}$ as well as GR^{null} lungs identified more apoptotic cells in both mutants compared to their control littermates (Figure 16). To corroborate those findings, TUNEL staining (data not shown) and immunohistochemistry for cleaved caspase 3 (Figure 16) were performed on paraffin sections. In line with other investigators, apoptosis was found to be in general a very rare event during murine lung development (Bellusci et al., 1996; Lindahl et al., 1997). Hence, although apoptotic cells were found more frequently in the lungs of $GR^{Col1\text{-}Cre}$ mice, this affects still a very small proportion of less then 1% of all cells.

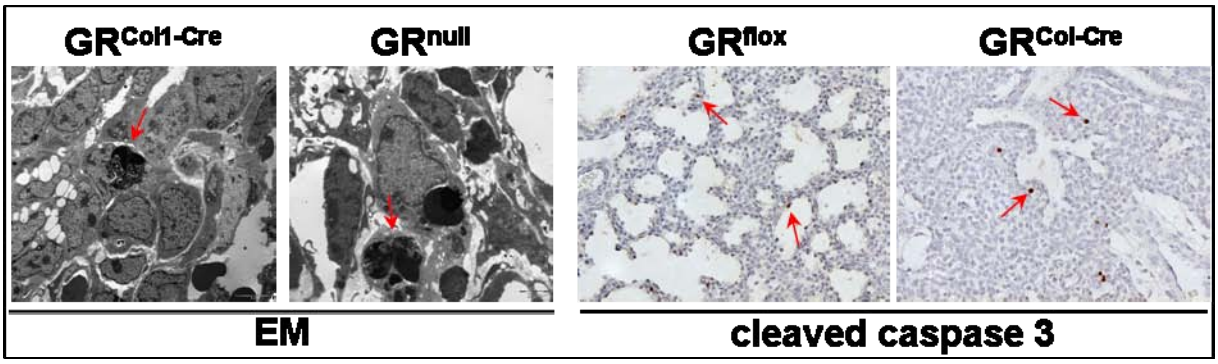

Figure 16: Increased apoptosis in lungs of GR$^{Col1\text{-}Cre}$ embryos compared to controls

Electron microscopy identified apoptotic cells in lungs from GR$^{Col1\text{-}Cre}$ as well as GR^{null} embryos collected at E18.5. IHC on 6µm paraffin sections also identified a higher number of cells positive for cleaved caspase 3 in GR$^{Col1\text{-}Cre}$ compared to littermate control lungs. Arrows indicate apoptotic cells.

To analyze whether a prolonged pregnancy would allow GR$^{Col1\text{-}Cre}$ animals to overcome the observed developmental block during lung development, pregnant mothers were injected with progesterone. Figure 17 shows HE stainings of GR$^{Col1\text{-}Cre}$ and control lungs of a litter collected at E20 (one day beyond calculated delivery). While the controls show signs of beginning alveogenesis, mutant lungs are in the process of tubular dilation which is characteristic for the canalicular phase and thus advanced compared to GR$^{Col1\text{-}Cre}$ mice delivered at P0. However, observation of

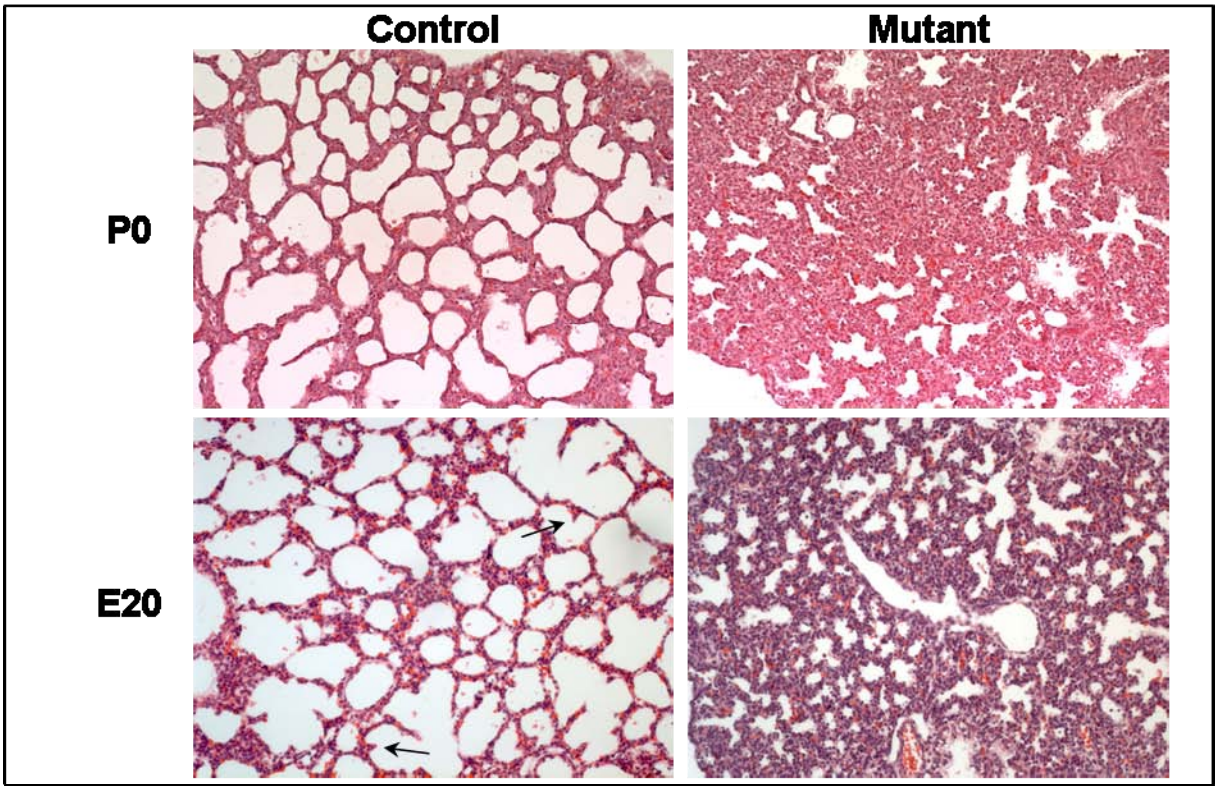

Figure 17: Prolonged pregnancy advances lung morphology in GR$^{Col1\text{-}Cre}$ embryos

Pregnancies were artificially prolonged by progesterone treatment. Control lungs at E20 display secondary septae (arrows) and thus progressed to the alveolar phase of murine lung development. Mutant lungs show widespread dilation of the alveolar saccules at E20 and appear advanced compared to mutants born at natural P0.

litters after delivery by caesarean section revealed that in contrast to their littermates, mutants of similar and even older age were still not able to survive and died within 20 to 30 minutes after birth. Hence, an artificially prolonged pregnancy indeed improves lung morphology and enables $GR^{Col1\text{-}Cre}$ mice to progress through the early canalicular phase of murine lung development. Nevertheless, this is not sufficient to sustain postnatal survival and within the temporal limits of fetal development this strong delay effectively leads to an arrest at the transition from the pseudoglandular to the canalicular phase.

4.6. Gene expression profiling on lungs from $GR^{Col1\text{-}Cre}$ embryos

To monitor transcriptional differences caused by mesenchymal GR inactivation, gene expression profiling was performed using Affymetrix microarrays. Whole lysates from the left lobe of mutant and control lungs, respectively, were used for RNA extraction and two time points were chosen: E16.5 when mutant and control lungs are morphologically indistinguishable but the differential transcriptional basis for the subsequent developmental changes is expected to be established. In contrast, E18.5 describes differences in gene expression reflecting the morphological phenotype observed in $GR^{Col1\text{-}Cre}$ mice (Figure 18A).

Quality and integrity of the RNA were verified by RNA LabChips prior to the labelling, hybridization and scanning procedure. Chip quality was confirmed in dChip (data not shown) and expression values were calculated based on the GC-RMA method.

At E16.5, a comparatively small set of 40 genes was differentially regulated in mutant compared to control lungs (>1.5-fold, $p<0.005$) (Figure 18A and Table 4 in the appendix). As expected, GR (Nr3c1) was among the 23 down-regulated genes, demonstrating the conditional inactivation at this time point.

The Gene Ontology (GO) database (www.geneontology.com) provides hierarchical clustering of biological terms within its three organizing principles: biological processes, cellular components and molecular functions. Above that, it connects gene products with these ontologies which allows the identification of specific terms associated with a particular set of genes. GO analysis of probe sets differentially expressed at E16.5 identified genes connected to “lung and respiratory tube formation” to be significantly over-represented, consistent with the idea that targeting GR will affect central processes of lung development. Moreover, the same gene set was also over-represented in GO terms related to “collagen and extracellular matrix”.

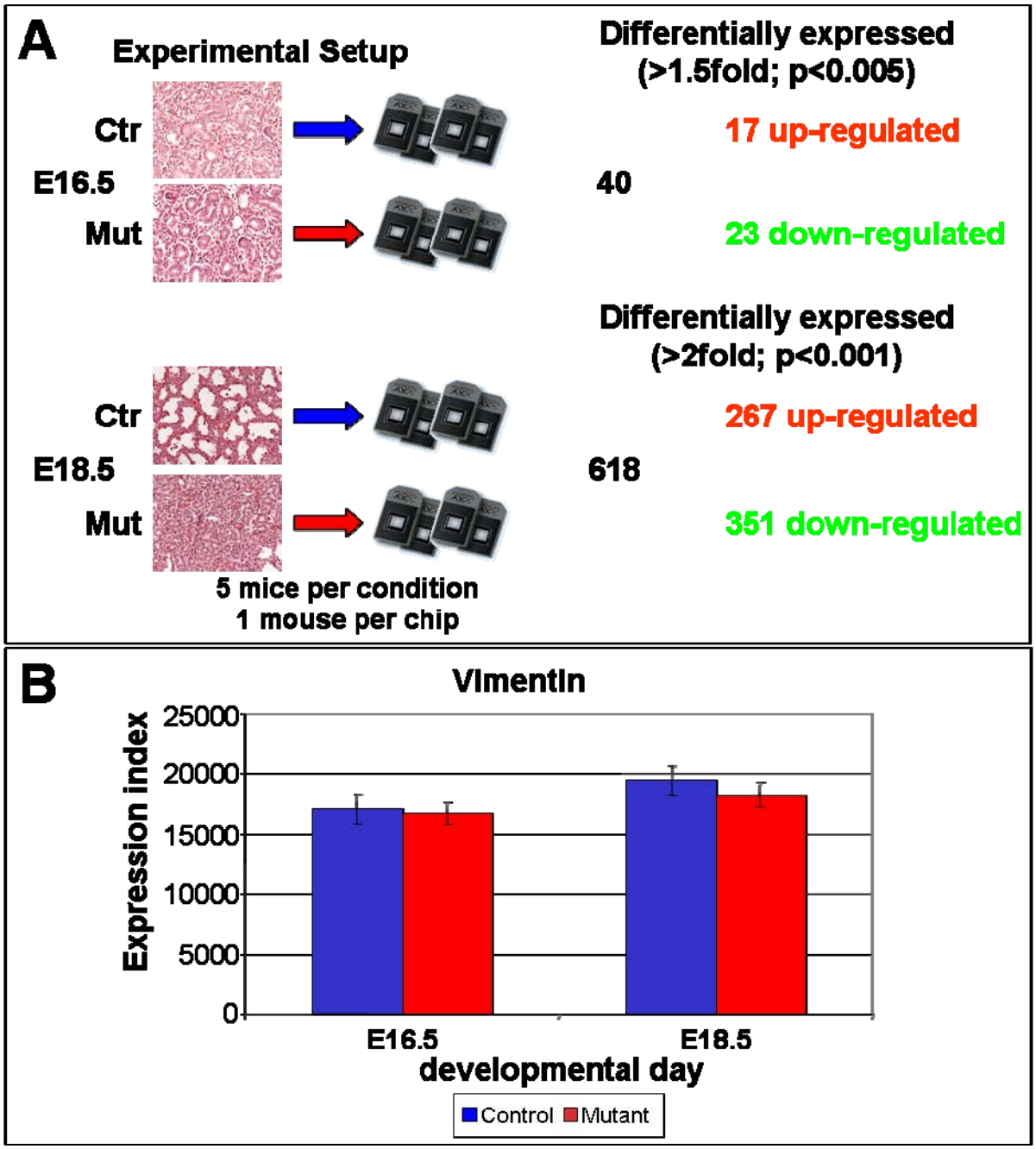

Figure 18: Gene expression profiling

A) RNA was extracted from $GR^{Col1\text{-}Cre}$ and control lungs at E16.5 and E18.5. Numbers of differentially regulated genes at both time points are indicated. B) The proportional contribution of epithelial and mesenchymal cells is comparable between the genotypes at both time points. Expression analysis of mesenchymal marker vimentin did not reveal considerable differences between mutants and controls at any time point.

A large number of 618 genes was found to be differentially expressed in mutants compared to control animals at E18.5. Among these, 267 were up-regulated while 351 showed a decreased expression in $GR^{Col1\text{-}Cre}$ lungs (Figure 18A).

Interpretation of the obtained expression values is complicated by the fact that RNA was extracted from whole lung lysates containing the whole variety of cell types of the developing lung. Thus, observed differences do not necessarily represent

changes at the transcriptional level but may also reflect altered proportions of cell populations. Vimentin is frequently used as a marker for mesenchymal cells as well as for normalization to mesenchymal proportions of mixed cell pools from mesenchymal and epithelial origin (Shirakihara et al., 2007). Therefore, its expression values were extracted from the gene expression profiling, revealing that the abundance of vimentin mRNA did not differ significantly between the genotypes neither at E16.5 nor at E18.5 (Figure 18B). This indicates that the proportional contribution of epithelial and mesenchymal cells to the observed expression values in whole lung lysates is comparable in $GR^{Col1\text{-}Cre}$ and control mice, respectively.

4.7. Identification of changes in gene expression associated with developmental progress

Apart from a direct comparison at a particular stage, the chosen time points allow in addition the description of changes in gene expression which are associated with the developmental progression from E16.5 to E18.5 in control and $GR^{Col1\text{-}Cre}$ mice, respectively. For this analysis, the criteria for significance were set at a fold change

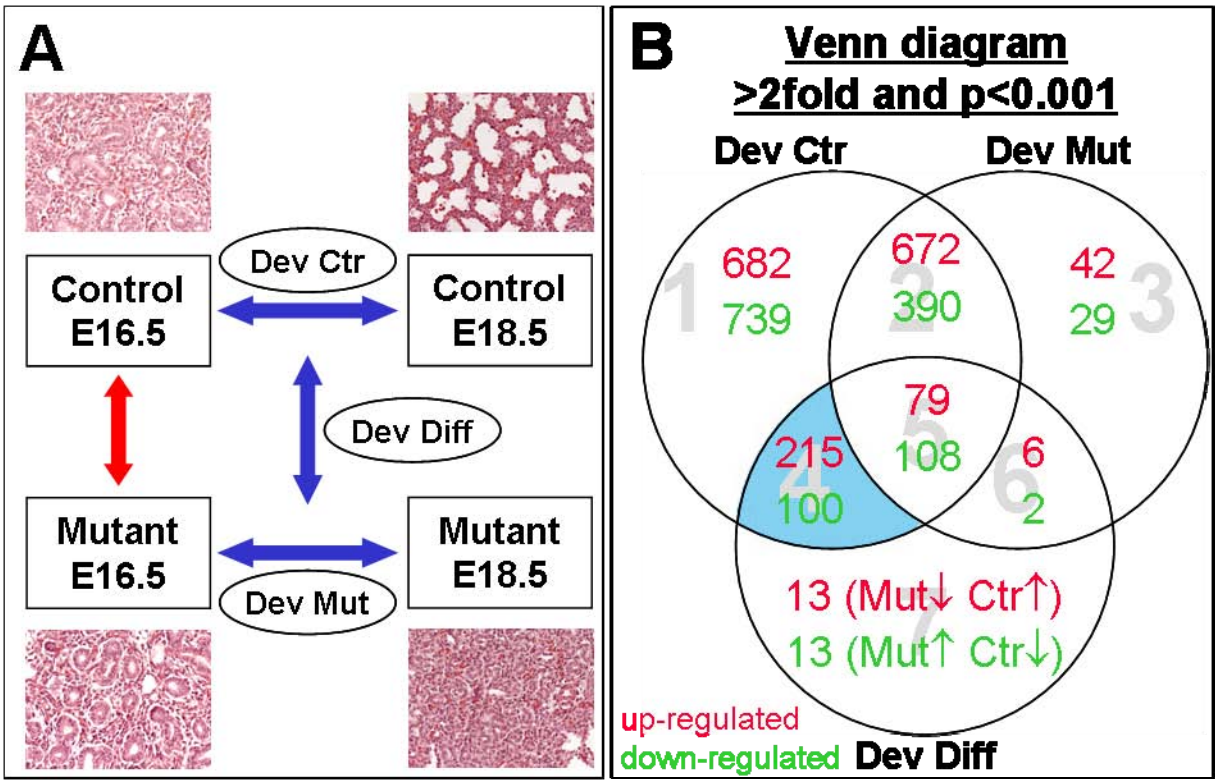

Figure 19: Changes in gene expression associated with the differential development in $GR^{Col\text{-}Cre}$ and control lungs

A) Illustration of the analytical approach used to monitor genes differentially expressed throughout development from E16.5 to E18.5 in mutant and control lungs. Blue arrows indicate the comparison of expression profiles used for the calculation of the Venn diagram in B).

>2 combined with a p-value <0.001 and the probe sets following these criteria are illustrated in a Venn diagram (Figure 19B). The numbers within the circles represent those genes showing a significant change in expression from E16.5 to E18.5 in lungs of controls (Dev Ctr) and/or in $GR^{Col1\text{-}Cre}$ mice (Dev Mut). In addition, it is taken into consideration whether there is a significant quantitative difference between the changes observed in the two genotypes and the number of those genes is found in the circle Dev Diff (Figure 19A).

To identify GR-regulated genes explaining the observed phenotypical changes in $GR^{Col1\text{-}Cre}$ mice, probe sets of the indicated area 4 in the Venn diagram were selected which therefore A) were differentially regulated in controls from E16.5 to E18.5, B) did not respond with a significant change in mutant lungs during the same period and C) showed in addition a significant change in the differential expression. This gene set was subsequently subjected to GO analysis to detect ontological pattern, which might help to define critical mediators of glucocorticoid action (Table 1). This GO analysis revealed that the vast majority of these genes could be classified in two main topics, “proliferation” and “extracellular matrix”. Therefore, these aspects were analyzed in more detail.

Changes in developmental expression pattern – Area 4 (>2fold and p<0.001)	
	Exemplary cluster of gene ontologies
Extracellular matrix	Proteinacous extracellular matrix and heparin binding Polysaccharid and aminoglycan binding Biological and cell adhesion
Proliferation	Cell division and chromosome segregation Cell cycle and M phase Positive regulation of proliferation and G-protein signalling
	Organisation and localization of intracellular organelles Protein kinase regulatory activity Response to wounding and external stimulus
Changes at E16.5 (>1.5fold and p<0.005)	
	Exemplary cluster of gene ontologies
Extracellular matrix	Proteinacous extracellular matrix
Lung development	Respiratory tube development Tube development

Table 1: Gene ontology analysis of particular gene sets

The probe sets extracted from the area 4, indicated blue in Figure 19, were subjected to GO analysis and exemplary clusters are described in the upper part of the table. These can be compared to results obtained by GO analysis of the genes differentially regulated between mutants and controls at E16.5 as indicated by the red arrow in Figure 19.

4.8. Increased proliferation in the lungs of $GR^{Col1\text{-}Cre}$ mice

At the single gene level, area 4 included a number of known effectors of cell cycle regulation (Table 2). While genes important for the progression through the cell cycle such as cyclins A2 and B2 or Cdc2A (cell division cycle 2 homolog A) and Cdc20 were less down-regulated, the induction of well described differentiation markers is absent in $GR^{Col1\text{-}Cre}$ animals. In particular, the expression of the cyclin-dependent kinase inhibitor $p21^{cip}$ was strongly increased in control animals from E16.5 to E18.5 and remained virtually unchanged in mutants.

In order to detect changes in the proliferation rate of fetal lungs, mothers were injected with Bromodeoxyuridine (BrdU) two hours prior to embryo collection. BrdU is a synthetic analogue of thymidine and is incorporated into the DNA of replicating cells during the S-phase of the cell cycle. Specific antibodies then allow the immunohistochemical detection of these cells on tissue sections.

Mesenchyme- as well as epithelium-specific mutants ($GR^{Col1\text{-}Cre}$ and $GR^{Spc\text{-}Cre}$, respectively) were analyzed at embryonic day E18.5 and compared to their littermate controls. The proliferation index is defined as the percentage of proliferating cells per total cell number and was found to be significantly increased in lungs of $GR^{Col1\text{-}Cre}$ mice compared to control lungs. In contrast, $GR^{Spc\text{-}Cre}$ mice displayed a pulmonary proliferation rate comparable to their control littermates (Figure 20A).

To distinguish in $GR^{Col1\text{-}Cre}$ mutants proliferating cells in the epithelium and the

Developmental changes in expression from E16.5 to E18.5 (log2 ratios)		
Gene	**Control**	**Mutant**
Cyclin A2	-2.1	-0.9
Cell division cycle 2 homolog A	-2.2	-0.9
Cyclin B2	-2.0	-0.7
N-myc	-2.0	-0.7
Mki67	-2.0	-0.7
Ndr1	1.5	0.4
Cyclin-dependent kinase inhibitor 1A (p21)	2.4	0.3

Table 2: Exemplary genes from the proliferation cluster identified by GO analysis

These genes were represented in area 4, indicated blue, in Figure 19, i.e. they showed a significant change in controls from E16.5 to E18.5 but not in mutants and these developmental changes were in addition significantly different among the genotypes (criteria for significance were a fold change >2 and $p<0.001$). Furthermore, GO analysis identified them to be associated with proliferation and control of cell cycle regulation.

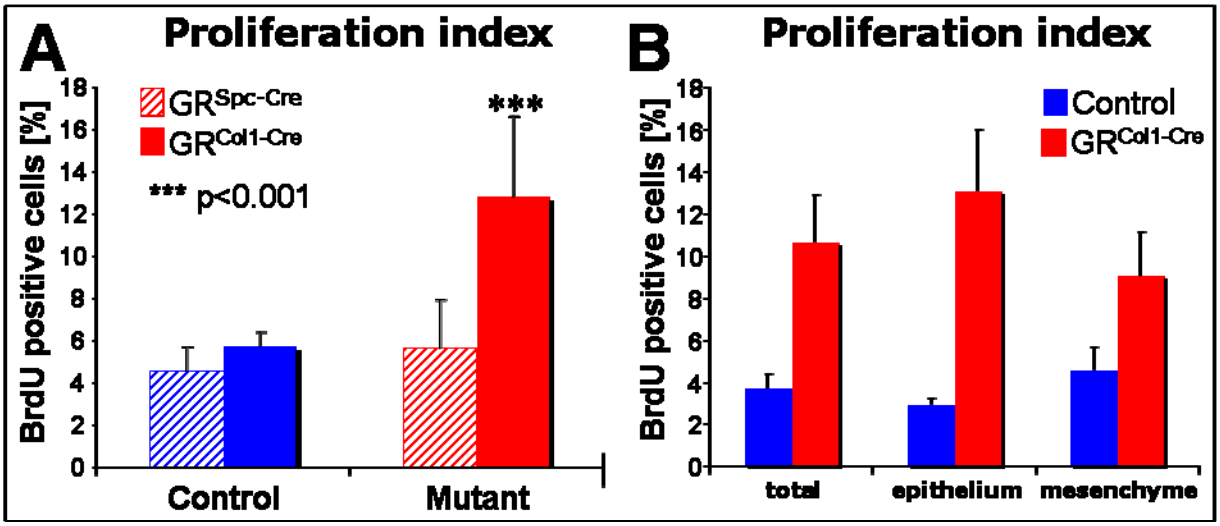

Figure 20: Increased proliferation in $GR^{Col1\text{-}Cre}$ embryonic lungs

A) 6µm paraffin sections of E18.5 lungs from mutant and controls treated with BrdU two hours prior to embryo collection were stained with an anti-BrdU antibody and counterstained with hematoxylin. The proliferation index is defined as the percentage of BrdU positive cells relative to all nuclei. It was calculated as overall proliferation index for E18.5 $GR^{Spc\text{-}Cre}$ and $GR^{Col1\text{-}Cre}$ mutants as well as their respective control littermates showing a significant increase of $GR^{Col1\text{-}Cre}$ but not in $GR^{Spc\text{-}Cre}$ litters.
B) Double labelling of BrdU and the epithelial marker T1α allows the calculation of separate values for the epithelium and the mesenchyme. This did not reveal a significant difference in the increased proliferation rate in the two compartments compared to the total proliferation index.

mesenchyme, double-labelling with antibodies against BrdU and the epithelial marker T1α was performed. However, calculation of separate values for the two compartments revealed that the proliferation index increased in the epithelium as well as in the mesenchyme to a similar extent and both did not reveal a significant difference to the rise in the total proliferation index (Figure 20B).

In summary, mesenchyme-specific inactivation of the GR gene leads to a significant increase in the general proliferation rate which is in accordance with the results of the expression profiling.

4.9. Changes in ECM composition in the lungs of $GR^{Col1\text{-}Cre}$ mice

In addition to genes associated with the regulation of proliferation, the expression profiling also identified numerous components of the extracellular matrix (ECM) as well as ECM-modifying enzymes to be differentially expressed (Table 3). This included representatives of all major constituents of the lung ECM, i.e. collagens, elastic fibres and proteoglycans, but also cell surface molecules interacting with those.

For instance, elastin expression in $GR^{Col1\text{-}Cre}$ embryos did not follow the strong increase observed in their control littermates from E16.5 to E18.5 and the most important elastin-crosslinking enzyme lysyl-oxidase was significantly down-regulated

Developmental changes in expression from E16.5 to E18.5 (log2 ratios)		
Gene	**Control**	**Mutant**
Procollagen, type IX, alpha 1	-4.7	-0.9
Chondroitin sulfate proteoglycan 2 (Versican)	-3.3	-0.2
Fibromodulin	-2.5	-0.8
Heparan sulfate 6-O-sulfotransferase 2	-2.0	-0.8
Fibrillin 2	-2.0	-0.0
Fibulin 1	-1.7	-0.5
Adam 12	-1.2	-0.0
Adamts 15	1.9	0.4
Plasminogen activator, urokinase receptor	1.7	0.1
Integrin β6	1.7	0.3
Elastin	2.0	0.9
Fibronectin	2.0	0.9
Ceruloplasmin	3.6	0.5
Chitinase, acidic	3.7	0.4
Spondin 1	4.0	0.1

Table 3: Exemplary genes from the extracellular matrix cluster identified by GO analysis

These genes were represented in area 4, indicated blue in Figure 19, i.e. they showed a significant change in controls from E16.5 to E18.5 but not in mutants and these developmental changes were in addition significantly different among the genotypes (criteria for significance were a fold change >2 and $p<0.001$). Furthermore, GO analysis identified them to be associated with the extracellular matrix.

at both time points (Figure 21A). Elastogenesis also involves the balanced synthesis of microfibril proteins such as fibrillins and fibulins, which act as a scaffold for elastin assembly and are essential for this process (El-Hallous et al., 2007; Hubmacher et al., 2006; Kostka et al., 2001). In line with the emergence of all these probe sets, Goldner-Elastika staining revealed that the formation of elastic fibres could not be detected in the distal lungs of $GR^{Col1\text{-}Cre}$ animals while elastogenesis around larger bronchi and vessels was not affected (Figure 21B).

Laminins are a central part of basal membranes and known to show a dynamic expression pattern throughout lung development (Nguyen and Senior, 2006). Although the developmental switch for instance from laminin $\alpha1$ to $\alpha5$ was delayed in mutant lungs, these changes did not reach significance (data not shown). In contrast, significant differences could be observed for members of the integrin family which form the cellular laminin receptors as well as laminin interaction partners such as fibronectin and certain collagens (Table 3) (Kreidberg et al., 1996).

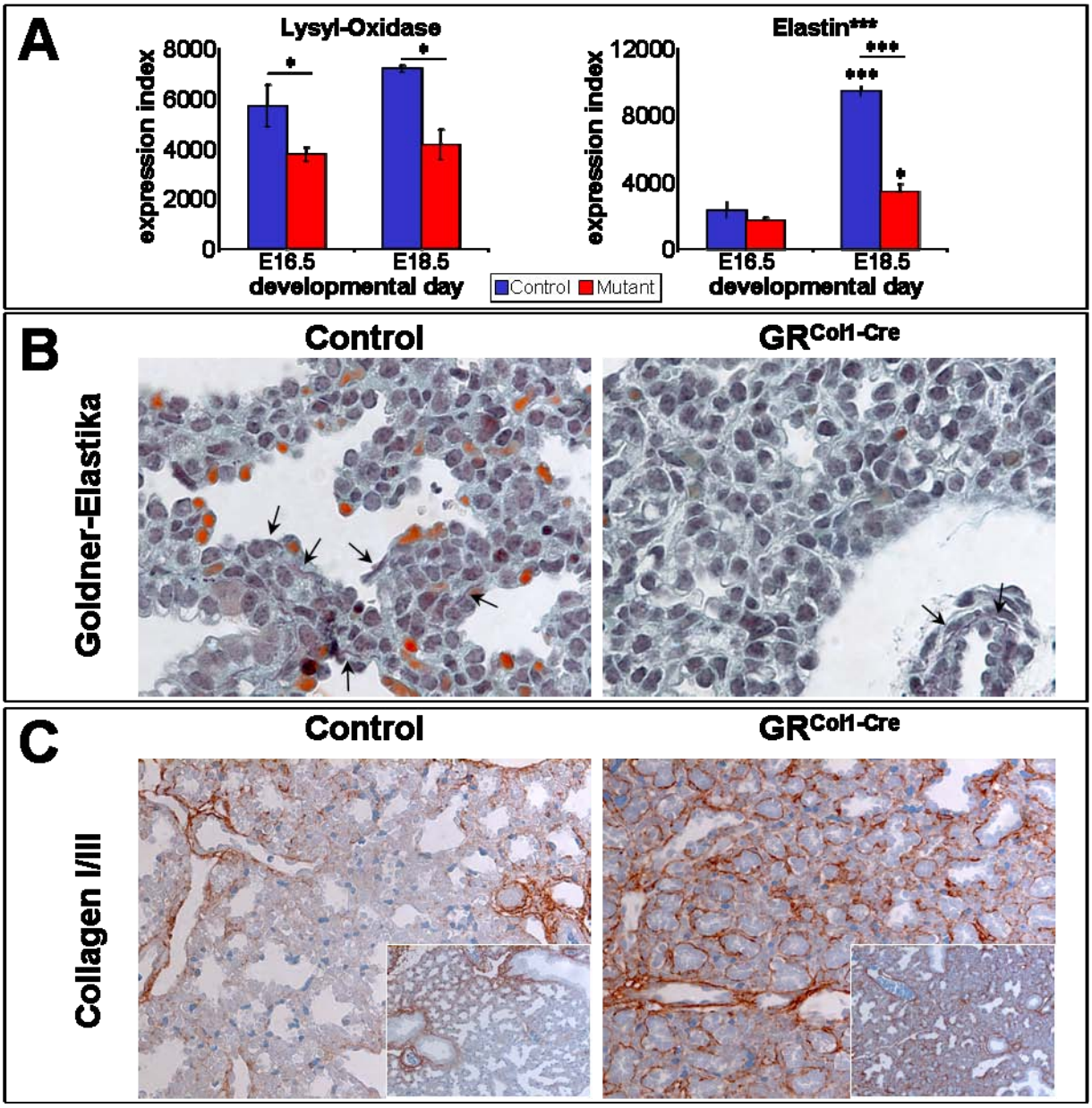

Figure 21: Changes in components of the ECM

A) Elastin and its major cross-linking enzyme lysyl-oxidase show different expression values in mutant compared to control lungs. * indicates a fold change >1.5 and p<0.005; *** indicates a fold change >2 and p<0.001, *** in the title indicates a significant difference in the developmental profile B) Goldner-Elastika staining of E18.5 lungs demonstrates violet elastic fibers (arrows) in the alveolar area in controls. In mutant lungs, elastin deposition is only detected around larger airways (not shown) and vessels (indicated by arrowheads) C) Immunohistochemistry for collagen I/III shows widespread collagen deposition in mutant lungs. In controls, maturation coincides with loss of immunoreactivity. Insets show a lower magnification overview.

Immunohistochemically, these changes in the overall composition of the ECM were exemplified using an antibody against the collagens I/III, demonstrating persistent and strong staining of collagen fibres in $GR^{Col1\text{-}Cre}$ animals. In control animals instead, pulmonary maturation coincided with reduced immunoreactivity for these collagens and prominent staining was only observed in the most distal parts, in particular near bronchi and bronchioles (Figure 21C).

4.10. Mesenchyme-specific loss of GR influences known signalling pathways of pulmonary morphogenesis

For a number of signalling molecules, a critical role during proper lung development is well documented, such as transforming growth factor β (TGFβ), fibroblast growth factors (FGFs) or sonic hedgehog (Shh). In their target cells, these molecules exert actions which affect the activity of diverse transcription factors and ultimately give rise to the differential expression of target genes (Shannon and Hyatt, 2004). Therefore, expression values from the microarray experiment were used to monitor the effect of mesenchyme-specific GR ablation on the activity of accepted regulators of lung development and some of these are shown in Figure 22.

TGFβ signalling and in particular its influence on the regulation of the ECM are well known effectors during lung development (Shi et al., 1999; Zeng et al., 2001). While the increase in TGFβ1 expression during late development in controls is only mildly attenuated in $GR^{Col1\text{-}Cre}$ mice, TGFβ2 and 3 show a contrary behaviour in mutants compared to controls. Their strong decrease from E16.5 to E18.5 in controls is contrasted by a significant up-regulation in mutant lungs. In accordance, a variety of constituents of the ECM were found to be differentially regulated as well and have been described above.

Members of the FGF family and their receptors have been described to mediate respiratory tube growth and branching but also functional maturation prior to birth. In particular, FGF9 expressed in the mesothelium and the epithelium has been shown to act together with Shh signalling to promote mesenchymal proliferation and growth factor synthesis (White et al., 2006). Apart from gene products associated with proliferating cells, FGF7 is up-regulated which in turn promotes epithelial maturation and alveolar dilation (Shi et al., 1999; Tichelaar et al., 2000; Zeng et al., 2001). In $GR^{Col1\text{-}Cre}$ mice, FGF9 as well as a particular set of Shh target genes do not follow the developmental pattern observed in the control lungs and this translates into an increased expression of proliferation markers (see section 4.8.) in parallel with a lower expression of FGF7. The Shh target genes Gli1 and Gli2 are significantly down-regulated in controls at E18.5 compared to E16.5 while the decrease over the same period in $GR^{Col1\text{-}Cre}$ lungs does not reach significance. In the case of Gli1, this significantly different developmental change leads to a similarly significant difference

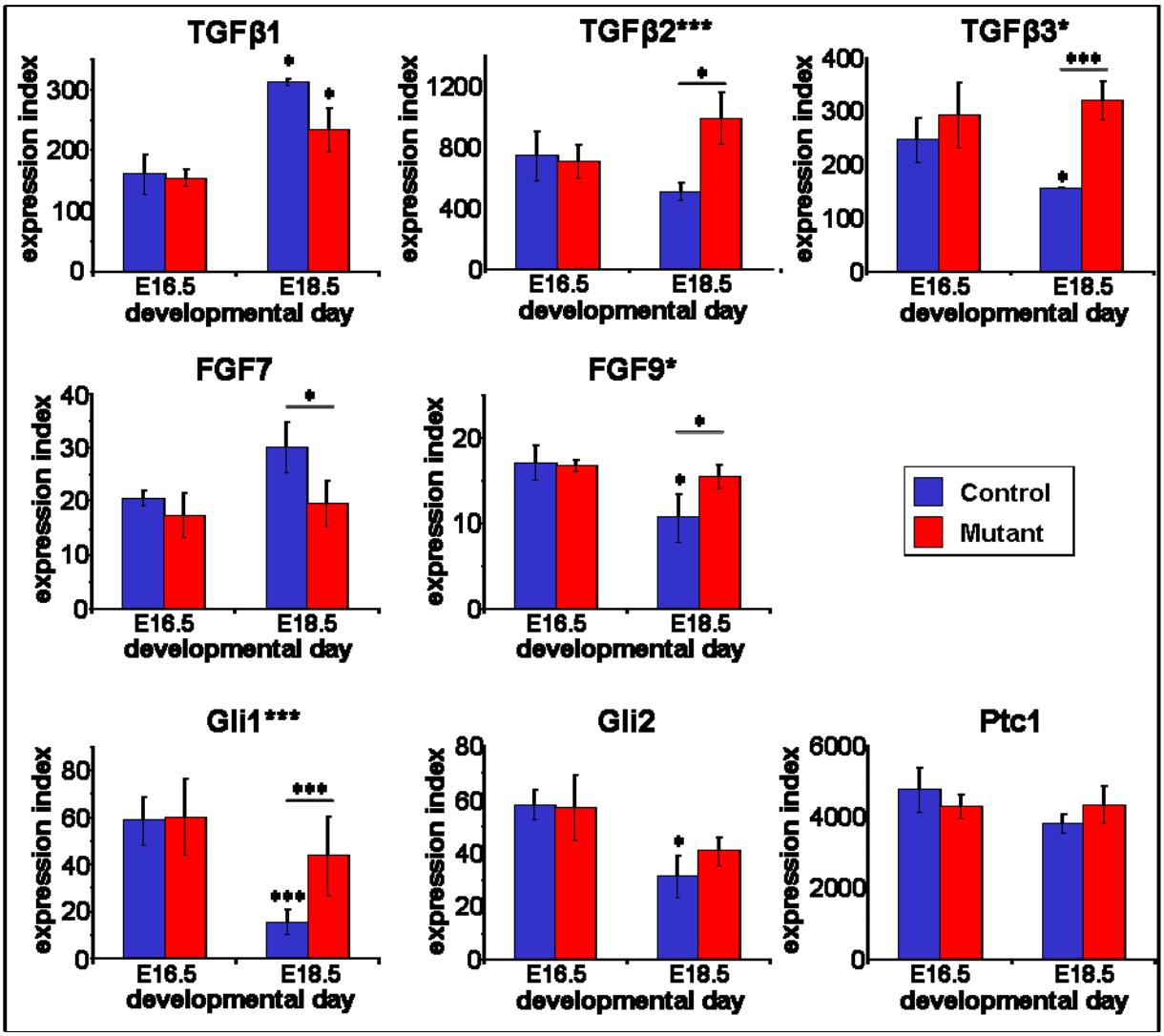

Figure 22: Expression values of genes known to be involved in the regulation of lung morphogenesis

Expression values were extracted from the gene expression profiling. * indicates a fold change >1.5 and p<0.005; *** indicates a fold change >2 and p<0.001, */*** in the title indicates a significant difference in the developmental profile (Dev Diff). Significant differences between genotypes are indicated with bars while */*** at E18.5 indicates a significant change compared to E16.5.

in expression at E18.5 between the genotypes. In contrast, another Shh target gene, Ptc1, does not display significant differences among any of the two conditions.

4.11. Analysis of vascular differentiation in $GR^{Col1\text{-}Cre}$ mice and endothelium-specific inactivation of the GR gene

The capillary system surrounding the alveoli has been shown to arise from the primitive lung mesenchyme through vasculogenesis, a process involving various interactions between the differentiating endothelial and epithelial compartments (Stenmark and Abman, 2005). Importantly, interference with the precise control of these signalling events causes malformations of the respiratory system, leading to

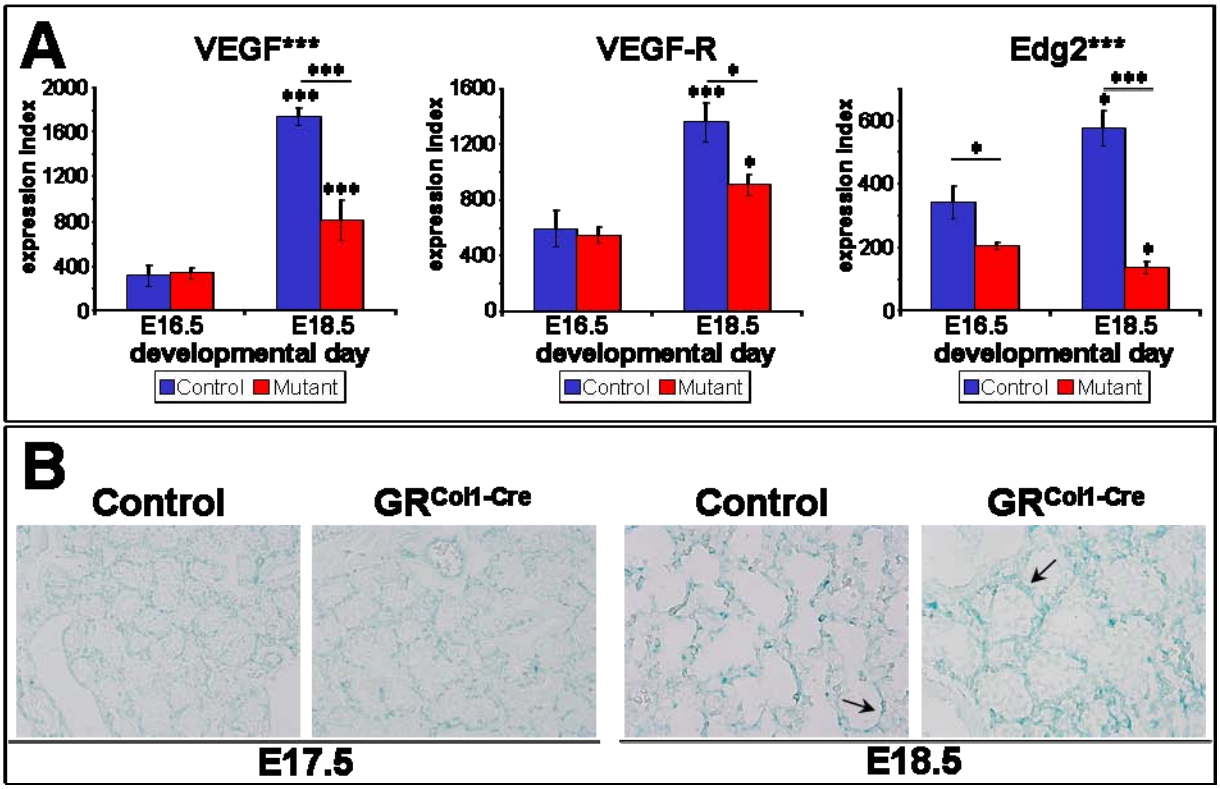

Figure 23: Endothelial differentiation in GR$^{Col1\text{-}Cre}$ animals

A) Expression values of selected genes involved in endothelial differentiation. * indicates a fold change >1.5 and p<0.005; *** indicates fold change >2 and p<0.001, */*** in the title indicates a significant difference in the developmental profile (Dev Diff). Significant differences between genotypes are indicated with bars while */*** at E18.5 indicates a significant change compared to E16.5.
B) Immunohistochemistry for the endothelial marker Pecam1 shows continuous staining around the alveoli in mutants and controls at E17.5. At E18.5, the staining in control lungs becomes more condense while GR$^{Col1\text{-}Cre}$ animals maintain the staining pattern observed in the E17.5 lung (indicated by arrows).

inadequate lung function and even death (Del Moral et al., 2006b; Yamamoto et al., 2007; Zeng et al., 1998).

The expression profiling identified a number of differentially regulated genes which are known to participate in the regulation of endothelial development such as vascular endothelial growth factor (VEGF), VEGF receptor (VEGF-R) and endothelial differentiation gene 2 (Edg2) (Figure 23A). To investigate the extent of vascular differentiation in GR$^{Col1\text{-}Cre}$ mice, lung sections were stained with an antibody against Pecam1 (CD31) which labels specifically endothelial cells and their progenitors (Figure 23B). A continuous staining surrounding the complete alveolus can be observed at E17.5 in control as well as mutant embryos. In controls, this staining becomes condensed and intensifies throughout the subsequent maturation as the alveolar lumen dilates and the thickness of the septae is reduced. In contrast, GR$^{Col1\text{-}Cre}$ lungs preserve the immunohistochemical appearance of the

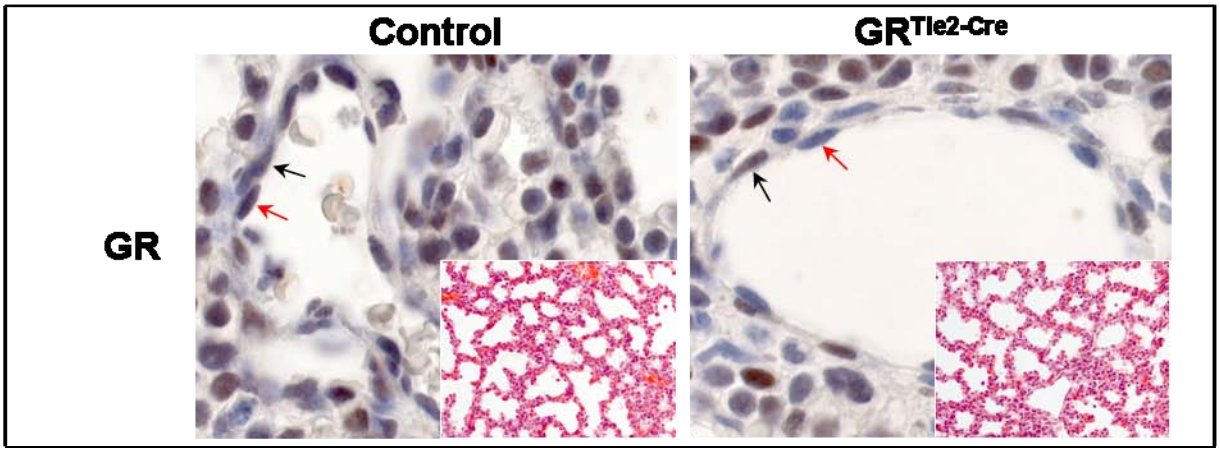

Figure 24: Endothelium-specific inactivation of the GR gene

Immunohistochemistry against GR on 6µm paraffin sections shows GR protein in endothelial cells (red arrow) and pericytes (black arrow) in control animals. In mutants, GR is still detected in pericytes (black arrow) while endothelial cells do not show immunoreactivity (red arrow). Insets show HE staining of 4.5µm paraffin sections. No significant differences in lung morphology were noted between the two genotypes.

pseudoglandular vasculature, corresponding to the general phenotype of these mutants (Figure 23B).

In order to investigate a potential role of GR in cells of the vascular system during murine lung development, animals lacking GR specifically in the endothelium were generated. Mice expressing the Cre recombinase under regulatory promotor/enhancer elements of the Tie2 gene (Constien et al., 2001) were crossed with GR^{flox} animals (Tronche et al., 1999). The resulting $GR^{flox/flox}$/Tie2-Cre ($GR^{Tie2\text{-}Cre}$) mutants did neither show respiratory distress nor other obvious dysfunctions after birth. Consequently, E18.5 embryos were analyzed for pulmonary maturation but no significant differences were noted upon morphological examination of HE stained paraffin sections (Figure 24, insets).

The efficacy of the endothelial recombination was confirmed by immunohistochemistry. GR staining is detectable in endothelial cells as well as pericytes in control animals whereas in $GR^{Col1\text{-}Cre}$ lungs only the pericytes preserve positive immunoreactivity (Figure 24).

4.12. Generation of an inducible, endothelium-specific Cre line Tie2-CreER^{T2}

The constitutive Tie2-Cre line applied before is known to recombine unspecifically in cells of the hematopoietic system during development (Constien et al., 2001). To further improve the analysis of gene function in endothelial cells specifically at the adult stage, a Cre line was established expressing the CreER^{T2} fusion protein under control of the regulatory elements of the mouse Tie2 gene. To generate these mice,

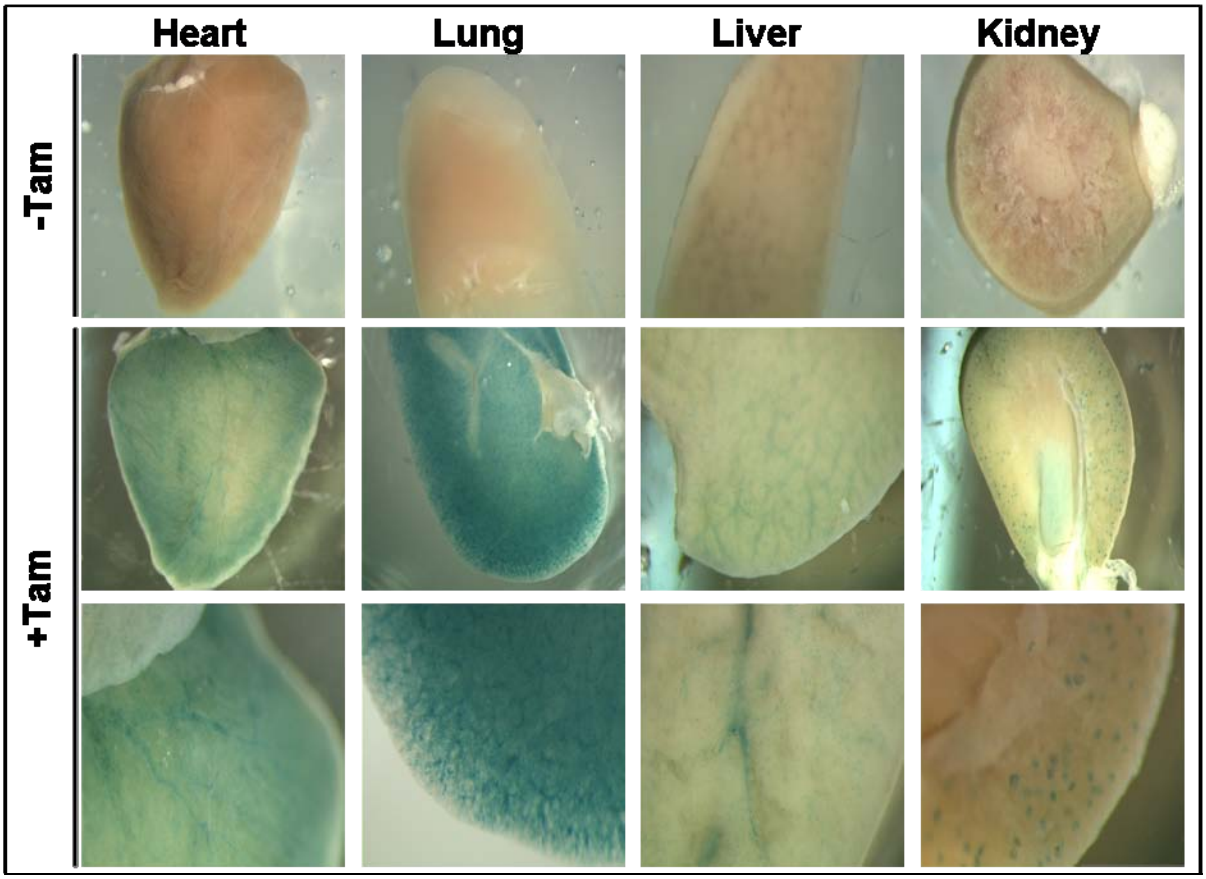

Figure 25: Tie2-CreER^{T2}-mediated recombination in endothelial cells of various organs

Whole mount β-galactosidase staining of organs collected from mice positive for the Rosa26 Cre reporter and carrying the Tie2-CreER^{T2} transgene. Only after treatment with tamoxifen, widespread blue staining is observed in a pattern consistent with the vasculature system.

a BAC was selected which contained ~80kb upstream and ~60kb downstream of the Tie 2 gene and the processing was essentially performed as described in 4.1., except that the targeting construct contained the sequence of the CreER^{T2}. This fusion protein consists of the Cre recombinase and a mutated ligand binding domain (LBD) of the estrogen receptor (ER) which binds specifically the synthetic ligand tamoxifen but not endogenous estrogens. The ER-LBD retains the Cre molecule in the cytoplasm and only upon tamoxifen application the fusion protein translocates into the nucleus where it mediates recombination (Feil et al., 1997; Kellendonk et al., 1999; Kellendonk et al., 1996; Weber et al., 2001).

Purification, oocyte injection and analysis of the resulting mice were performed as described before (section 4.1.). Fourteen animals carrying the transgene were identified as potential founders and crossed to Rosa26 Cre reporter mice for the validation of Cre activity. Eight founders successfully transmitted the transgene and resulting R26R/Tie2-Cre^{ERT2} (Rosa26$^{Tie2\text{-}CreERT2}$) offspring of six founders was subjected to an established induction protocol (Erdmann et al., 2007). At the age of

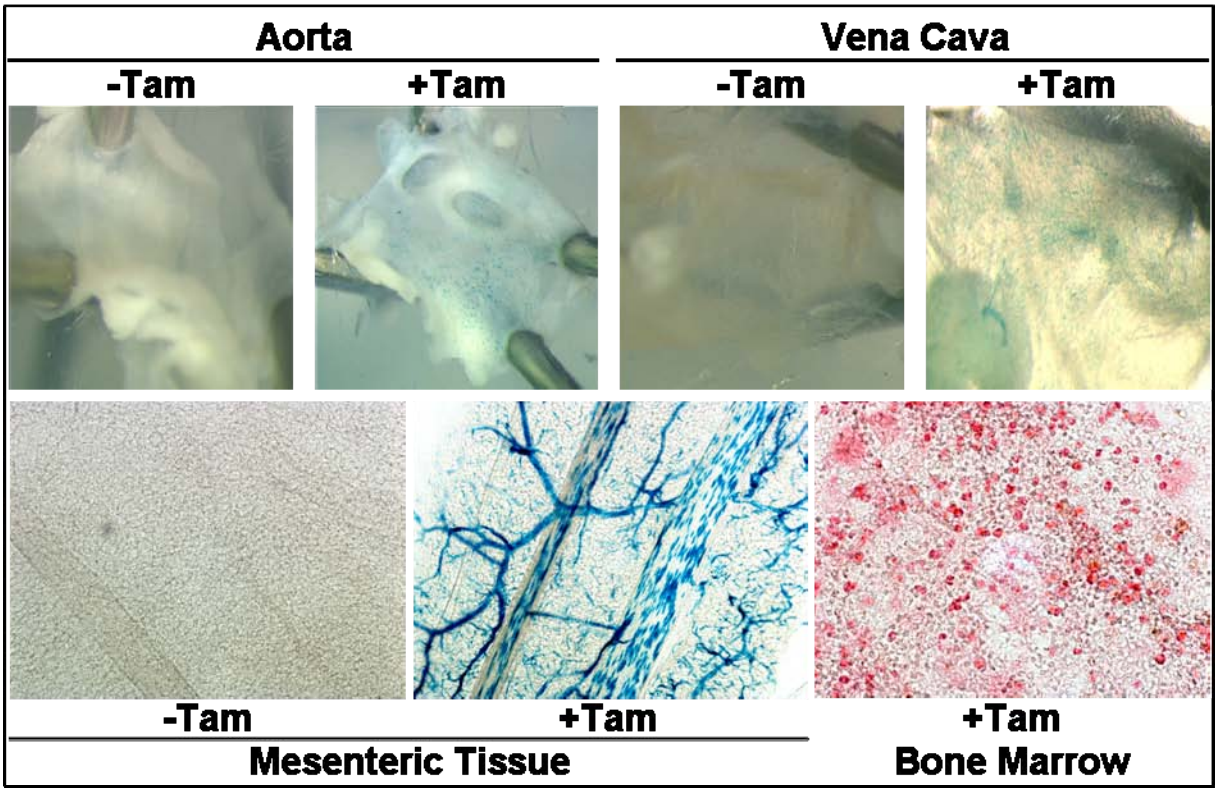

Figure 26: The Tie2-CreER^{T2} transgene mediates recombination in endothelial cells of various vessel types but not in the bone marrow

β-galactosidase staining is discontinuous in the aorta and the vena cava but complete recombination is observed in the capillary system exemplified by the mesenteric tissue. With increasing vessel size, the staining becomes progressively discontinuous and is mosaique in the aorta and the vena cava. No recombination was detected in cells of the hematopoietic system (bone marrow).

eight weeks, the mice received two injections of 1mg tamoxifen or vehicle for five consecutive days and were sacrificed another ten days thereafter. Three lines displayed the expected recombination pattern and LacZ data are shown for one of them (Figures 25 and 26). Recombination was specifically detected in endothelial cells in various organs whereas β-galactosidase staining was neither observed in cells of the hematopoietic system (bone marrow), nor in other non-endothelial cell types. Importantly, Cre activity was also not revealed in vehicle-injected animals.

The extent of Cre-mediated recombination was strongly dependent on the size and type of the vessels. Upon tamoxifen treatment, strong β-galactosidase activity was observed in virtually all cells of the capillary system, for instance in the lung, kidney or most clearly visualized in mesenteric tissue. Instead, the β-galactosidase staining became mosaique with increasing size of the vessels and this effect was more pronounced in the arterious compared to the venous compartment. Reflecting this pattern, β-galactosidase staining becomes discontinuous in the vena cava and the aortic endothelium shows only scattered recombination (Figure 26).

5. Discussion

The beneficial effects of glucocorticoids for the acceleration of fetal lung maturation are well known after the initial experiments performed by Liggins and colleagues on sheep in 1969 (Liggins, 1969). Since then, corresponding actions have been described for a broad range of mammalian species, ranging from rodents over cattle to, and most importantly, humans (Liggins and Howie, 1972; Snyder et al., 1981; Zaremba et al., 1997). Clinical studies have further confirmed the advantageous outcome of glucocorticoid application and have led to their recommendation as standard regimen of care in preterm infants (Gilstrap et al., 1995).

However, pharmacological doses of glucocorticoids are known to be associated with considerable side-effects. Experiments in rodents, (non-human) primates and humans have revealed that glucocorticoid treatment leads to growth retardation, premature differentiation of several organs and an increased risk for cardiovascular disease as well as mental disorders such as unipolar depression (Reinisch et al., 1978; Seckl, 2004). Thus, further insights into the mechanisms of glucocorticoid action in the fetal lung are desirable and might provide alternative strategies to treat preterm infants.

Apart from pharmacological stimulation, the critical role of glucocorticoid signalling has also been demonstrated by gene ablation and consequent loss of glucocorticoid action in mice. GR knockout mice die immediately after birth due to respiratory failure and display strong pulmonary alterations including mesenchymal thickening and strongly reduced airspace (Cole et al., 1995). The essential role of glucocorticoid signalling was corroborated by results from mice with genetic inactivation of the CRH gene (Muglia et al., 1999). Leading to a marked glucocorticoid deficiency and postnatal lethality, this mutation causes a lung morphology strongly reminiscent of the GR knockout phenotype.

GR actions can be mediated by direct binding to GREs as a homodimer or by interaction with other transcription factors. Dimerization-defective mice were generated to allow the distinction of different modes of GR action (Reichardt et al., 1998). In these animals, GR retains its ability to transactivate and transrepress via interactions with other transcription factors whereas classical homodimeric binding to

GREs is perturbed. Interestingly, these mice are viable indicating that the essential functions of GR in the developing lung are mediated via protein-protein interactions.

5.1. Conditional inactivation of the GR gene in different cellular compartments of the developing lung

Targeted gene inactivation in mice is a powerful tool for the analysis of gene function and has been proven valuable in the investigation of glucocorticoid signalling. It provides strong specificity and reliable ablation of gene function while pharmacological blockade or adrenalectomy with subsequent glucocorticoid replacement bear considerable disadvantages. Receptor antagonists show a certain degree of un-specificity and do not guarantee complete blockade while adrenalectomy removes apart from glucocorticoids also mineralocorticoids and catecholamines. Finally, investigation of embryonic development further complicates the pharmacologic intervention while surgical manipulation is virtually precluded.

The Cre/loxP recombination system has enabled the investigation of gene function in cases where complete gene inactivation leads to early lethality. Moreover, it also allows a cell type-specific analysis to distinguish contributions of certain cell populations to a given paradigm.

In the developing lung, morphogenesis and maturation depend on a delicate signalling network involving various cell types of epithelial and mesenchymal origin. Therefore, a series of Cre-transgenic lines was applied to investigate the role of these respective cell types for the glucocorticoid-mediated maturation of the murine lung and two of these lines were generated in the course of the present studies.

5.1.1. mSftpc-Cre

Efforts to generate a BAC-derived transgene expressing the Cre recombinase specifically in the lung epithelium under the regulatory elements of the Sftpc gene locus failed. Only a small number of three transgenic founder animals was obtained and none of these was able to transmit the transgene to the F1 generation. While BACs imply the advantage of reliable copy number-dependent and integration site-independent expression, they also bear the risk of co-expression of potentially unfavourable genes present on the BAC. In the case of the applied BAC RP24-252D18, a number of other genes are found in close proximity to the Sftpc locus, such as the nuclear receptor co-repressor hairless, the 47kd polypeptide of the DNA-

directed RNA polymerase III or Bmp1 encoding bone morphogenic protein (BMP1) and mammalian Tolloid (mTLD). Although detailed knowledge through over-expression studies in the mouse is missing in most cases, some candidates might explain or contribute to the failure to establish a BAC-based mSftpc-Cre line. For instance BMP1 is an extracellular metalloproteinase which orchestrates ECM assembly but also activates the TGFβ-like proteins BMP2 and BMP4. Overexpression studies demonstrated a crucial role of BMP1 in dorsal-ventral patterning (Hopkins et al., 2007), whereas mice with a targeted mutation in the Bmp1 gene do not survive beyond birth (Suzuki et al., 1996). In conclusion, plasmid-based transgenes might prove superior in particular cases when suitable BACs are not available.

5.1.2. Spc-Cre

In the course of these studies, a plasmid-based epithelium-specific Cre transgenic mouse line was published (Okubo and Hogan, 2004; Okubo et al., 2005). It employs 3.7kb of the promotor from the human gene encoding surfactant associated protein C (SPC), which has been extensively characterized and used to drive the expression of various proteins in cells of the developing lung epithelium (Glasser et al., 1991; Korfhagen et al., 1990; Perl et al., 2002; Tichelaar et al., 2000; Wert et al., 1993). The specificity was confirmed using the Rosa26 Cre reporter line (Soriano, 1999) and faithful recombination was achieved in combination with the conditional GR allele.

5.1.3. Col1-Cre

This transgenic mouse line expresses the Cre recombinase from a 100kb P_1 artificial chromosome (PAC) containing the locus of the collagen type (I)-alpha 2 gene (Florin et al., 2004). During embryogenesis as well as in adult animals it mediates recombination in cells of mesenchymal origin such as dermal fibroblasts, mesenchymal cells of blood vessel walls and cells of the connective tissue. In the developing lung, the Col1-Cre transgene efficiently targets the whole mesenchymal compartment including the endothelium of the capillary system which surrounds the developing alveolus and is derived from the primitive lung mesenchyme through vasculogenesis.

5.1.4. Tie2-Cre

The applied plasmid-based transgenic line employs promotor/enhancer elements of the mouse Tie2 gene to direct Cre expression specifically to endothelial cells (Constien et al., 2001). This includes vessels originating from angiogenesis but also the endothelial progenitor cells which arise from the primitive mesenchyme during vasculogenesis of the lung capillary system and which have been characterized by the expression of TIE2 (White et al., 2006).

5.1.5. Tie2-CreER^{T2}

In order to enable a versatile applicability of the Cre/loxP recombination system in endothelial cells, a BAC-transgenic mouse line was generated which expresses a tamoxifen-inducible recombinase CreER^{T2} under the regulatory elements of the Tie2 gene. A variety of Tie2-Cre lines has been published so far, however, all these transgenes relied on various combinations of promotor and/or enhancer fragments and resulted in very diverse and mostly incomplete recombination pattern (Forde et al., 2002; Kisanuki et al., 2001; Li et al., 2005b). The constitutive plasmid-based Tie2-Cre applied in the present study provides faithful recombination in endothelial cells but activity has also been observed in cells of the hematopoietic system during embryonic development. Moreover, targeting of genes essential for the developing vascular system extends also to the yolk sack and the extraembryonic vasculature. Frequently, this renders the mutants particularly vulnerable to early midgestational lethality precluding detailed analysis in later development and adulthood (George et al., 1993; Schorpp-Kistner et al., 1999; Shalaby et al., 1995). Employment of an inducible CreER^{T2} allows activation at any desired time point and therefore circumvents potential fatal outcomes as well as unwanted recombination in cells of the hematopoietic system during development.

In line with previous attempts, the oocyte injections of the Tie2-CreER^{T2} construct yielded founders with mostly surprisingly high copy numbers of the BAC transgene (J. Elzer, personal communication; Table 5 in the appendix). Analysis of β-galactosidase activity in R26R$^{Tie2\text{-}CreERT2}$ animals identified three lines which showed the expected recombination pattern and one of these was investigated in more detail. Importantly, recombination was neither detectable in the absence of tamoxifen nor in cells of the hematopoietic system in induced animals.

$R26R^{Tie2\text{-}CreERT2}$ animals demonstrated prominent β-galactosidase activity in the capillary system of a variety of organs including lung, kidney and the mesenteric tissue. With increasing vessel size, this staining became progressively mosaique and was only scattered in the aorta. Since similar recombination pattern were observed in all three lines, this most likely reflects the restricted activity of the Tie2 locus in sub-populations of endothelial cells. Further investigation is warranted to analyze the suitability of this Cre line for the generation of mice with inducible endothelium-specific protein loss.

5.2. Lung epithelium-specific inactivation of the GR gene retards lung maturation but does not impair survival

Beneficial effects of corticosteroids for lung maturation have commonly been attributed to their ability to induce the functional maturation of lung epithelial cells. Glucocorticoids have been shown to induce the synthesis and secretion of pulmonary surfactant in epithelial ATII cells, reducing the surface tension within the alveolus and thus preventing collapse (Mendelson, 2000). Moreover, corticosteroid receptors are known to induce the transepithelial sodium and water transport via regulation of the epithelial sodium channel (ENaC) (Itani et al., 2002; Nakamura et al., 2002). Apart from their general function in homeostasis, this is of particular importance for the rapid clearance of lung liquid during the perinatal transition from a fluid-filled lung to air-breathing, and mice lacking functional ENaC die within ten hours after birth due to respiratory distress (Hummler et al., 1996). In adult humans, glucocorticoids are also applied for the induction of lung liquid removal for instance in the case of high altitude pulmonary edema (Keller et al., 1995).

For the investigation of GR function in lung epithelial cells, we used the Cre/loxP recombination system to generate mice lacking the receptor specifically in these cells. Animals expressing the Cre recombinase under control of a 3.7kb promotor of the human Sftpc gene (Spc-Cre) were crossed with mice carrying a conditional GR allele. The resulting $GR^{Spc\text{-}Cre}$ mutants were born in mendelian frequency and survived to adulthood without macroscopic disturbances. Even when the GR dosage in non-targeted cells was reduced by introduction of one GR^{null} allele, these $GR^{null/flox}$/Spc-Cre animals were still obtained with the expected frequency of about 25%. The efficacy of the Spc-Cre line has been characterized before (Okubo and Hogan, 2004; Okubo et al., 2005) and immunohistochemistry confirmed the

successful ablation of GR protein specifically in all epithelial cells of the developing lung. As a consequence, these findings demonstrate that lung epithelial GR is not essential for survival.

Nevertheless, further histological analysis revealed a delayed progression through lung development in $GR^{Spc\text{-}Cre}$ embryos. Intriguingly, these effects were more prominently associated with the mesenchyme emphasizing the importance of epithelial-mesenchymal interactions and the developmental interconnectivity of the two compartments. Electron microscopy and morphometry revealed an increased thickness of the mesenchymal layer within the alveolar walls leading to significantly reduced airspace in mutant mice. In contrast, attenuation and differentiation of the epithelium were preserved and allowed the formation of a functional alveolar gas exchange unit. However, the observed developmental delay in $GR^{Spc\text{-}Cre}$ animals is only transient and can be compensated within the first days of life or during an artificially prolonged pregnancy.

5.3. Mesenchymal GR promotes progression through the canalicular phase of murine lung development and is indispensible for postnatal survival

The mild phenotype in the epithelial $GR^{Spc\text{-}Cre}$ mutants strongly indicated an important function of GR in the surrounding lung mesenchyme. Consequently, mice lacking GR specifically in mesenchymal cells ($GR^{Col1\text{-}Cre}$) were generated to investigate this conclusion. Remarkably, no mutants were found at weaning and observation of delivering mothers revealed that mutant pups died within the first hour after birth. They displayed respiratory distress and cyanosis reminiscent of the GR knockout phenotype.

This striking similarity of $GR^{Col1\text{-}Cre}$ lungs to the phenotype of GR knockout animals was further substantiated by histological examination of $GR^{Col1\text{-}Cre}$ and control lungs. As in the germ line mutation, branching morphogenesis and general lung development were not affected in $GR^{Col1\text{-}Cre}$ embryos until E16.5. Subsequently, however, mutant lungs failed to progress through the canalicular and saccular phase and still displayed the primitive morphology of the pseudoglandular phase at E18.5. Unexpanded alveolar tubes were surrounded by cuboidal epithelial cells resulting in the lack of both, alveolar airspace as well as a functional gas exchange unit. The mesenchymal compartment was significantly increased but showed a disorganized appearance and was characterized by extensive deposition of ECM. Nevertheless,

proximo-distal patterning of the epithelium was preserved, and although delayed, epithelial differentiation occurred as judged by differentiation markers and the presence of lamellar bodies.

Electron microscopy as well as immunohistochemistry identified an increased number of apoptotic cells in $GR^{Col1\text{-}Cre}$ mutants. However, considering the extremely low incidence of apoptosis during murine lung development (<1%) observed in this and other studies, it is unlikely that the moderate increase in $GR^{Col1\text{-}Cre}$ lungs has major consequences on the functional maturation of the mutant fetal lung (Bellusci et al., 1996; Lindahl et al., 1997).

Knowledge about GR functions in the lung mesenchyme has been limited. In lung epithelial cell lines, the maximal induction of surfactant synthesis by glucocorticoids was dependent on the co-culture of lung fibroblasts, leading to the suggestion of a so-called fibroblast pneumocyte factor (FPF) (Smith, 1979). Although the latter has never been identified, a number of signalling molecules with appropriate properties has been identified. In particular, FGF7 is expressed in lung mesenchymal cells and has been shown to be induced by glucocorticoids in cultured pulmonary fibroblasts. Conditioned medium of these cells exerted a stimulating effect on the surfactant synthesis in cultured lung epithelial cells and this could be partially blocked by an antibody against FGF7 (Chelly et al., 2001). Interestingly, FGF7 was found to be differentially regulated in $GR^{Col1\text{-}Cre}$ lungs compared to control littermates and this finding will be discussed below (see section 5.5.).

5.4. Profiling gene expression during the canalicular and saccular phase of murine lung development in controls and mutant mice

In general, GR acts as a ligand-dependent transcription factor and can thus be expected to mediate its essential effects through regulated expression of target genes. Profiling of gene expression using microarrays therefore not only advances the understanding of the observed phenotype to the transcriptional level but may also allow the identification of regulatory pathways critical for the GR-mediated maturation of the fetal lung.

The vast majority of studies on mice with lung phenotypes monitored gene expression exclusively at embryonic day E18.5, a time point when the morphological alterations are typically already fully established (Basseres et al., 2006; Okubo et al., 2005; Wan et al., 2004). This complicates a conclusive interpretation of the obtained

data, since the observed differences are unlikely to reflect primary effects of the mutation but rather characterize the transcriptional profile associated with the pathophysiological end point. Moreover, deployment of whole lung lysates for RNA extraction does in most cases not allow an assignment of the detected expression values to a specific cellular compartment. Alternatively, observed differences may be caused by relative changes in cell populations which affect their respective contribution to the RNA pool.

Therefore, physical separation of epithelial and mesenchymal cells would be desirable to allow the application of RNA extracts from specific cell types. While the clear separation of these two compartments until E16.5 may enable sampling by techniques such as laser assisted microdissection, their fusion and close interaction during terminal maturation precludes these approaches. In addition, microdissection as well as the alternative enzymatic treatment with consecutive cell sorting requires intensive and time-consuming manipulation of the lung samples, deteriorating RNA quality and giving rise to possible experimental artefacts.

Considering these general caveats of gene expression profiling on the developing lung, the following design for sampling and analysis was chosen. Whole lysates from mutant and control lungs were analyzed at E16.5 and E18.5, respectively, and special importance was given to the developmental profile between these two time points. The latter allows monitoring of the transcriptional changes which are associated with the progression through the canalicular and saccular phase of murine lung development in control embryos, as well as an assessment to which extent these processes are affected by the mesenchyme-specific loss of GR in the mutants. Importantly, analysis of expression levels for the mesenchymal marker gene vimentin did not reveal significant differences between $GR^{Col1\text{-}Cre}$ and control lungs indicating that mesenchymal and epithelial cells contributed to the RNA pool in a similar proportion in both genotypes. Moreover, this finding contributes an interesting aspect to the expansion of the mesenchymal compartment observed in the morphometric analysis. Together, these results suggest that the described phenotype in $GR^{Col1\text{-}Cre}$ lungs is caused by a failure to undergo appropriate morphogenetic maturation rather than mesenchymal hyperplasia alone. This is in accordance with the observation that the increase in proliferating cells was not restricted to the mesenchyme but affected the epithelium to a similar extent.

5.5. Mesenchymal GR interferes with known regulatory pathways of murine lung development to alter the proliferative state and the composition of the extracellular matrix

The analytical approach described above identified two critical processes to be affected by the conditional inactivation of GR in the developing lung mesenchyme, and these were further investigated by histological methods: Gene ontology analysis revealed an over-representation of genes connected to proliferation and cell cycle control, including well-known marker genes and regulators of lung development such as Cyclins A2 and B2, Ki67 and Nmyc. The latter has been shown to fulfil critical functions during lung development and is continuously expressed in mutant lungs from E16.5 to E18.5 while it is down-regulated in controls during the same period. Lung epithelium-specific deletion of Nmyc leads to a virtual absence of the lung while over-expression resulted in a phenotype similar to $GR^{Col1\text{-}Cre}$ animals characterized by impaired differentiation and ongoing proliferation. It has to be noted however, that Nmyc is exclusively expressed in the epithelium which precludes a direct effect of GR on its regulation (Okubo et al., 2005). $P21^{cip}$ is a cyclin-dependent kinase inhibitor and regarded as an important regulator promoting terminal differentiation and inhibiting proliferation (Besson et al., 2008). Accordingly, $p21^{cip}$ is significantly up-regulated in controls from E16.5 to E18.5 and this induction is completely abolished in mutant lungs. Interestingly, $p21^{cip}$ has been shown to be regulated by glucocorticoids in lung fibroblasts and other cell types, involving interaction of GR with the C/EBP (CCAAT/enhancer binding protein) family of transcription factors (Cram et al., 1998; Yang et al., 2007).

These findings of cell cycle dysregulation were corroborated by *in vivo* BrdU labeling of proliferating cells and consecutive histological analysis. Compared to controls, the proliferation index was significantly increased in $GR^{Col1\text{-}Cre}$ lungs. Yet, subsequent determination of separate values for mesenchymal and epithelial compartments did not reveal significant differences, indicating that mesenchymal loss of GR does not exclusively regulate proliferation in the mesenchyme but affects the general proliferation rate of the developing lung including the epithelium. One important group of growth factors involved in the pulmonary cell cycle control are Shh together with the FGF family, and mesenchymal loss of GR altered the expression levels of various effectors of this signalling complex (del Moral et al., 2006a; White et al., 2006).

Produced in the epithelium, Shh and FGF9 act on the mesenchyme to promote proliferation and their decline in the canalicular phase co-incides with a rise in FGF7 expression. In $GR^{Col1\text{-}Cre}$ lungs, FGF9 expression was only mildly attenuated, there was a considerable dysregulation of Shh and FGF9 target genes and the expression of FGF7 which is important for epithelial maturation and dilation was not induced (Cardoso et al., 1997; Tichelaar et al., 2000).

In addition to the impairment in the proliferative control in $GR^{Col1\text{-}Cre}$ lungs, the gene expression profiling also revealed a massive dysregulation of ECM components as well as ECM-modifying enzymes such as chitinase 3 or lysyl-oxidase. The observed changes affected all major constituents of the lung ECM, collagens (e.g. procollagen type IX alpha 1), elastic fibers (elastin, fibrillin and lysyl-oxidase) and proteoglycans (chondroitin sulfate proteoglycan), but also numerous cell surface molecules which interact with the ECM, for instance integrins.

This is likely to affect the morphogenetic development of the lungs in various ways: The ECM provides structural support, which is particularly critical for a largely hollow organ, and becomes additionally important during processes such as cell adhesion and migration (Francis et al., 2002; Nguyen and Senior, 2006; Sakai et al., 2003). Moreover, lung maturation involves aspects of remodelling such as the attenuation of the epithelium or the thinning of the alveolar septae, including the fusion of the bi-layered capillary system with the two epithelial layers. These processes can be expected to depend on the exertion of mechanical stretch and contraction, which in turn requires an appropriate anchorage. In addition, ECM functions have more recently been extended to the modulation of growth factor signalling by multiple modes such as enzymatic activation or inactivation of signalling molecules but also their sequestration or release. Thereby, the composition of the ECM influences the availability and activity of these molecules and thus determines their range of action (ten Dijke and Arthur, 2007).

Indeed, *in vivo* models revealed important functions during lung development for many of the ECM genes identified by the gene expression profiling. For example, the induced expression of elastin as well as its major crosslinking enzyme lysyl-oxidase was significantly attenuated in $GR^{Col1\text{-}Cre}$ animals and knockout studies demonstrated an essential role during the alveolar maturation for both genes (Maki et al., 2005; Wendel et al., 2000). Fibronectin is another major component of the ECM which is strongly induced in control animals during the late phase of lung development, and

this induction is almost completely absent in $GR^{Col1\text{-}Cre}$ embryos. While the inactivation of the fibronectin gene results in early lethality before E10.5 (George et al., 1993), fibronectin deposition and its interaction with its cellular receptors, the integrins, has been shown to mediate critical functions during lung morphogenesis (Araya et al., 2006; De Langhe et al., 2005; Kreidberg et al., 1996).

TGFβ-signalling plays a critical role in the orchestration of ECM composition and its resulting properties (Derynck and Akhurst, 2007; ten Dijke and Arthur, 2007). In the present study, mesenchyme-specific loss of GR was associated with the differential expression of various genes and processes regulated by TGFβ, and expression values for different types of TGFβ proteins were changed as well. This ventures speculations that GR might interact in particular with TGFβ signalling to promote maturation of the respiratory system. Indeed, GR has been shown to interact with the TGFβ effector SMAD3 leading to ligand-dependent transcriptional repression of the type-1 plasminogen activator inhibitor (PAI-1) gene (Song et al., 1999).

5.6. Fibroblast but not endothelial GR mediates the essential effects of glucocorticoids on lung maturation

Ablation of GR protein using the Col1-Cre transgene identified the lung mesenchyme as the critical site for glucocorticoid action during maturation of the respiratory system. However, the mesenchyme gives rise to a variety of cell types, including endothelial cells, smooth muscle cells as well as lipofibroblast and alveolar myofibroblasts. Therefore, investigating the effects on particular subpopulations may help to reveal potentially involved mechanisms.

The capillary system surrounding the alveoli arises through vasculogenesis from the mesenchymal compartment and is one of its major derivatives (Stenmark and Gebb, 2003). Moreover, mouse models have shown that disruption of signalling complexes important for this process such as VEGF or PDGF signalling interferes with normal lung development (Del Moral et al., 2006b; Lindahl et al., 1997; Yamamoto et al., 2007; Zeng et al., 1998). In addition, GR has been proposed to mediate glucocorticoid effects through transcriptional regulation of the VEGF receptor (Clerch et al., 2004). Since several of these factors known to determine endothelial development were differentially regulated in the expression profiling, a potentially critical function of GR in the lung through participation in the regulation of vascular differentiation was investigated.

However, immunohistochemistry for the endothelial marker Pecam1 did not reveal significant differences in staining pattern beyond those attributable to the morphological differences. In addition, mice lacking GR specifically in endothelial cells were generated, and these animals survived and did not show alterations in lung morphology at E18.5. These results exclude that GR fulfils an essential function through actions in endothelial cells.

Apart from that, the primitive lung mesenchyme gives rise to smooth muscle cells (SMC) and cells of the fibroblast lineage, namely alveolar myofibroblasts and lipofibroblasts. SMCs enclose the shaft of the developing respiratory tube during branching morphogenesis and surround the complete bronchial airways in the mature lung (Kim and Vu, 2006). Branching morphogenesis is not altered in $GR^{Col1\text{-}Cre}$ animals and the mutation affects primarily the differentiation and dilation of the most distal alveolar saccules. Therefore, SMCs are unlikely to participate significantly in the glucocorticoid-mediated maturation of the fetal lung.

Myofibroblasts and lipofibroblasts are predominantly characterized by their ability to provide contractile forces and lipid supply to the alveolar unit, respectively. However, their distinct actions have been studied mostly *in vitro*, and instead, overlapping functional and biochemical characteristics have been described *in vivo* (Kim and Vu, 2006; McGowan and Torday, 1997). Indeed, both cell types express smooth muscle actin and are involved in the deposition of ECM as well as the active participation in epithelial-mesenchymal signalling, which is in agreement with the observed effects in $GR^{Col1\text{-}Cre}$ animals. Taken together, the exclusion of all other major cell types implies that GR exerts its essential function during lung development in cells of the fibroblast lineage, namely lipo- and/or myofibroblasts.

It should be also noted that previous studies ablating GR in the central nervous system precluded that GR has a critical impact on lung function through regulatory action in the nervous system and in particular within the nervous control of respiratory movements and/or reflexes (Tronche et al., 1999).

5.7. Conclusion and Outlook

Progression through the later phases of murine lung development requires a developmental switch from the pseudoglandular phase characterized by proliferation and growth, towards growth arrest and differentiation, which are necessary for terminal maturation during the canalicular and saccular stage. The developmental

timing of this process co-incides with the increase of pulmonary GR expression as well as the surge in fetal corticosteroid levels observed from E16.5 until birth. In agreement with these pre-conditions, gene targeting experiments in this study proved that GR exerts key functions during lung morphogenesis by initiating the transition to the developmental phase of reduced proliferation and terminal differentiation.

In contrast to common understanding, the present work demonstrates that epithelial GR is dispensable for the completion of murine lung development. Instead, conditional gene inactivation evidenced that GR serves its essential role in the mesenchyme and more precisely in cells of the fibroblast lineage. Glucocorticoid signalling in these cells has a major impact on the composition of the extracellular matrix and thereby modulates mesenchymal-epithelial interactions. Moreover, it influences regulatory complexes of lung development such as TGFβ or FGF signalling which are known to participate in the proliferative and morphogenetic control.

Identification of the critical cell type and the central effects *in vivo* should facilitate the investigation of the molecular mechanisms at their basis and this may finally allow the identification of interaction partners participating in the essential functions of GR during lung development.

6. Materials and Methods

5.8. Materials

6.1.1. Chemicals and enzymes

In general, chemicals and enzymes were purchased from the following companies:

Chemicals
BioRad, Munich
Difco, Detroit
Fluca, Neu-Ulm
VWR international, Darmstadt
Roth, Karlsruhe
Serva, Heidelberg
Sigma-Aldrich, Munich
Applichem, Darmstadt

Radionucleotides
Amersham, Braunschweig

Enzymes
Roche, Mannheim
New England Biolabs, Schwalbach
Invitrogen, Karlsruhe
Stratagene, Heidelberg
Promega, Heidelberg

6.1.2. Standard solutions

10x PBS (phosphate buffered saline)

1.37M	NaCl
100mM	Na_2HPO_4
27mM	KCl
20mM	KH_2PO_4

pH 7.2

TE

10mM	Tris/HCl, pH8.0
1mM	EDTA

50x TAE (Tris acetate EDTA buffer)

2M	Tris base
50mM	EDTA
250mM	NaAc

pH 7.8 (glacial acidic acid)

20x SSC (standard sodium citrate buffer)
3M NaCl
0.3M NaCitrate
pH 7.0

10x TBE
2M Tris
250mM NaAc
50mM EDTA
pH 7.8 (glacial acetic acid)

6.1.3. Media

LB-medium
10g Bacto-Trypto (Difco)
5g yeast extract (Difco)
5g NaCl
ad 1l H_2O
pH 7.2 (NaOH), autoclaved

LB-agar
1x LB-medium
1.5% (w/v) bacto agar (Difco)

6.1.4. Bacteria

NM554
This bacterial strain provided by Stratagene was used as standard host for the cloning of plasmids. Transformation of plasmids into preparations of competent bacteria was performed by heat-shock at 42°C.

EL250
These bacteria were used for ET-recombination according to Copeland/Court (Lee et al., 2001), described in 6.3.1. They contain the lambda prophage recombination system (Yu et al., 2000) and a gene encoding the Flp recombinase. The transcription of the Flp recombinase can be induced by arabinose while the recombination system is under control of a temperature-sensitive repressor. Therefore, the bacteria are grown at 32°C and are only shifted to 42°C when recombination is desired.

6.1.5. Plasmids

pConst and pIndu
These plasmids, generated and provided by Dr. Erich Greiner (Evotec, Germany), were used to prepare the targeting constructs for the insertion of a Cre or $CreER^{T2}$ cassette into a BAC vector by homologous recombination in bacteria. The plasmids contain a cassette encoding the codon-improved Cre recombinase (Shimshek et al., 2002) or a fusion protein consisting of the latter and a mutated ligand-binding domain of the human estrogen receptor (Feil et al., 1997). In addition, the plasmids harbor an ampicillin resistance cassette flanked by two FRT sites, which can therefore be removed by the Flp recombinase.

6.1.6. Primers for genotyping

Primers were purchased from MWG Biotech AG, Munich and the following conditions were applied:

GR alleles and Rosa26:

95°C	5min	
95°C	30s	
63°C	45s	35x
72°C	60s	
72°C	5min	
4°C	∝	

GR1	Forward	5´ – GGC ATG CAC ATT ACG GCC TTC T – 3´
GR4	Reverse	5´ – GTG TAG CAG CCA GCT TAC AGG A – 3´
GR8	Reverse	5´ – CCT TCT CAT TCC ATG TCA GCA TGT – 3´

amplicons: GR^{wt} → 225bp, GR^{flox} → 275bp, GR^{null} → 390bp

Rosa1	Forward	5´ – TCT GCT GCC TCC TGG CTT CTG A – 3´
Rosa2	Reverse	5´ – CCA GAT GAC TAC CTA TCC TCC CA – 3´
Rosa3	Reverse	5´ – AAG CGC ATG CTC CAG ACT GCC T – 3´

amplicons: ROSA26 locus → 270bp, ROSA26 Cre reporter → 420bp

Col1-Cre and Tie2-Cre^{ERT2}:

95°C	5min	
95°C	30s	
59°C	45s	35x
72°C	60s	
72°C	5min	
4°C	∝	

CreERT2_f	Forward	5´ – TCC AAC CTG CTG ACT GTG CAC CA – 3´
CreERT2_r	Reverse	5´ – GTC AGT GCG TTC AAA GGC CAG G – 3´

amplicon: Cre → 450bp

Spc-Cre:

95°C	5min	
95°C	30s	
54°C	45s	35x
72°C	60s	
72°C	5min	
4°C	∝	

Spc-Cre1	Forward	5´ – GGC TAT ACG TAA CAG GG – 3´
Spc-Cre2	Reverse	5´ – TCG ATG CAA CGA GTG ATG AG – 3´

amplicon: Cre → 500bp

5.9. Standard techniques in molecular biology

6.2.1. Cloning into plasmid vectors and sequencing

Cloning of DNA fragments into plasmid vectors was performed following standard protocols as described in Sambrock et al. (1989). Methods to obtain DNA fragments and vectors to clone the different plasmid constructs included PCR amplification, (sequential) digestion with restriction enzymes, dephosphorylation of DNA ends with Shrimp alkaline phosphatase (Roche), phosphorylation of DNA ends with polynucleotidekinase as well as ligation of DNA fragments using T4-DNA-ligase. Isolation of DNA fragments from agarose gels was performed using the Qiaquick Gel-Extraction Kit (Qiagen). Competent bacteria of the strain *E.Coli* NM554 were generally transformed by heat-shock at 42°C and spread on LB-agar plates. Recombinant plasmid DNA was then isolated from positive transformants as described in section 6.2.3.1.
Sequencing was performed at MWG Biotech AG, Munich from plasmid DNA using 10µM of an appropriate primer.

6.2.2. Homology arms of the construct used to generate the mSftpc-Cre transgene

Preparative PCRs were performed using *Pfu*-polymerase and the following program:

95°C, 30s/63°C, 1min/72°C, 1min, 35 cycles; finally 72°C, 10min

5´homology arm for mSftp-Cre transgene
as template served a mSftpc BAC DNA preparation

Spc5endfor	forward	5´ – GTT TAA ACA CAC CCA CGG TGA GA – 3´
Spc5endrev	reverse	5´ – ATC CAT TTT GTA AGG TTT CTC TCT C – 3´

amplicon: 397bp

3´homology arm for mSftpc-Cre transgene
as template served a mSftpc BAC DNA preparation

Spc3endfor	forward	5´ – AGC GTA TCT AGA GTG AGT GTG ATT GTG TGT GT – 3´
Spc3endrev	reverse	5´ – AAC CAT GCT AGC GTT TAA ACA GTG TGC ACC TCT ATG – 3´

amplicon: 365bp

6.2.3. Isolation of DNA

6.2.3.1 Isolation of plasmid DNA from bacteria

Bacterial cultures were inoculated and grown overnight in 2ml (mini-prep) or 50ml (midi-prep) of LB-medium containing the appropriate antibiotic (100µg/ml ampicillin or 50µg/ml kanamycin). Isolation of plasmid DNA was done using the Quiagen Mini spin or Midi/Maxi Kit (Cartridges) according to instructions supplied by the manufacturer.

6.2.3.2 Isolation of BAC DNA from bacteria

Due to its size (about 150-200kb circular supercoiled DNA) and low abundance (1-2 copies/bacterium), modified protocols were applied for the isolation of BAC DNA from bacteria. All reagents and columns were from Quiagen.

6.2.3.3 Mini-prep of BAC DNA

Bacterial cultures were inoculatied and grown overnight in 2ml LB-medium containing 25µg/ml chloramphenicol. After centrifugation at 3 000rpm for 10min, the pellet was resuspended in 300µl buffer P1 and alkaline lysis was achieved by addition of 300µl buffer P2. Following neutralization by 300µl buffer P3, the preparation was centrifuged at 14 000rpm for 10min, the supernatant was transferred into a new tube and the DNA was precipitated by addition of 600µl isopropanol. The pellet, resulting from centrifugation at 14 000rpm for 10min was washed once in 70% ethanol to remove salt, air dried and resuspended in 40µl TE buffer. The concentration and quality of the preparation were verified spectrophotometrically and by gel electrophoresis after appropriate restriction digestion of the BAC.

6.2.3.4 Midi-prep of BAC DNA

50ml LB-medium containing 25µg/ml chloramphenicol were inoculated and grown overnight. Lysates were prepared as described for the mini-prep using 5ml of the respective buffers P1-P3. After centrifugation at 4 000rpm for 10min, the supernatant was filtered through cheese cloth and the DNA was precipitated by addition of 10ml isopropanol and centrifugation at 8 000rpm for 15min. The pellet was resuspended in 1ml QBT buffer and applied to an equilibrated Q20 column. The DNA was washed twice with 2ml QC buffer before elution with 800µl warm QF buffer (70°C) The eluate was again precipitated with 560µl isopropanol (centrifugation at 14 000rpm for 10min), the pellet washed with 70% ethanol, air dried and resuspended in 25µl TE buffer. As for the Mini-prep, the concentration and quality of the preparation were verified spectrophotometrically and by gel electrophoresis after appropriate restriction digestion of the BAC.

6.2.3.5 Isolation of DNA from mouse tails and organs

NID-prep
After weaning around four weeks after birth, mice were labelled with an earmark and a piece of tail was taken (1-2mm). The latter was digested in 200µl NID buffer containing 2µl proteinase K at 56°C overnight. The next morning, proteinase K was heat-inactivated by incubation at 96°C for 10min and the resulting DNA preparation was used as template for genotyping the mice by PCR (section 5.1.6.).

NID buffer

50mM	KCl
10mM	Tris/HCl (pH8.3)
2mM	$MgCl_2$
0.1mg/ml	gelatin
0.45%	NP40
0.45%	Tween20

Tail-prep
To obtain higher amounts of pure DNA for Southern or dot blot analysis, a larger piece of tail (~5mm) was taken and digested in 760µl tail buffer with 40µl proteinase K (10mg/ml) at 56°C overnight. The reactions were agitated on a shaking incubator for 5min, 260µl of saturated NaCl were added and the mixture agitated again. The precipitate was spun down by centrifugation for 10min at 13 000rpm and 800µl of the supernatant were transferred into a pre-spun 2ml Heavy Phase Lock Gel tube (Eppendorf). The same volume of Phenol/Chloroform/Isoamyl Alcohol (25:24:1) was added and mixed well by repeated inversion before centrifugation at 13 000rpm for 5min. The aqueous phase was transferred to a new tube, 600µl isopropanol were added and the DNA was allowed to precipitate for 5min with light agitation. Subsequent to centrifugation at 13 000rpm for 10min, the resulting pellet was washed with 70% ethanol, air dried and resuspended in 100µl TE buffer.

Tail buffer

50mM	Tris/HCl, pH8
100mM	EDTA
100mM	NaCl
1%	SDS

6.2.4. Southern blot analysis

6.2.4.1 Synthesis of radioactively labeled DNA probes

The generation of radioactive labelled DNA probes was performed using a modified protocol of Feinberg (Feinberg and Vogelstein, 1983). Around 100ng of the appropriate DNA fragment were filled up with water to achieve a final volume of 33µl. The DNA strands were separated by incubation at 95°C for 5min followed by immediate transfer to ice. After addition of 10µl 5x OLB-C, 5µl [α-^{32}P]-dCTP

(3000Ci/mmol) and 2µl Klenow polymerase (2U/µl) the reaction was incubated for a minimum of 2h at 37°C.
Prior to addition to the pre-heated hybridization buffer, the labeled probe was denatured for 5min at 95°C followed by immediate transfer on ice.

5x OLB-C (stored at –20°C)
100µl Sol.A
250µl Sol.B
150µl Sol.C

Sol.O

625µl	2M Tris/HCl, pH 8
125µl	1M $MgCl_2$
250µl	H_2O_{dd}

Sol.A

1ml	Sol.O
18 µl	β-mercaptoethanol
5µl each	100mM dATP, dGTP, dTTP

Sol.B
2M HEPES, pH6.6 (adjust pH with 4M NaOH)

Sol.C
random Hexamers pd $(N)_6$
50 OD_{260}units dissolved in 550µl TE

6.2.4.2 Southern transfer of genomic DNA

Appropriate DNA preparations were digested by restriction enzymes, separated on an agarose gel, transferred to a membrane and hybridized with a radioactive probe. The transfer of the separated DNA from the gel to the membrane was performed following the protocol of Southern (Southern, 1975).
Approximately 30µg of a tail-prep were digested with the desired restriction enzyme/s overnight, loaded onto a 1% agarose gel (poured with 1x TAE) and separated for 5-6hrs with 90V using 1x TAE as running buffer. The DNA was first partially depurinated by 10min incubation of the gel in 0.25M HCl followed by denaturation of DNA through 3x15min treatment of the gel with 0.4M NaOH.
The DNA was transferred to a positively charged nylon membrane in 20x SSC with a capillary blot (Sambrook and Russell, 2001) overnight. After equilibrating the membrane in 20x SSC, the blot was built in the following order: 1x Whatman, gel, membrane, 3x Whatman rinsed in 20x SSC, 3x Whatman (dry), stack of filter papers mounted with a small weight. The next morning, the membrane was rinsed briefly in 25mM NaP-buffer, 1mM EDTA pH 8.0 and dried at room temperature (RT). The DNA was fixed on the membrane by UV-light (Stratalinker UV 1800, Stratagene) using the auto crosslinking program.

1M NaP buffer
71g Na_2HPO_4 (hydrogen-free) or 89g Na_2HPO_4 $(H_2O)_2$ were dissolved in 800ml H_2O_{dd} and adjusted with H_3PO_4 (85%) to pH 7.2. H_2O_{dd} was added to 1l total volume and the buffer was autoclaved.

6.2.4.3 Transfer of genomic DNA by dot blot

Dot blot allows large-scale screening of genomic DNA for the presence of a specific sequence, e.g. a transgene. The DNA is fixed on a nylon membrane using a vacuum dot blot manifold system (Schleicher & Schüll).
3µl 2M NaOH were added to 27µl of a tail-prep and the mix was incubated for 10min at RT. The blot is built according to the manufacturer's instructions including 2x Whatman followed by the membrane, both rinsed in 2x SSC. The DNA was applied and sucked into the membrane followed by addition of 200µl 10x SSC per well. The membrane was removed, rinsed briefly in 25mM NaP buffer, 1mM EDTA pH 8.0 and dried at RT. The DNA was fixed on the membrane by UV-light (Stratalinker UV 1800, Stratagene) using the auto crosslinking program.

6.2.4.4 Hybridization with radioactively labelled probes

The hybridization of the genomic DNA, fixed on a nylon membrane (by Southern or dot blot), was performed following the protocol of Church and Gilbert (Church and Gilbert, 1984). The membrane was briefly rinsed in 25mM NaP buffer, 1mM EDTA pH 8.0 and transferred to a glass tube filled with pre-heated hybridization buffer (Church-Gilbert buffer). The denatured probe was added to the Church-Gilbert buffer and hybridization was performed overnight at 65°C. The next morning, the membrane was rinsed 2x10min in the glass tube in washing buffer, wrapped in Saran foil and exposed to either a film (Kodak) in a cassette containing an intensifier screen at -80°C or a phosphoimager screen at RT.
For determination of transgene copy number, the membrane was exposed to a phosphoimager screen for several days and relative band intensities were assessed by phosphoimager (BAS-1800; Fuji) and subsequent quantification by Aida V 2.0. The band originating from the endogenous gene was calculated as two copies.
If the membrane needed to be hybridized with a second probe, the old probe was removed by 20min incubation of the membrane in 0.4M NaOH at RT followed by subsequent rinsing in 0.25M NaP buffer, 1mM EDTA 3x for 10min.

6.2.4.5 Hybridization buffer (Church-Gilbert)

50ml	1M NaP buffer, pH 7.2
35ml	20% SDS (Bio-RAD)
200µl	0,5M EDTA, pH 8.0
	H_2O_{dd} ad 100ml

<u>Washing buffer</u>

40ml	1M NaP-buffer
50ml	20% SDS (Bio-RAD)
2ml	0,5M EDTA, pH 8.0
	H_2O_{dd} ad 1l

pre-heated to 80°C before use, otherwise stored at RT

6.2.5. Genotype determination by PCR

To determine the genotype of a mouse by PCR, 2µl genomic DNA prepared from a piece of tail (section 6.2.3.5.) were analyzed using *Taq*-DNA-polymerase (Roche) in a 25µl reaction volume according to the manufacturer's instruction.
The conditions for all genotyping PCRs performed in this study were as indicated in section 6.1.6. together with the oligo sequences.

PCR products were mixed with 6x loading buffer and separated on a 2% agarose gel containing 2µl ethidiumbromide (10mg/ml) per 150ml gel.

6x loading buffer

0.25%	bromophenol blue
0.25%	xylene cyanol FF
15%	Ficoll 400

6.2.6. Pulse-field gel electrophoresis (PFGE)

This technique applies an alternating voltage gradient and has been developed to electrophoretically separate large pieces of DNA beyond the resolution of standard agarose gel electrophoresis (>15-20kb) (Schwartz and Cantor, 1984). BAC DNA preparations were appropriately digested and resolved on a 1% Sea-plug low melting point agarose (Sigma) gel in 0.5x TAE running buffer using the following parameters: initial t_{switch}=0.5s, final t_{switch}=20s, included angle α=120°, $|E|$=6V/cm, I≈140mA, total time T=14h and cooling at 14°C. The gel was afterwards stained with ethidium bromide 1:20 000 in water.

5.10. Generation of transgenic mice

6.3.1. Modification of a BAC by homologous recombination in bacteria

Recombinant DNA molecules were generated by homologous recombination in bacteria (ET-cloning) using the method of Copeland and Court (Lee et al., 2001; Yu et al., 2000). This method allows the integration of a linear DNA sequence into a homologous region of an acceptor vector. In the present study, the acceptor vector was a bacterial artificial chromosome (BAC) harboring ~163kb of genomic DNA (RP24-252D18) that was chosen from the NCBI CloneFinder homepage (http://www.ncbi.nlm.nih.gov/genome/clone/clonefinder/CloneFinder.html). The BAC was ordered at the Children's Hospital Oakland Research Institute (http://bacpac.chori.org) and the ends of the genomic insert were sequenced and blasted to the mouse genome to verify the identity and integrity of the BAC clone.
This BAC was modified by homologous recombination in EL250 cells to insert a cassette encoding a codon-improved Cre recombinase (Cre) (Shimshek et al., 2002) and an ampicillin resistance cassette flanked by two FRT sites. For the Tie2-CreER^{T2} this cassette contained the CreER^{T2} fusion protein consisting of a codon-improved Cre recombinase (Cre) (Shimshek et al., 2002) and a mutated ligand-binding domain of the human estrogen receptor (ER^{T2}) (Feil et al., 1997).

6.3.2. Preparation of the Cre-containing plasmid and the linear fragment for homologous recombination

To introduce a linear DNA fragment by homologous recombination into a genomic DNA sequence, the linear fragment has to be flanked by fragments homologous to the acceptor sequence, the homology arms. It has been shown (Zhang et al., 1998) that the homology arms and the acceptor DNA have to contain about 50bp overlap to achieve high recombination efficiency.
In order to introduce the Cre cassette into the BAC harboring the genomic sequence of the mouse Sftpc locus, a 397bp 5´homology arm and a 365bp 3´homology arm were amplified by PCR. The 5´homology arm contained the ATG of the mSftpc gene at its 3´end and the 3´homology arm started with the beginning of the first intron. With the primers additional restriction sites were introduced into the homology arms allowing the cloning of the arms into the plasmid pConst, subsequent analytical digestion of the modified plasmid and finally the release of the linear targeting construct. The following restriction sites were introduced into the 5´homology arm: An EcoRV halfsite at the 3´end (reconstitution of the EcoRV restriction site in pConst) and a PmeI halfsite at the 5´end (generation of a PmeI restriction site in pConst). Into the 3´homology arm an XbaI restriction site was introduced at the 5´end. At its 3'end, a PmeI site was followed by a NheI halfsite (generation of a NheI restriction site in pConst).
The PCR products were separated on an agarose gel and isolated as described before (section 6.2.5.). The 5´homology arm ending with the ATG was phosphorylated using polynucleotidekinase (Roche) and cloned in front of the Cre coding sequence into the pConst plasmid (EcoRV digested and dephosphorylated). The 3´homology arm was first digested with XbaI and NheI to generate sticky ends and cloned downstream of the FRT-flanked ampicillin cassette into the modified pIndu (containing the 5´homology arm; NheI digested and dephosphorylated). The final targeting vector containing both homology arms, one upstream of the Cre coding sequence and one downstream of the FRT-flanked ampicillin resistance cassette was released from the plasmid by PmeI digestion and the linear fragment was isolated by phenol/chloroform extraction.

6.3.3. Preparation of competent bacteria for transformation with the BAC

Single colonies of EL250 bacteria (Copeland/Court) were inoculated in 5ml LB-medium at 32°C. 2ml of the overnight culture were transferred to 50ml LB-medium and incubated at 32°C for 3-4hrs. When reaching the log phase (OD=0.4-0.5), the cells were cooled on ice and centrifuged for 10min at 4°C, 3 000rpm. The cell pellet was resuspended in 50ml of ice cold 10% glycerol and centrifuged again for 10min at 4°C, 3 000rpm. After a total of three washing steps, the supernatant was poured off and the pellet was resuspended in the remaining 10% glycerol resulting in a final volume of 0.6-0.7ml. 50µl aliquots of the cells were transferred into pre-cooled eppendorf tubes and frozen in liquid nitrogen.

6.3.4. Re-transformation of the BAC

Mini-prep of the BAC, present in the former host bacteria, was prepared according to section 6.2.3.3. The competent EL250 cells were thawed on ice and the electroporation cuvettes were pre-cooled on ice as well. A series of 1µl, 2µl and 5µl

of the BAC mini-prep were added to 50µl competent cells respectively, followed by electroporation at 2.3kV (BioRad Gene Pulser, 25µF with Pulse controller set to 200Ω). 1ml LB-medium was added afterwards, the cells were transferred into Eppendorf tubes and incubated for 1h at 32°C. Finally 100µl of the cells were plated directly on LB-plates containing chloramphenicol (25µg/ml), whereas the remaining cells were centrifuged, resuspended in 100µl LB-medium and plated on a second chloramphenicol plate.

6.3.5. Preparation of competent bacteria for homologous recombination

Single colonies were picked from EL250 bacteria containing the desired BAC clone and inoculated in 5ml LB-medium/chloramphenicol (25µg/ml) at 32°C overnight (O/N). The next day, 2ml of the O/N culture were transferred into 50ml LB-medium and incubated at 32°C for 3-4hrs. When cells reached the log phase (OD=0.4-0.5), the RED-recombination system was induced by 15min shaking in a 42°C water bath. After incubation, the cells were rapidly cooled down and incubated on ice for 10-40min. Subsequent washing steps with 10% glycerol, resuspension and freezing in 50µl aliquots followed, as described in section 6.3.3.

6.3.6. ET recombination and removal of the ampicillin resistance cassette

0.1pmol of the linearized and purified construct were electroporated into the RED-induced bacteria at 2.3kV (BioRad Gene Pulser, 25µF with Pulse controller set to 200Ω). The cells were incubated in additional 1ml LB-medium for 1h as described before and plated on LB-plates containing chloramphenicol (25µg/ml) and ampicillin (50µg/ml) followed by incubation at 32°C (at least for 16hrs). Colonies were picked and BAC mini-preps were performed followed by diagnostic digestion with frequent cutting enzymes to verify successful ET-recombination.
The Cre and CreER^{T2} constructs contain an ampicillin resistance cassette to select for the BAC that underwent homologous recombination with the construct. After homologous recombination in bacteria, the resistance cassette was removed from the modified BAC. Since the cassette is flanked by two FRT sequences, it can be excised by the Flp-recombinase, which can be induced in EL250 bacteria by L-arabinose (Sigma). Of the recombined clone, a 5ml O/N culture (containing 25µg/ml chloramphenicol) was incubated at 32°C and the next day a 1:50 dilution of the culture was prepared and incubated at 32°C until cells reached an OD of 0.5. Then cells were treated for 1h with 0.1% L-arabinose at 32°C, diluted 1:10, incubated an additional hour and plated onto chloramphenicol (25µl/ml) LB-plates followed by incubation at 32°C. After O/N incubation, colonies were picked and transferred into 5ml LB-medium (containing 25µg/ml chloramphenicol). After O/N incubation, a small aliquot of the culture was incubated for few hours in LB-medium containing chloramphenicol (25µl/ml) and ampicillin (50µg/ml) to verify the loss of the ampicillin resistance cassette by negative selection. From a culture that was not growing in ampicillin LB-medium, a BAC mini-prep was performed with subsequent diagnostic digestion by analytical pulse-field gel electrophoresis (PFGE).

6.3.7. Preparation of linearized BAC DNA using a gel filtration column

100µg of BAC Midi DNA from the verified clone were digested O/N with NotI which was then heat-inactivated at 65°C for 10min. ~50ml Sepharose CL4b were

equilibrated to injection buffer, degassed and used to pour a column in a 5ml plastic pipette. After application of the digested BAC, injection buffer was continuously added from a reservoir and 300µl fractions were collected. Fractions containing DNA were identified by UV-spectroscopy and analyzed by pulse-field gel electrophoresis.

Injection buffer

10mM	Tris/HCl, pH 7.5
0.1M	EDTA
100mM	NaCl

6.3.8. DNA microinjection in mouse oocytes

The microinjection of DNA into mouse oocytes was performed according to the protocol of Hogan (Hogan et al., 1994). Superovulated fertilized FVB/N females were used as source of oocytes. To induce superovulation, females were first injected intraperitoneally with PMS-gonadotropin (Sigma) and 48 hours later with chorion-gonadotropin (Sigma). After administration of chorion-gonadotropin, the females were mated with FVB/N males and were analyzed for the presence of a vaginal plaque the following morning. Positive females were sacrificed the morning after the mating by cervical dislocation, the oviducts were removed and transferred into 37°C-warm M2-medium. Oocytes were isolated and cumulus cells surrounding the oocytes were removed by hyaluronidase treatment (100mg/ml in M2-medium; Sigma). Oocytes were then rinsed in M2-medium, transferred into M16-medium and incubated at 37°C. For microinjection, 30 oocytes were transferred in an injection syringe containing M2-medium and placed under a microscope with two micromanipulator setups connected to a hydraulic control system (Eppendorf femtoJet). Oocytes were fixed with a blunt pipette and the tip of the injection needle was filled with the prepared DNA. The DNA was injected at a concentration of 1µg/µl or 2µg/µl in a volume of 1-2pl into the larger male pronucleus and oocytes were subsequently incubated for 2hrs in M16-medium at 37°C and controlled for their vitality.
To transfer the oocytes into foster mothers, pseudopregnant FVB/N females (mated with vasectomized males one day before) were intraperitoneally injected with Ketavet and Rompun (0.01ml of a 1:10 in PBS diluted solution per g bodyweight) to anesthetize the animals. To transfer the oocytes, the operation site was desinfected with EtOH, the abdominal cavity was opened and the oviduct was pulled out. Using a binocular the oocytes were injected into the oviduct, it was returned to the abdominal cavity and the wound was closed with clamps. The females delivered 18 days after the surgery and 5-15% of the offspring were expected to be transgenic.

M2-medium

20ml	10x A
3.2ml	10x B
2ml	33mM sodiumpyruvate (Serva)
2ml	171.4mM $CaCl_2$ $(H_2O)_2$
16.8ml	250mM HEPES (sodiumsalt, Sigma)
156ml	H_2O
800mg	BSA (Serva)

pH 7.4 (NaOH)

M16-medium

20ml	10x A
20ml	10x B
2ml	33mM sodiumpyruvate (Serva)
2ml	171.4mM $CaCl_2$ $(H_2O)_2$
156ml	H_2O
800mg	BSA (Serva)

pH 7.4 (NaOH)

10x A

47mM	NaCl
47.75mM	KCl
11.9mM	KH_2PO_4
232.8mM	sodium lactate (Sigma)
55.6mM	D-glucose
0.6g/l	penicillin (Seromed)
0.5g/l	streptomycin (Seromed)

10x B

250mM	$NaHCO_3$
max. 5mg	phenol red (Sigma)

5.11. Mouse work

All mouse lines were maintained on a C57Bl6 background and respective wildtype mice for backcrosses were obtained by Charles River Laboratories (Wilmington, USA). In the case of the two germ line mutations, heterozygous animals were mated to generate litters containing mutants ($GR^{null/null}$, dedicated GR^{null}, or $GR^{dim/dim}$, dedicated GR^{dim}) as well as controls ($GR^{wt/wt}$). Litters containing conditional mutant mice were generally produced by crossing $GR^{flox/wt}$ and Cre-positive animals with $GR^{flox/flox}$ animals.

6.4.1. Animal treatment

6.4.1.1 Treatment with tamoxifen

Tamoxifen (Sigma) was dissolved in sunflower seed oil/ethanol (10:1) mixture at a final concentration of 10mg/ml. Eight weeks old mice were injected intraperitoneally with 1mg of tamoxifen twice per day for five consecutive days. Vehicle-treated animals were injected with 100µl of sunflower seed oil/ethanol mixture.

Tamoxifen

500µl $EtOH_{abs}$ and 4,5ml sunflower seed oil (Sigma) were added to 50mg tamoxifen (Sigma). After slow rotation for about 2hrs at room temperature to dissolve the tamoxifen, the solution was stored at 4°C and used for up to three days.

6.4.1.2 Treatment with bromodeoxyuridine (BrdU)

2hrs before the cesarean section, mothers were injected intraperitoneally with 300mg BrdU/kg bodyweight.

BrdU
250mg BrdU (Sigma) were dissolved in 16.7ml PBS (15mg/ml stock) by incubation at 50°C. 20µl stock solution were injected per g bodyweight.

6.4.1.3 Treatment with Dexamethasone

Animals were intraperitoneally injected with 0.1mg dexamethasone/kg bodyweight and sacrificed 2hrs later.

Dexamethasone and vehicle
1mg Dexamethasone (γ-irradiated, Sigma) was solved in 1ml $EtOH_{abs}$. This stock solution was diluted 1:100 in H_2O_{dd} resulting in a final concentration of 0.01µg/µl. The animals were injected with 10µl/g bodyweight.

5.12. Collection of organs

Staged matings were set up to harvest embryonic organs at desired stages of fetal development. The presence of a vaginal plug in the morning indicated successful mating and noon of the same day was designated E0.5. At the embryonic day of interest, mothers were killed by CO_2 and the pups were collected by caesarean section. Complete uteri were removed and transferred to ice-cold PBS. Only when the potential of the embryos to survive was to be tested, they were quickly dissected out at RT and allowed to recover on a warming plate. A piece of the tail was taken from dead pups for later genotyping and the lungs were dissected. After a quick wash in PBS they were transferred to 4% PFA and further processed as described below.

5.13. RNA analyses – gene expression profiling

Profiling of gene expression was performed on lungs from $GR^{Col1\text{-}Cre}$ animals and controls that were collected as described in section 6.5. Left lung lobes were immersed in RNALater solution (Sigma-Aldrich Chemie GmbH, Munich, Germany), snap frozen in liquid nitrogen and stored at -80°C. Total RNA was prepared with the RNeasy Mini Kit (Qiagen, Hilden, Germany) and its quality was assessed on RNA LabChips (Agilent, Santa Clara, CA, USA). Microarray experiments were carried out using GeneChip Mouse Genome 430A 2.0 arrays (Affymetrix, Santa Clara, CA, USA). Labeling of the target RNAs (1-2µg total RNA), hybridization and scanning of the microarrays was performed according to manufacturer's instruction.
Two time points, E16.5 and E18.5, were analyzed for mutants and controls, respectively. For each of the four conditions, five GeneChips were used each representing one animal.
Analysis of array data was performed using the R/Bioconductor and MeV 4.0. Data was normalized and expression values were computed using the gcrma method. Ontology analyses were performed using GOstat and ErmineJ. Analysis of transcription factor binding sites in co-expressed genes was performed using oPossum (Ho Sui et al., 2005) using the following parameters: top 20% of mouse-to-

human conserved non-coding regions (minimum 65% identity) within 2 000bp of the transcription site (in both directions) were considered. Matrix match score was set to 80%, results with z-score>10 and Fischer exact test p<0.001 were considered as significant.

5.14. Protein analyses – extraction of mouse organs and preparation for immunohistochemical analysis

Preparation of paraffin sections

Lungs were collected as described in section 6.5. and fixed in 4% PFA overnight. Organs were subsequently washed 3x for 5min in PBS at RT and dehydrated through an increasing ethanol gradient: 3x 30min 70%EtOH, 1h 80%EtOH, 1h 95%EtOH, 3x 1h $EtOH_{abs}$. The dehydrated organs were incubated in glass cuvettes for 30min in xylene followed by O/N incubation in xylene. The next day, the xylene was replaced with fresh xylene and organs were heated up to 56°C for 1h. The following steps took place at 56°C. Half of the xylene was replaced with liquid paraffin and the organs were incubated in this 1:1 xylene/paraffin mixture for 1h. Subsequently, the samples were immersed in pure paraffin which was exchanged three times every hour. Finally the organs were embedded in paraffin in small plastic molds and cooled down to solidify the paraffin. These paraffin blocks were stored at 4°C.

Paraffin sections of the embedded organs, with a thickness of 6µm for immunohistochemistry or 4.5µm for histology, were prepared using a microtome (Leica). The sections were smoothened on a 42°C water bath, transferred onto Superfrost Plus glass slides (Roth) and fixed O/N at 56°C. The paraffin sections were stored at RT.

4% PFA

300ml H_2O_{dd} were heated to 100°C in a microwave and subsequently mixed with 150ml room temperature H_2O_{dd}. 20g PFA were helped to dissolve therein by addition of 100µl 10M NaOH on a stirring plate. When the PFA was dissolved completely, 50ml of 10x PBS were added and the solution cooled down to 4°C.

For all applications with β-galactosidase staining, 5mM EGTA and 2mM $MgCl_2$ were added.

PBS

120mM	NaCl
28mM	Na_2HPO_4
2.5mM	KH_2HPO_4

5.15. Histology and immunohistochemistry

6.8.1. Immunohistochemistry using paraffin sections

Paraffin sections were deparaffinized 3x for 10min in xylene and rehydrated through a decreasing ethanol gradient: 2x5min $EtOH_{abs}$, 2x5min 95%EtOH and 2x5min 70%EtOH followed by H_2O_{dd}. The endogenous peroxidase activity was blocked by 3%H_2O_2 diluted in PBS/MetOH (1:1) at RT for 10min. After washing in PBS, antigen retrieval was performed by microwave treatment (100s 900W, 7min 270W) in 1x Antigen Retrieval Citra buffer (Biogentex). The cooled sections were rinsed 4x in

H_2O_{dd} and 1x in PBS, circled with Pap-Pen (Beckman Coulter) and incubated for 30min with blocking solution (5% normal swine serum (NSS; Dako) in PBST) in a humid chamber. Incubation with the first antibody was performed at 4°C O/N. Sections were rinsed next day 3x for 5min in PBS and afterwards incubated for 30min with the appropriate biotinylated secondary antibody (Vector). After 3x5min washing in PBS, 30min incubation with the VECTASTAIN ABC system was performed according to the instruction of the manufacturer (streptavidin-biotin-complex coupled with horse radish peroxidase; Vector Laboratories). The sections were stained with 3,3-diaminobenzidine (DAB; Sigma) dissolved in Tris/HCl or Histogreen (Vector) and the staining was controlled using a binocular. After the reaction was stopped by replacing DAB with PBS, Hematoxylin QS (Vector) was applied to lightly counterstain. Finally, the sections were dehydrated in an increasing ethanol gradient (H_2O_{dd}, 70%EtOH, 95%EtOH and $EtOH_{abs}$ 2x3min each) followed by 2x5min incubation in xylene and mounted with Eukitt (O.Kindler).
Following primary antibodies were used in the indicated dilution in 5%NSS/PBST: polyclonal rabbit anti-GR (M-20 - Santa Cruz) 1:200; polyclonal rabbit anti-Cre (Kellendonk et al., 1999) 1:2000; monoclonal mouse anti-BrdU (Bu20a - Dako) 1:100; monoclonal hamster anti-T1α (8.1.1 - Developmental Studies Hybridoma Bank) 1:500; polyclonal rabbit anti-collagen I/III (#2150-2555 - Biotrend) 1:20; mouse anti-alpha smooth muscle actin (mouse ascites fluid, clone 1A4, #2547 - Sigma).

PBST
PBS with 0.1% Triton-X-100 (Sigma)

DAB
10mg DAB (diaminobenzidine tablet; Sigma) were dissolved in 15ml Tris/HCl pH7.5, filtered through paper filter and 12µl H_2O_2 were added immediately prior to use.

Histogreen POD substrate kit

1ml	buffer (solution #2)
2drops	solution #1
vortex	
2drops	solution #3
vortex	

6.8.2. Hematoxylin/eosin staining of paraffin sections

4.5µm paraffin sections were deparaffinized for 3x10min in xylene and rehydrated through a decreasing ethanol gradient (2x5min $EtOH_{abs}$, 2x5min 95%EtOH, 2x5min 70%EtOH and 3min tap water). 3min incubation in Gill's hematoxylin No.3 (Sigma) was followed by a quick wash in H_2O_{dd} and 1min in 0.5%HCl in 70%EtOH. The signal was allowed to differentiate for 5min under running tap water before the sections were transferred to eosin staining solution for 2min. After a quick wash in H_2O_{dd} and dehydration through an increasing ethanol gradient (30s 70%EtOH, 30s 95%EtOH, 1min $EtOH_{abs}$) the sections were incubated 2x5min in xylene and finally mounted with Eukitt (O. Kindler).

Eosin staining solution

30ml	1% Eosin (Sigma)
270ml	70%EtOH
3ml	glacial acetic acid

6.8.3. β-galactosidase staining

For whole mount β-galactosidase stainings, organs of interest were dissected and fixed in 4% PFA (5mM EGTA, 2mM $MgCl_2$) for 30-45min. After 10min in PBS (5mM EGTA, 2mM $MgCl_2$) and washing buffer, respectively, the specimen were incubated at 37°C overnight in X-gal staining solution. The next day, organs were washed in washing buffer and kept in PBS at 4°C for analysis. In some cases, stained organs were postfixed overnight with 4% PFA at 4°C and further processed for paraffin sections as described in section 6.7.
For β-galactosidase staining on cryosections, dissected organs were frozen in O.C.T. compound (Tissue Tek, Sakura Finetek) on ethanol/dry ice and 10µm sections were prepared using a cryostat (Leica). The slides were immersed for 15min in 4% PFA and β-galactosidase staining was performed as described for whole mount samples. Sections were counterstained with Eosin (Sigma), dehydrated and mounted with Eukitt (O.Kindler).

Washing buffer

5mM	EGTA
2mM	$MgCl_2$
0.01%	sodium-deoxycholat
0.02%	NP-40

dissolved in PBS

X-gal staining solution

5mM	EGTA, pH8.0
2mM	$MgCl_2$
0.01%	sodium-deoxycholat
0.02%	NP-40
10mM	$K_3[Fe(CN)_6]$
10mM	$K_4[Fe(CN)_6]$
0.5mg/ml	X-gal (50mg/ml in Dimethylformamide; Applichem)

dissolved in PBS

6.8.4. Electron microscopy and semi-thin sections

Specimen were fixed in Karnovsky's solution for 24h at RT, dehydrated in an increasing ethanol gradient and embedded in Araldit. Sections were prepared on a Leica Ultracut UCT with a thickness of 500nm for semi-thin section and 70nm for electron microscopy. For the latter, sections were contrasted with uranyl acetate and lead citrate before inspection with the Zeiss EM900. Semi-thin sections were stained with toluidine blue and used for morphometric measurements. Series of pictures were acquired and evaluated using the processing and analysis software imageJ (available at http://rsb.info.nih.gov/ij/index.html).

7. Appendix

Table 4: Genes differentially regulated at E16.5 in $GR^{Col1\text{-}Cre}$ lungs compared to control littermates

			Dev Mut		Dev Ctr		E16.5		E18.5		Dev Diff	
Probe -ID	Symbol	Description	M	p-val	M	p-val	M	p-val	M	p-val	M	p-val
1424903_at	Jarid1d	jumonji, AT rich interactive domain 1D (Rbp2 like)	3,14	0,018	-4,32	0,003	-4,32	0,002	3,14	0,024	7,46	0,001
1449038_at	Hsd11b1	hydroxysteroid 11-beta dehydrogenase 1	3,73	0,000	4,44	0,000	-3,48	0,000	-4,19	0,000	-0,71	0,300
1437932_a_at	Cldn1	claudin 1	0,29	0,160	0,45	0,049	-2,06	0,000	-2,22	0,000	-0,16	0,599
1448700_at	G0s2	G0/G1 switch gene 2	0,99	0,000	0,83	0,000	-1,96	0,000	-1,80	0,000	0,16	0,490
1460303_at	Nr3c1	nuclear receptor subfamily 3, group C, member 1	0,75	0,001	0,73	0,001	-1,72	0,000	-1,70	0,000	0,02	0,937
1449851_at	Per1	period homolog 1 (Drosophila)	0,90	0,005	1,98	0,000	-1,56	0,000	-2,64	0,000	-1,08	0,017
1418936_at	Maff	v-maf musculoaponeurotic fibrosarcoma oncogene family, protein F (avian)	1,20	0,003	2,41	0,000	-1,42	0,001	-2,63	0,000	-1,21	0,029
1425428_at	Hif3a	hypoxia inducible factor 3, alpha subunit	-0,02	0,926	0,25	0,356	-1,38	0,000	-1,65	0,000	-0,27	0,461
1420760_s_at	Ndrl	N-myc downstream regulated-like	1,99	0,000	1,86	0,001	-1,34	0,004	-1,21	0,012	0,13	0,830
1422677_at	Dgat2	diacylglycerol O-acyltransferase 2	0,08	0,670	0,61	0,009	-1,27	0,000	-1,80	0,000	-0,52	0,082
1422904_at	Fmo2	flavin containing monooxygenase 2	1,63	0,000	5,02	0,000	-1,23	0,003	-4,62	0,000	-3,39	0,000
1417143_at	Edg2	endothelial differentiation, lysophosphatidic acid G-protein-coupled receptor, 2	-0,63	0,000	0,70	0,000	-0,81	0,000	-2,14	0,000	-1,33	0,000
1424633_at	Camk1g	calcium/calmodulin-dependent protein kinase I gamma	-0,37	0,043	-1,23	0,000	-0,72	0,001	0,14	0,465	0,85	0,003
1425631_at	Ppp1r3c	protein phosphatase 1, regulatory (inhibitor) subunit 3C	0,56	0,000	-0,19	0,152	-0,69	0,000	0,07	0,609	0,75	0,000
1428455_at	Col14a1	procollagen, type XIV, alpha 1	-0,03	0,816	0,81	0,000	-0,68	0,000	-1,53	0,000	-0,85	0,001
1416714_at	Irf8	interferon regulatory factor 8	1,16	0,000	2,15	0,000	-0,68	0,001	-1,67	0,000	-0,98	0,001
1448228_at	Lox	lysyl oxidase	-0,02	0,862	0,04	0,753	-0,68	0,000	-0,73	0,000	-0,06	0,728
1420854_at	Eln	elastin	1,21	0,000	3,01	0,000	-0,67	0,001	-2,47	0,000	-1,80	0,000
1418596_at	Fgfr4	fibroblast growth factor receptor 4	0,80	0,000	1,26	0,000	-0,66	0,000	-1,12	0,000	-0,46	0,034
1451407_at	Jam4	junction adhesion molecule 4	1,46	0,000	1,05	0,000	-0,61	0,000	-0,20	0,115	0,41	0,026
1418086_at	Ppp1r14a	protein phosphatase 1, regulatory (inhibitor) subunit 14A	0,51	0,000	0,61	0,000	-0,60	0,000	-0,71	0,000	-0,11	0,283
1421275_s_at	Socs4	suppressor of cytokine signaling 4	-0,16	0,214	-0,81	0,000	-0,59	0,000	0,06	0,655	0,65	0,002
1432543_a_at	Klf13	Kruppel-like factor 13	0,53	0,002	1,16	0,000	-0,59	0,001	-1,22	0,000	-0,63	0,010
1424131_at	Col6a3	procollagen, type VI, alpha 3	1,10	0,000	1,26	0,000	-0,59	0,005	-0,75	0,001	-0,16	0,543
1452025_a_at	Zfp2	zinc finger protein 2	-0,95	0,000	-0,76	0,000	0,62	0,000	0,44	0,006	-0,19	0,347
1449310_at	Ptger2	prostaglandin E receptor 2 (subtype EP2)	1,40	0,000	2,21	0,000	0,63	0,002	-0,17	0,362	-0,81	0,006
1416958_at	Nr1d2	nuclear receptor subfamily 1, group D, member 2	0,77	0,000	0,79	0,000	0,64	0,000	0,62	0,000	-0,01	0,927
1420377_at	St8sia2	ST8 alpha-N-acetyl-neuraminide alpha-2,8-sialyltransferase 2	0,27	0,178	-1,63	0,000	0,64	0,004	2,54	0,000	1,90	0,000
1427527_a_at	Pthlh	parathyroid hormone-like peptide	-1,51	0,000	-1,02	0,000	0,67	0,002	0,18	0,365	-0,49	0,081
1422893_at	Sfmbt1	Scm-like with four mbt domains 1	-0,77	0,001	-0,79	0,002	0,68	0,004	0,70	0,004	0,02	0,947
1450191_a_at	Sox13	SRY-box containing gene 13	0,27	0,151	0,69	0,002	0,70	0,001	0,28	0,164	-0,42	0,123
1417552_at	Fap	fibroblast activation protein	0,05	0,823	0,15	0,520	0,73	0,003	0,63	0,013	-0,10	0,751
1425528_at	Prrx1	paired related homeobox 1	0,34	0,009	-0,20	0,118	0,74	0,000	1,29	0,000	0,55	0,005
1454953_at	Rnf157	ring finger protein 157	-1,16	0,000	-0,47	0,030	0,76	0,001	0,08	0,708	-0,69	0,023
1449005_at	Slc16a3	solute carrier family 16 (monocarboxylic acid transporters), member 3	-0,58	0,018	-0,16	0,508	0,81	0,002	0,39	0,118	-0,43	0,205
1422924_at	Tnfsf9	tumor necrosis factor (ligand) superfamily, member 9	-0,88	0,000	-0,40	0,021	0,86	0,000	0,38	0,028	-0,48	0,038
1418937_at	Dio2	deiodinase, iodothyronine, type II	-0,94	0,000	-0,07	0,723	0,98	0,000	0,11	0,580	-0,88	0,004
1418989_at	Ctse	cathepsin E	0,98	0,000	-0,87	0,002	1,10	0,000	2,95	0,000	1,85	0,000
1418139_at	Dcx	doublecortin	-0,49	0,084	-0,36	0,224	1,28	0,000	1,14	0,001	-0,13	0,735
1455893_at	Rspo2	R-spondin 2 homolog (Xenopus laevis)	0,46	0,058	-1,83	0,000	1,33	0,000	3,62	0,000	2,29	0,000
1418580_at	Rtp4	receptor transporter protein 4	3,81	0,000	5,89	0,000	1,72	0,003	-0,35	0,517	-2,08	0,012

Table 5: Overview of the analysis of Tie2-CreER^{T2} transgenic offspring

Founder	Sex	Transgenic Offspring	Copy Number	LacZ analysis	Expected Recombination Pattern
T1	♀	✓	13	✓	-
T2	♀	✓	15	✓	-
T3	♂	✓	13	✓	✓
T4	♀	✓	5	-	
T5	♀	-	n.d.	-	
T6	♂	-	n.d.	-	
T7	♂	✓	6	✓	✓
T8	♀	✓	5		
T9	♀	✓	14	✓	✓
T10	♂	-	n.d.	-	
T11	♂	-	n.d.	-	
T12	♀	✓	17	-	
T13	♂	-	n.d.	-	
T14	♂	✓	1	✓	-

8. Literature

Albiston, A. L., et al., 1994. Cloning and tissue distribution of the human 11 beta-hydroxysteroid dehydrogenase type 2 enzyme. Mol Cell Endocrinol. 105**,** R11-7.

Araya, J., et al., 2006. Integrin-mediated transforming growth factor-beta activation regulates homeostasis of the pulmonary epithelial-mesenchymal trophic unit. Am J Pathol. 169**,** 405-15.

Arriza, J. L., et al., 1988. The neuronal mineralocorticoid receptor as a mediator of glucocorticoid response. Neuron. 1**,** 887-900.

Arriza, J. L., et al., 1987. Cloning of human mineralocorticoid receptor complementary DNA: structural and functional kinship with the glucocorticoid receptor. Science. 237**,** 268-75.

Barnes, P. J., Adcock, I., 1993. Anti-inflammatory actions of steroids: molecular mechanisms. Trends Pharmacol Sci. 14**,** 436-41.

Basseres, D. S., et al., 2006. Respiratory failure due to differentiation arrest and expansion of alveolar cells following lung-specific loss of the transcription factor C/EBPalpha in mice. Mol Cell Biol. 26**,** 1109-23.

Beato, M., 1989. Gene regulation by steroid hormones. Cell. 56**,** 335-44.

Beato, M., et al., 1995. Steroid hormone receptors: many actors in search of a plot. Cell. 83**,** 851-7.

Beato, M., Klug, J., 2000. Steroid hormone receptors: an update. Hum Reprod Update. 6**,** 225-36.

Bellusci, S., et al., 1997a. Involvement of Sonic hedgehog (Shh) in mouse embryonic lung growth and morphogenesis. Development. 124**,** 53-63.

Bellusci, S., et al., 1997b. Fibroblast growth factor 10 (FGF10) and branching morphogenesis in the embryonic mouse lung. Development. 124**,** 4867-78.

Bellusci, S., et al., 1996. Evidence from normal expression and targeted misexpression that bone morphogenetic protein (Bmp-4) plays a role in mouse embryonic lung morphogenesis. Development. 122**,** 1693-702.

Berger, S., et al., 2006. Loss of the limbic mineralocorticoid receptor impairs behavioral plasticity. Proc Natl Acad Sci U S A. 103**,** 195-200.

Besson, A., et al., 2008. CDK Inhibitors: Cell Cycle Regulators and Beyond. Dev Cell. 14**,** 159-69.

Bourbon, J., et al., 2005. Control mechanisms of lung alveolar development and their disorders in bronchopulmonary dysplasia. Pediatr Res. 57**,** 38R-46R.

Boyle, M. P., et al., 2005. Acquired deficit of forebrain glucocorticoid receptor produces depression-like changes in adrenal axis regulation and behavior. Proc Natl Acad Sci U S A. 102**,** 473-8.

Calandra, T., et al., 1995. MIF as a glucocorticoid-induced modulator of cytokine production. Nature. 377**,** 68-71.

Calfa, G., et al., 2003. Characterization and functional significance of glucocorticoid receptors in patients with major depression: modulation by antidepressant treatment. Psychoneuroendocrinology. 28**,** 687-701.

Cardoso, W. V., et al., 1997. FGF-1 and FGF-7 induce distinct patterns of growth and differentiation in embryonic lung epithelium. Dev Dyn. 208**,** 398-405.

Cardoso, W. V., Lu, J., 2006. Regulation of early lung morphogenesis: questions, facts and controversies. Development. 133**,** 1611-24.

Chelly, N., et al., 2001. Role of keratinocyte growth factor in the control of surfactant synthesis by fetal lung mesenchyme. Endocrinology. 142**,** 1814-9.

Church, G. M., Gilbert, W., 1984. Genomic sequencing. Proc Natl Acad Sci U S A. 81**,** 1991-5.

Clerch, L. B., et al., 2004. DNA microarray analysis of neonatal mouse lung connects regulation of KDR with dexamethasone-induced inhibition of alveolar formation. Am J Physiol Lung Cell Mol Physiol. 286**,** L411-9.

Cole, T. J., et al., 1995. Targeted disruption of the glucocorticoid receptor gene blocks adrenergic chromaffin cell development and severely retards lung maturation. Genes Dev. 9**,** 1608-21.

Cole, T. J., et al., 1993. Expression of the mouse glucocorticoid receptor and its role during development. J Steroid Biochem Mol Biol. 47**,** 49-53.

Condon, J. C., et al., 2004. Surfactant protein secreted by the maturing mouse fetal lung acts as a hormone that signals the initiation of parturition. Proc Natl Acad Sci U S A. 101**,** 4978-83.

Constien, R., et al., 2001. Characterization of a novel EGFP reporter mouse to monitor Cre recombination as demonstrated by a Tie2 Cre mouse line. Genesis. 30**,** 36-44.

Copeland, N. G., et al., 2001. Recombineering: a powerful new tool for mouse functional genomics. Nat Rev Genet. 2**,** 769-79.

Cram, E. J., et al., 1998. Role of the CCAAT/enhancer binding protein-alpha transcription factor in the glucocorticoid stimulation of p21waf1/cip1 gene promoter activity in growth-arrested rat hepatoma cells. J Biol Chem. 273**,** 2008-14.

De Kloet, E. R., et al., 1998. Brain corticosteroid receptor balance in health and disease. Endocr Rev. 19**,** 269-301.

De Langhe, S. P., et al., 2005. Dickkopf-1 (DKK1) reveals that fibronectin is a major target of Wnt signaling in branching morphogenesis of the mouse embryonic lung. Dev Biol. 277**,** 316-31.

De Martino, M. U., et al., 2004. The glucocorticoid receptor and the orphan nuclear receptor chicken ovalbumin upstream promoter-transcription factor II interact with and mutually affect each other's transcriptional activities: implications for intermediary metabolism. Mol Endocrinol. 18**,** 820-33.

del Moral, P. M., et al., 2006a. Differential role of FGF9 on epithelium and mesenchyme in mouse embryonic lung. Dev Biol. 293**,** 77-89.

Del Moral, P. M., et al., 2006b. VEGF-A signaling through Flk-1 is a critical facilitator of early embryonic lung epithelial to endothelial crosstalk and branching morphogenesis. Dev Biol. 290**,** 177-88.

Derynck, R., Akhurst, R. J., 2007. Differentiation plasticity regulated by TGF-beta family proteins in development and disease. Nat Cell Biol. 9**,** 1000-4.

Diamond, M. I., et al., 1990. Transcription factor interactions: selectors of positive or negative regulation from a single DNA element. Science. 249**,** 1266-72.

Ding, W., et al., 2007. Sprouty2 downregulation plays a pivotal role in mediating crosstalk between TGF-beta1 signaling and EGF as well as FGF receptor tyrosine kinase-ERK pathways in mesenchymal cells. J Cell Physiol. 212**,** 796-806.

El-Hallous, E., et al., 2007. Fibrillin-1 interactions with fibulins depend on the first hybrid domain and provide an adaptor function to tropoelastin. J Biol Chem. 282**,** 8935-46.

Engblom, D., et al., 2007. Direct glucocorticoid receptor-Stat5 interaction in hepatocytes controls body size and maturation-related gene expression. Genes Dev. 21**,** 1157-62.

Erdmann, G., et al., 2007. Inducible gene inactivation in neurons of the adult mouse forebrain. BMC Neurosci. 8**,** 63.

Feil, R., et al., 1997. Regulation of Cre recombinase activity by mutated estrogen receptor ligand-binding domains. Biochem Biophys Res Commun. 237**,** 752-7.

Feinberg, A. P., Vogelstein, B., 1983. A technique for radiolabeling DNA restriction endonuclease fragments to high specific activity. Anal Biochem. 132**,** 6-13.

Florin, L., et al., 2004. Cre recombinase-mediated gene targeting of mesenchymal cells. Genesis. 38**,** 139-44.

Forde, A., et al., 2002. Temporal Cre-mediated recombination exclusively in endothelial cells using Tie2 regulatory elements. Genesis. 33**,** 191-7.

Francis, S. E., et al., 2002. Central roles of alpha5beta1 integrin and fibronectin in vascular development in mouse embryos and embryoid bodies. Arterioscler Thromb Vasc Biol. 22**,** 927-33.

Freedman, N. D., Yamamoto, K. R., 2004. Importin 7 and importin alpha/importin beta are nuclear import receptors for the glucocorticoid receptor. Mol Biol Cell. 15**,** 2276-86.

Funder, J. W., 1992. Glucocorticoid receptors. J Steroid Biochem Mol Biol. 43**,** 389-94.

Funder, J. W., et al., 1988. Mineralocorticoid action: target tissue specificity is enzyme, not receptor, mediated. Science. 242**,** 583-5.

Gass, P., et al., 2001. Mice with targeted mutations of glucocorticoid and mineralocorticoid receptors: models for depression and anxiety? Physiol Behav. 73**,** 811-25.

Gauthier, J. M., et al., 1993. Functional interference between the Spi-1/PU.1 oncoprotein and steroid hormone or vitamin receptors. EMBO J. 12**,** 5089-96.

Gehring, U., 1993. The structure of glucocorticoid receptors. J Steroid Biochem Mol Biol. 45**,** 183-90.

George, E. L., et al., 1993. Defects in mesoderm, neural tube and vascular development in mouse embryos lacking fibronectin. Development. 119**,** 1079-91.

Gilstrap, L. C., et al., 1995. EFFECT OF CORTICOSTEROIDS FOR FETAL MATURATION ON PERINATAL OUTCOMES. Jama-Journal of the American Medical Association. 273**,** 413-418.

Glasser, S. W., et al., 1991. Genetic element from human surfactant protein SP-C gene confers bronchiolar-alveolar cell specificity in transgenic mice. Am J Physiol. 261**,** L349-56.

Green, S., et al., 1988. The N-terminal DNA-binding 'zinc finger' of the oestrogen and glucocorticoid receptors determines target gene specificity. Embo J. 7**,** 3037-44.

Gu, H., et al., 1994. Deletion of a DNA polymerase beta gene segment in T cells using cell type-specific gene targeting. Science. 265**,** 103-6.

Halliday, H. L., 2004. Use of steroids in the perinatal period. Paediatr Respir Rev. 5 Suppl A**,** S321-7.

Hanson, R. W., Reshef, L., 1997. Regulation of phosphoenolpyruvate carboxykinase (GTP) gene expression. Annu Rev Biochem. 66**,** 581-611.

Heck, S., et al., 1994. A distinct modulating domain in glucocorticoid receptor monomers in the repression of activity of the transcription factor AP-1. EMBO J. 13**,** 4087-95.

Herbert, J., et al., 2006. Do corticosteroids damage the brain? J Neuroendocrinol. 18**,** 393-411.

Herman, J. P., et al., 2003. Central mechanisms of stress integration: hierarchical circuitry controlling hypothalamo-pituitary-adrenocortical responsiveness. Front Neuroendocrinol. 24**,** 151-80.

Ho Sui, S. J., et al., 2005. oPOSSUM: identification of over-represented transcription factor binding sites in co-expressed genes. Nucleic Acids Res. 33**,** 3154-64.

Hogan, B., et al., 1994. Manipulating the Mouse Embryo. A Laboratory Manual. Cold Spring Harbor Laboratory Press.

Hollenberg, S. M., et al., 1985. Primary structure and expression of a functional human glucocorticoid receptor cDNA. Nature. 318**,** 635-41.

Hopkins, D. R., et al., 2007. The bone morphogenetic protein 1/Tolloid-like metalloproteinases. Matrix Biol. 26**,** 508-23.

Hubmacher, D., et al., 2006. Fibrillins: from biogenesis of microfibrils to signaling functions. Curr Top Dev Biol. 75**,** 93-123.

Hummler, E., et al., 1996. Early death due to defective neonatal lung liquid clearance in alpha-ENaC-deficient mice. Nat Genet. 12**,** 325-8.

Imai, E., et al., 1993. Glucocorticoid receptor-cAMP response element-binding protein interaction and the response of the phosphoenolpyruvate carboxykinase gene to glucocorticoids. J Biol Chem. 268**,** 5353-6.

Itani, O. A., et al., 2002. Glucocorticoid-stimulated lung epithelial Na(+) transport is associated with regulated ENaC and sgk1 expression. Am J Physiol Lung Cell Mol Physiol. 282**,** L631-41.

Jacobson, L., Sapolsky, R., 1991. The role of the hippocampus in feedback regulation of the hypothalamic-pituitary-adrenocortical axis. Endocr Rev. 12**,** 118-34.

Jantzen, H. M., et al., 1987. Cooperativity of glucocorticoid response elements located far upstream of the tyrosine aminotransferase gene. Cell. 49**,** 29-38.

Kassel, O., et al., 2004. A nuclear isoform of the focal adhesion LIM-domain protein Trip6 integrates activating and repressing signals at AP-1- and NF-kappaB-regulated promoters. Genes Dev. 18**,** 2518-28.

Kellendonk, C., et al., 1999. Inducible site-specific recombination in the brain. J Mol Biol. 285**,** 175-82.

Kellendonk, C., et al., 1996. Regulation of Cre recombinase activity by the synthetic steroid RU 486. Nucleic Acids Res. 24**,** 1404-11.

Keller, H. R., et al., 1995. Simulated descent v dexamethasone in treatment of acute mountain sickness: a randomised trial. BMJ. 310**,** 1232-5.

Khan, A. A., et al., 1996. Lymphocyte apoptosis: mediation by increased type 3 inositol 1,4,5-trisphosphate receptor. Science. 273**,** 503-7.

Kim, N., Vu, T. H., 2006. Parabronchial smooth muscle cells and alveolar myofibroblasts in lung development. Birth Defects Res C Embryo Today. 78**,** 80-9.

Kisanuki, Y. Y., et al., 2001. Tie2-Cre transgenic mice: a new model for endothelial cell-lineage analysis in vivo. Dev Biol. 230**,** 230-42.

Kleiman, A., Tuckermann, J. P., 2007. Glucocorticoid receptor action in beneficial and side effects of steroid therapy: lessons from conditional knockout mice. Mol Cell Endocrinol. 275**,** 98-108.

Klieber, M. A., et al., 2007. Corticosteroid-binding globulin, a structural basis for steroid transport and proteinase-triggered release. J Biol Chem. 282**,** 29594-603.

Korfhagen, T. R., et al., 1990. Cis-acting sequences from a human surfactant protein gene confer pulmonary-specific gene expression in transgenic mice. Proc Natl Acad Sci U S A. 87**,** 6122-6.

Kostka, G., et al., 2001. Perinatal lethality and endothelial cell abnormalities in several vessel compartments of fibulin-1-deficient mice. Mol Cell Biol. 21**,** 7025-34.

Kreidberg, J. A., et al., 1996. Alpha 3 beta 1 integrin has a crucial role in kidney and lung organogenesis. Development. 122**,** 3537-47.

Krieger, D. T., 1983. Physiopathology of Cushing's disease. Endocr Rev. 4**,** 22-43.

Lee, E. C., et al., 2001. A highly efficient Escherichia coli-based chromosome engineering system adapted for recombinogenic targeting and subcloning of BAC DNA. Genomics. 73**,** 56-65.

Lewis, J. F., Veldhuizen, R., 2003. The role of exogenous surfactant in the treatment of acute lung injury. Annu Rev Physiol. 65**,** 613-42.

Li, C., et al., 2005a. Wnt5a regulates Shh and Fgf10 signaling during lung development. Dev Biol. 287**,** 86-97.

Li, W. L., et al., 2005b. Endothelial cell-specific expression of Cre recombinase in transgenic mice. Yi Chuan Xue Bao. 32**,** 909-15.

Liggins, G. C., 1969. Premature delivery of foetal lambs infused with glucocorticoids. J Endocrinol. 45**,** 515-23.

Liggins, G. C., Howie, R. N., 1972. A controlled trial of antepartum glucocorticoid treatment for prevention of the respiratory distress syndrome in premature infants. Pediatrics. 50**,** 515-25.

Lindahl, P., et al., 1997. Alveogenesis failure in PDGF-A-deficient mice is coupled to lack of distal spreading of alveolar smooth muscle cell progenitors during lung development. Development. 124**,** 3943-53.

Luecke, H. F., Yamamoto, K. R., 2005. The glucocorticoid receptor blocks P-TEFb recruitment by NFkappaB to effect promoter-specific transcriptional repression. Genes Dev. 19**,** 1116-27.

Luisi, B. F., et al., 1991. Crystallographic analysis of the interaction of the glucocorticoid receptor with DNA. Nature. 352**,** 497-505.

Mader, S., et al., 1989. Three amino acids of the oestrogen receptor are essential to its ability to distinguish an oestrogen from a glucocorticoid-responsive element. Nature. 338**,** 271-4.

Maki, J. M., et al., 2005. Lysyl oxidase is essential for normal development and function of the respiratory system and for the integrity of elastic and collagen fibers in various tissues. Am J Pathol. 167**,** 927-36.

Mangelsdorf, D. J., et al., 1995. The nuclear receptor superfamily: the second decade. Cell. 83**,** 835-9.

Mantamadiotis, T., et al., 2002. Disruption of CREB function in brain leads to neurodegeneration. Nat Genet. 31**,** 47-54.

McGowan, S. E., Torday, J. S., 1997. The pulmonary lipofibroblast (lipid interstitial cell) and its contributions to alveolar development. Annu Rev Physiol. 59**,** 43-62.

Mendelson, C. R., 2000. Role of transcription factors in fetal lung development and surfactant protein gene expression. Annu Rev Physiol. 62**,** 875-915.

Miesfeld, R., et al., 1986. Genetic complementation of a glucocorticoid receptor deficiency by expression of cloned receptor cDNA. Cell. 46**,** 389-99.

Mittelstadt, P. R., Ashwell, J. D., 2003. Disruption of glucocorticoid receptor exon 2 yields a ligand-responsive C-terminal fragment that regulates gene expression. Mol Endocrinol. 17**,** 1534-42.

Morishima, Y., et al., 2003. The hsp90 cochaperone p23 is the limiting component of the multiprotein hsp90/hsp70-based chaperone system in vivo where it acts to stabilize the client protein: hsp90 complex. J Biol Chem. 278**,** 48754-63.

Muglia, L. J., et al., 1999. Proliferation and differentiation defects during lung development in corticotropin-releasing hormone-deficient mice. Am J Respir Cell Mol Biol. 20**,** 181-8.

Muyrers, J. P., et al., 1999. Rapid modification of bacterial artificial chromosomes by ET-recombination. Nucleic Acids Res. 27**,** 1555-7.

Nagy, A., 2000. Cre recombinase: the universal reagent for genome tailoring. Genesis. 26**,** 99-109.

Nakamura, K., et al., 2002. Endogenous and exogenous glucocorticoid regulation of ENaC mRNA expression in developing kidney and lung. Am J Physiol Cell Physiol. 283**,** C762-72.

Nguyen, N. M., Senior, R. M., 2006. Laminin isoforms and lung development: all isoforms are not equal. Dev Biol. 294**,** 271-9.

Okubo, T., Hogan, B. L., 2004. Hyperactive Wnt signaling changes the developmental potential of embryonic lung endoderm. J Biol. 3**,** 11.

Okubo, T., et al., 2005. Nmyc plays an essential role during lung development as a dosage-sensitive regulator of progenitor cell proliferation and differentiation. Development. 132**,** 1363-74.

Otto, C., et al., 2001. Impairment of mossy fiber long-term potentiation and associative learning in pituitary adenylate cyclase activating polypeptide type I receptor-deficient mice. J Neurosci. 21**,** 5520-7.

Patel, P. D., et al., 1989. Molecular cloning of a mineralocorticoid (type I) receptor complementary DNA from rat hippocampus. Mol Endocrinol. 3**,** 1877-85.

Pearce, D., Yamamoto, K. R., 1993. Mineralocorticoid and glucocorticoid receptor activities distinguished by nonreceptor factors at a composite response element. Science. 259**,** 1161-5.

Perl, A. K., et al., 2002. Early restriction of peripheral and proximal cell lineages during formation of the lung. Proc Natl Acad Sci U S A. 99**,** 10482-7.

Pilkis, S. J., Granner, D. K., 1992. Molecular physiology of the regulation of hepatic gluconeogenesis and glycolysis. Annu Rev Physiol. 54**,** 885-909.

Pratt, W. B., Toft, D. O., 1997. Steroid receptor interactions with heat shock protein and immunophilin chaperones. Endocr Rev. 18**,** 306-60.

Pratt, W. B., Toft, D. O., 2003. Regulation of signaling protein function and trafficking by the hsp90/hsp70-based chaperone machinery. Exp Biol Med (Maywood). 228**,** 111-33.

Ramasamy, S. K., et al., 2007. Fgf10 dosage is critical for the amplification of epithelial cell progenitors and for the formation of multiple mesenchymal lineages during lung development. Dev Biol. 307**,** 237-47.

Reichardt, H. M., et al., 1998. DNA binding of the glucocorticoid receptor is not essential for survival. Cell. 93**,** 531-41.

Reily, M. M., et al., 2006. The GRIP1:IRF3 interaction as a target for glucocorticoid receptor-mediated immunosuppression. EMBO J. 25**,** 108-17.

Reinisch, J. M., et al., 1978. Prenatal exposure to prednisone in humans and animals retards intrauterine growth. Science. 202**,** 436-8.

Ridder, S., et al., 2005. Mice with genetically altered glucocorticoid receptor expression show altered sensitivity for stress-induced depressive reactions. J Neurosci. 25**,** 6243-50.

Rogatsky, I., et al., 2001. Factor recruitment and TIF2/GRIP1 corepressor activity at a collagenase-3 response element that mediates regulation by phorbol esters and hormones. EMBO J. 20**,** 6071-83.

Rupprecht, R., et al., 1993. Transactivation and synergistic properties of the mineralocorticoid receptor: relationship to the glucocorticoid receptor. Mol Endocrinol. 7**,** 597-603.

Sakai, T., et al., 2003. Fibronectin requirement in branching morphogenesis. Nature. 423**,** 876-81.

Sambrook, J., Russell, D. W., 2001. Molecular Cloning. A Laboratory Manual. Cold Spring Harbor: Cold Spring Harbor Laboratory Press.

Schacke, H., et al., 2002. Mechanisms involved in the side effects of glucocorticoids. Pharmacol Ther. 96**,** 23-43.

Schedl, A., et al., 1993a. A method for the generation of YAC transgenic mice by pronuclear microinjection. Nucleic Acids Res. 21**,** 4783-7.

Schedl, A., et al., 1993b. A yeast artificial chromosome covering the tyrosinase gene confers copy number-dependent expression in transgenic mice. Nature. 362**,** 258-61.

Schmid, W., et al., 1985. Deletions near the albino locus on chromosome 7 of the mouse affect the level of tyrosine aminotransferase mRNA. Proc Natl Acad Sci U S A. 82**,** 2866-9.

Schorpp-Kistner, M., et al., 1999. JunB is essential for mammalian placentation. EMBO J. 18**,** 934-48.

Schule, R., et al., 1990. Functional antagonism between oncoprotein c-Jun and the glucocorticoid receptor. Cell. 62**,** 1217-26.

Schwartz, D. C., Cantor, C. R., 1984. Separation of yeast chromosome-sized DNAs by pulsed field gradient gel electrophoresis. Cell. 37**,** 67-75.

Seckl, J. R., 2004. Prenatal glucocorticoids and long-term programming. Eur J Endocrinol. 151 Suppl 3**,** U49-62.

Sengupta, S., et al., 2000. Negative cross-talk between p53 and the glucocorticoid receptor and its role in neuroblastoma cells. Embo J. 19**,** 6051-64.

Sengupta, S., Wasylyk, B., 2001. Ligand-dependent interaction of the glucocorticoid receptor with p53 enhances their degradation by Hdm2. Genes Dev. 15**,** 2367-80.

Shalaby, F., et al., 1995. Failure of blood-island formation and vasculogenesis in Flk-1-deficient mice. Nature. 376**,** 62-6.

Shannon, J. M., Hyatt, B. A., 2004. Epithelial-mesenchymal interactions in the developing lung. Annu Rev Physiol. 66**,** 625-45.

Shi, W., et al., 1999. TGF-beta3-null mutation does not abrogate fetal lung maturation in vivo by glucocorticoids. Am J Physiol. 277**,** L1205-13.

Shimshek, D. R., et al., 2005. Enhanced odor discrimination and impaired olfactory memory by spatially controlled switch of AMPA receptors. PLoS Biol. 3**,** e354.

Shimshek, D. R., et al., 2002. Codon-improved Cre recombinase (iCre) expression in the mouse. Genesis. 32**,** 19-26.

Shirakihara, T., et al., 2007. Differential regulation of epithelial and mesenchymal markers by deltaEF1 proteins in epithelial mesenchymal transition induced by TGF-beta. Mol Biol Cell. 18**,** 3533-44.

Simmons, P. S., et al., 1984. Increased proteolysis. An effect of increases in plasma cortisol within the physiologic range. J Clin Invest. 73**,** 412-20.

Sinclair, J. C., 1995. Meta-analysis of randomized controlled trials of antenatal corticosteroid for the prevention of respiratory distress syndrome: discussion. Am J Obstet Gynecol. 173**,** 335-44.

Smith, B. T., 1979. Lung maturation in the fetal rat: acceleration by injection of fibroblast-pneumonocyte factor. Science. 204**,** 1094-5.

Snyder, J. M., et al., 1981. The effect of cortisol on rabbit fetal lung maturation in vitro. Dev Biol. 85**,** 129-40.

Song, C. Z., et al., 1999. Glucocorticoid receptor inhibits transforming growth factor-beta signaling by directly targeting the transcriptional activation function of Smad3. Proc Natl Acad Sci U S A. 96**,** 11776-81.

Soriano, P., 1999. Generalized lacZ expression with the ROSA26 Cre reporter strain. Nat Genet. 21**,** 70-1.

Southern, E. M., 1975. Detection of specific sequences among DNA fragments separated by gel electrophoresis. J Mol Biol. 98**,** 503-17.

Stenmark, K. R., Abman, S. H., 2005. Lung vascular development: implications for the pathogenesis of bronchopulmonary dysplasia. Annu Rev Physiol. 67**,** 623-61.

Stenmark, K. R., Gebb, S. A., 2003. Lung vascular development: breathing new life into an old problem. Am J Respir Cell Mol Biol. 28**,** 133-7.

Stromstedt, P. E., et al., 1991. The glucocorticoid receptor binds to a sequence overlapping the TATA box of the human osteocalcin promoter: a potential mechanism for negative regulation. Mol Cell Biol. 11**,** 3379-83.

Suzuki, N., et al., 1996. Failure of ventral body wall closure in mouse embryos lacking a procollagen C-proteinase encoded by Bmp1, a mammalian gene related to Drosophila tolloid. Development. 122**,** 3587-95.

ten Dijke, P., Arthur, H. M., 2007. Extracellular control of TGFbeta signalling in vascular development and disease. Nat Rev Mol Cell Biol. 8**,** 857-69.

Ten, S., et al., 2001. Clinical review 130: Addison's disease 2001. J Clin Endocrinol Metab. 86**,** 2909-22.

Thompson, E. B., 1994. Apoptosis and steroid hormones. Mol Endocrinol. 8**,** 665-73.

Tichelaar, J. W., et al., 2000. Conditional expression of fibroblast growth factor-7 in the developing and mature lung. J Biol Chem. 275**,** 11858-64.

Tronche, F., et al., 1999. Disruption of the glucocorticoid receptor gene in the nervous system results in reduced anxiety. Nat Genet. 23**,** 99-103.

Tronche, F., et al., 1998. Genetic dissection of glucocorticoid receptor function in mice. Curr Opin Genet Dev. 8**,** 532-8.

Tronche, F., et al., 2004. Glucocorticoid receptor function in hepatocytes is essential to promote postnatal body growth. Genes Dev. 18**,** 492-7.

Tsien, J. Z., et al., 1996. Subregion- and cell type-restricted gene knockout in mouse brain. Cell. 87**,** 1317-26.

Umesono, K., Evans, R. M., 1989. Determinants of target gene specificity for steroid/thyroid hormone receptors. Cell. 57**,** 1139-46.

Vacca, A., et al., 1992. Glucocorticoid receptor-mediated suppression of the interleukin 2 gene expression through impairment of the cooperativity between nuclear factor of activated T cells and AP-1 enhancer elements. J Exp Med. 175**,** 637-46.

Vegiopoulos, A., Herzig, S., 2007. Glucocorticoids, metabolism and metabolic diseases. Mol Cell Endocrinol. 275**,** 43-61.

Wan, H., et al., 2004. Foxa2 is required for transition to air breathing at birth. Proc Natl Acad Sci U S A. 101**,** 14449-54.

Warburton, D., et al., 2005. Molecular mechanisms of early lung specification and branching morphogenesis. Pediatr Res. 57**,** 26R-37R.

Weaver, M., et al., 1999. Bmp signaling regulates proximal-distal differentiation of endoderm in mouse lung development. Development. 126**,** 4005-15.

Weber, P., et al., 2001. Temporally controlled targeted somatic mutagenesis in the mouse brain. Eur J Neurosci. 14**,** 1777-83.

Wendel, D. P., et al., 2000. Impaired distal airway development in mice lacking elastin. Am J Respir Cell Mol Biol. 23**,** 320-6.

Wert, S. E., et al., 1993. Transcriptional elements from the human SP-C gene direct expression in the primordial respiratory epithelium of transgenic mice. Dev Biol. 156**,** 426-43.

White, A. C., et al., 2006. FGF9 and SHH signaling coordinate lung growth and development through regulation of distinct mesenchymal domains. Development. 133**,** 1507-17.

Whitsett, J. A., Matsuzaki, Y., 2006. Transcriptional regulation of perinatal lung maturation. Pediatr Clin North Am. 53**,** 873-87, viii.

Wright, J. R., 2005. Immunoregulatory functions of surfactant proteins. Nat Rev Immunol. 5**,** 58-68.

Yamamoto, H., et al., 2007. Epithelial-vascular cross talk mediated by VEGF-A and HGF signaling directs primary septae formation during distal lung morphogenesis. Dev Biol.

Yang, J. Q., et al., 2007. Cell Density and Serum Exposure Modify the Function of the Glucocorticoid Receptor C/EBP Complex. Am J Respir Cell Mol Biol.

Yu, D., et al., 2000. An efficient recombination system for chromosome engineering in Escherichia coli. Proc Natl Acad Sci U S A. 97**,** 5978-83.

Zaremba, W., et al., 1997. Prophylaxis of respiratory distress syndrome in premature calves by administration of dexamethasone or a prostaglandin F2 alpha analogue to their dams before parturition. Am J Vet Res. 58**,** 404-7.

Zeng, X., et al., 2001. TGF-beta1 perturbs vascular development and inhibits epithelial differentiation in fetal lung in vivo. Dev Dyn. 221**,** 289-301.

Zeng, X., et al., 1998. VEGF enhances pulmonary vasculogenesis and disrupts lung morphogenesis in vivo. Dev Dyn. 211**,** 215-27.

Zennaro, M. C., et al., 1997. Tissue-specific expression of alpha and beta messenger ribonucleic acid isoforms of the human mineralocorticoid receptor in normal and pathological states. J Clin Endocrinol Metab. 82**,** 1345-52.

Zhang, Y., et al., 1998. A new logic for DNA engineering using recombination in Escherichia coli. Nat Genet. 20**,** 123-8.

9. Abbreviations

α-SMA	alpha smooth muscle actin
11β-HSD2	11β hydroxysteroid-dehydrogenase type 2
ACTH	adrenocorticotropic hormone
AF	transactivation domain
AP1	activator protein 1
AVP	arginine vasopressin
BAC	bacterial artificial chromosome
bp	base pairs
BrdU	Bromodeoxyuridine
BW	body weight
cDNA	complementary DNA
Ci	Curie
Cre	cyclization recombination (Cre) recombinase
CRH	corticotropin-releasing hormone
CTP	cytidine triphosphate
Da	Dalton
DAB	3,3'diaminobenzidine
DBD	DNA-binding domain
Dex	dexamethasone
DNA	deoxyribonucleic acid
dNTP	deoxyribonucleotide triphosphate
Ex	embryonic day x
ECM	extracellular matrix
EDTA	ehtylenediamine tetraacetic acid
EGTA	ehtyleneglycol tetraacetic acid
ER	estrogen receptor
ER^{T2}	LBD of the estrogen receptor harboring two point mutations
F1	first filial generation
FGF	fibroblast growth factor
Flp	flippase recombinase
FRT	Flp recombinase recognition site
g	gram
GR	glucocorticoid receptor
GRE	glucocorticoid response element
GTP	guanosine triphosphate
h	hour
HPA axis	hypothalamic-pituitary-adrenal axis
HRE	hormone response element
HRP	horseradish peroxidise
Hsp	heat shock protein
IHC	immunohistochemistry
i.p.	intraperitoneal

k	kilo (10^3)
kb	kilo base pair
kD	kilodalton
l	litre
LacZ	β-galactosidase gene
LB-medium	Luria-Bertani medium
LBD	ligand binding domain
loxP	Cre recombinase recognition site
µ	micro
M	molar
m	meter
m	milli (10^{-3})
min	minute
MR	mineralocorticoid receptor
mRNA	messenger RNA
n	nano
n	number
NF-kB	nuclear factor kappa B
NID	non ionic detergent (buffer)
NLS	nuclear localisation signal
NP40	nonidet P40
OD	optical density
p	pico (10^{-12})
p	p-value
PAS	periodic acid schiff
PBS	phosphate buffered saline
PCR	polymerase chain reaction
PECAM1	platelet endothelial cell adhesion molecule 1
PFA	paraformaldehyde
PFGE	pulse-field gel electrophoresis
RNA	ribonucleic acid
rpm	rotations per minute
RT	room temperature
s	second
SDS	sodiumdedecylsulfate
Shh	sonic hedgehog
TAE	trias acetate EDTA buffer
TBE	tris borate EDTA buffer
TE	tris EDTA
TGFβ	transforming growth factor β
U	enzymatic unit
UV	ultraviolet
V	volt
W	watt
wt	wild type
X-gal	5-bromo-4-chloro-3-indolyl-β-D-galactopyranoside
Yac	yeast artificial chromosome

10. Acknowledgements

First of all, I am very grateful to Prof. Dr. Günther Schütz for giving me the opportunity to work on these interesting projects in the comfortable environment of his group. His continuous support, his helpful advice and his scientific enthusiasm guided me through my PhD time.

I also want to thank Prof. Dr. Felix Wieland for serving as my second supervisor and Prof. Dr. Ingrid Grummt for serving as my external advisor in the DFKZ PhD program.

I am very grateful to Dr. Minqiang Chai for his great support and guidance during the first part of my PhD time. Thank you for all your efforts, all the good times and the insights into the Chinese culture.

A special thank you goes to Prof. Dr. Hermann-Josef Gröne and his colleagues Sylvia Kaden and Claudia Schmidt for the valuable support and their helpful advice. I also want to thank Prof. Dr. Peter Angel and his colleagues for the helpful discussions.

I want to thank past and present members of the Schütz lab for all the technical help, scientific advice and emotional support I obtained through the years. A big thank you goes to Dr. Stefan Berger, Dr. David Engblom, Dr. Gitta Erdmann and Dr. Wolfgang Schmid for reading this thesis and the helpful discussions. Particularly valuable scientific support was also provided by Dr. Jan Rodriguez and Dr. Jan Tuckermann. Thank you!

I am indebted and very grateful to my family, my parents Luzie and Gerhard Habermehl, my sister Susanne and my grandmother.

Finally, I would like to express my deepest gratitude to my partner Julia Baisch for her understanding, the unlimited support and all her love.